2005

Free vibration of sandwich plates with viscoelastic cores

Devlin Hayduke

Free Vibration of Sandwich Plates with Viscoelastic Cores

by

Devlin Hayduke

A Thesis Submitted in
Partial Fulfillment of the
Requirement for the

MASTER OF SCIENCE
IN
MECHANICAL ENGINEERING

Approved by:

Dr. H. Ghoneim
Department of Mechanical Engineering

Dr. J. Török
Department of Mechanical Engineering

Dr. A. Crassidis
Department of Mechanical Engineering

Dr. E. Hensel
Department Head of Mechanical Engineering

H. Ghoneim
(Thesis advisor)

J. S. Török

A. Crassidis

Edward Hensel

DEPARTMENT OF MECHANICAL ENGINEERING
ROCHESTER INSTITUTE OF TECHNOLOGY

MAY, 2005

PERMISSION FROM AUTHOR REQUIRED

Free Vibration of Sandwich Plates with Viscoelastic Cores

I, Devlin Hayduke, prefer to be contacted each time a request for reproduction is made. If permission is granted, any reproduction will not be for commercial use or profit. I can be reached at the following address:

Date: 05/06/05 **Signature of Author:** Devlin Hayduke

Acknowledgements

I am grateful to Dr. Ghoneim for his guidance and confidence in my ability through the inception, evolution and completion of this research; to Dr. Török and Dr. Crassidis for their support and suggestions.

I am especially thankful and deeply grateful to my parents Cindy and Walter Hayduke for their understanding and unwavering support of me; especially for trusting my commitment to my research and allowing me the time to properly complete it even though neither has an engineering background and to them most of this paper might as well we written in Greek.

Abstract

The analysis of the free vibration of rectangular sandwich plates with viscoelastic cores is purposed. The analysis focuses on evaluating two displacement theories of sandwich plates for various geometric and material properties and boundary conditions.

The first theory was developed for the vibratory bending of unsymmetrical sandwich plates by Rao and Nakra[1]. The theory is a layerwise theory that models the displacement of the face layers with classic plate theory (i.e. normals to the midplane remain normal to the midplane and undeformed after deformation of the plate) and the continuity of the displacements at the interfaces between the face layers and the core used to derive the displacements of the core. The core is assumed to be in a state of pure transverse shear and in-plane strains are considered negligible. This theory is not only restricted by the assumed displacement field, but is specific to a sandwich plate composed of three isotropic layers.

The second theory is a third order plate theory that was developed for composite plates that required the inclusion of transverse strains by Reddy[2]. The theory assumes a cubic displacement in terms of the thickness resulting in quadratic transverse shear stresses that vanish at the free surfaces of the plate. The advantage of this displacement field is that it does not require shear correction factors which are dependent on the specific plate materials and boundary conditions like first order plate theories (e.g. Mindlin plates). The theory is an equivalent single layer theory that integrates the displacement of the plate over the thickness, resulting in generalized stiffnesses that apply to a general plate composed of monoclinic layers.

Both theories are analyzed and compared to finite element models generated in ANSYS for simply supported boundary conditions. The purpose of the simply supported analysis is to determine the characteristics of each theory with respect to variations of the geometric and material properties of the sandwich plate. Damping is introduced to the sandwich plate using the linear elastic-viscoelastic correspondence principle for harmonic analysis and loss factors are calculated for several specific geometries of the simply supported plates.

The cantilever plate is also examined for both theories using the semi-analytical superposition method with a state space approach. The closed form superposition method developed by Gorman[3] for classic plate theory is extended to both sandwich plate theories and a new semi-numerical approach is taken. The only numerical error introduced in the analysis is the calculation of the eigenvalues and corresponding eigenvectors for the state space solutions that

---

[1] Rao, Y.V.K.S. and Nakra, B.C. 1973 *Archive of Mechanics* **25**, 213-225. Theory of vibratory bending of unsymmetrical sandwich plates.

[2] Reddy, J.N. 1984 *Journal of Applied Mechanics* **45**, 745-752. A simple higher-order theory for laminated composite plates.

[3] Gorman, D. J. 1982 Free Vibration Analysis of Rectangular Plates New York: Elsevier

are superimposed to solve for the cantilever boundary conditions. Fourier series solutions are obtained for the mode shapes such that each term of the series exactly satisfies the prescribed boundary conditions. The approach is directly compared to finite element models generated in ANSYS for the cantilever plate.

Table of Contents

1 Introduction

A review of the research and previous developments and contributions to the theory and analysis of sandwich plates is presented. Given the breath of the vast subject of elastic plates and the large amount of work that has been performed on subject of sandwich plates alone, the author concedes that his research cannot possibly include all of the work on the topic, but given this concession the sample of work used is adequate to give the reader a more than relevant background to understand the development and contribution of the work presented in this paper on the free vibration of rectangular sandwich plates.

1.1 Background

The classic theory of plates of plates (CPT) or the Poisson-Kirchoff theory of plates assumes normals to the mid-plane before deformation remain straight and normal to plane after deformation. The extension of the classic plate theory to the analysis of plates composed of layers of orthotropic plates which are treated as a single equivalent plate subject to the assumed deformation field of classic plate theory is known as the classic laminate plate theory (CLPT).

It is well known that the classic plate theory under predicts deflections and over predicts natural frequencies of vibration; this is directly attributed to the neglect of transverse shear strains in the classic plate theory. The movement to use advanced materials in a variety of applications (e.g. defense, aerospace, automotive and marine industries), in particular laminated (composite) plates which possess large elastic to shear modulus ratios (e.g. of the order 10^3 for sandwich plates, instead of 2.6 for a typical isotropic plate) has rendered classic theories inadequate and required the need for refined plate theories that incorporate the effects of transverse shear strains.

The analysis of composite plates has typically been performed by two methods: an equivalent single layer method, in which the specified displacement field is integrated over the entire thickness of the plate and a layerwise method where a displacement is integrated over the thickness of each layer (the displacement does not have to be identical for each layer) and a compatibility condition can is enforced between layers. The analysis of plates in particular composite plates is contingent not only to the assumed displacement field but also the application of that field whether it by an equivalent single layer of a layerwise application.

The improvements on the CPT have been made by incorporating transverse shear deformation. The first order shear deformation theory (FSDT) or Reisser-Mindlin plate theory [1, 2] assumes a displacement that is expanded in powers of the thickness and introduce shear deformation as well as rotary inertia effects but fail to satisfy the stress-free boundary conditions on the surface of the plate requiring shear correction factors.

The third order plate theory of Reddy (TSDT) [3] was developed to included the effects of shear deformation while satisfying the condition of vanishing stress on the free surfaces of the

plate. Many other higher order plate theories exist [4], but the TSDT presents equations of motion that are variationally consistent with the assumed displacement field and as stated the free surface conditions are satisfied. In addition the work on this theory and previous theories by Reddy is unparalleled and provided in [4] as well references to an extensive amount of previous and complimentary work on the theory and analysis of laminate plates. The TSDT is the minimum order expansion of the displacement in terms of the thickness coordinate to incorporate shear deformation and satisfy stress-free boundary conditions on the surface of the plate.

Given the overview of the immediate developments in plate theory we now turn our attention the subject of the analysis of sandwich plates, which can be view as a specialized subgroup of the general theory of elastic plates. A sandwich plate is a three layered plate composed of stiff face layers and a shear deformable core (i.e. the face layers are significantly stiffer than the core). The motivation for the use of sandwich plates is to introduce damping to materials have high stiffness to weight ratios (e.g. carbon-epoxy laminates), this is done by sandwiching a material with viscoelastic properties to dissipate energy (i.e. damping) between the stiff face layers.

Sandwich plates can generally be used in two ways: a sandwich plate with a thin core that has the sole purpose of dissipating energy while keeping the overall stiffness to weight ratio of the plate low, and a sandwich plate with a thick core that provides considerable damping but is usually applied in marine industries to greatly increase the buoyancy of the plate while still maintaining the high stiffness to weight ratio. In order to account for the energy dissipation of the viscoelastic core of sandwich plates transverse shear deformation must be considered in the theoretical model of the sandwich plate.

The pioneering work on sandwich plates can be attributed to Reissner [5], in which he considered a sandwich plate based on the assumption that the face layers are thin, stiff and heavy compared to the core. This type of theory is considered classic sandwich plate theory and can be characterized as a layerwise theory in which the face layers are modeled using classic plate theory and the core is subjected to transverse shear only as a result of the compatibility of the displacements at the interfaces between the core and the face layers.

The first fully unrestricted development of the classic sandwich plate theory and its extension to a sandwich plate with a viscoelastic core can be attributed to Rao and Nakra [6, 7] in which the assumed displacement field is developed directly from the assumptions of the classic sandwich plate theory and variational methods are used to derive the equations of motion and corresponding boundary conditions for rectangular sandwich plates. The theory known as the unsymmetric sandwich plate theory or USPT is novel in that it is variational consistent, includes rotary inertias of all layers and in only restricted with respect to the fact that it is developed for layers composed of isotropic material. This theory will be used as one of the two principle theories in this paper along with the TSDT.

However the USPT is suitable only for relatively thin cores and does not incorporate shear deformation in face layers which is not essential for isotropic material but must be considered for laminated plates which have large elastic stiffness to shear stiffness ratios. Advanced models of sandwich plates were formulated using the FSDT applied to each layer [8] and as an equivalent single layer [9].

Meunior and Shenoi [9-12] have developed the TSDT for the sandwich plate with a viscoelastic core using a single equivalent layer approach. They have obtained both analytical solutions for simply supported boundary conditions for free vibration as well as transient response in addition to various finite element solutions.

Sandwich plate theory development is closely related to developments in plate theory and both are driven by the need to accurately incorporate transverse shear strains.

1.2 Objective

This paper focuses on the free vibration of sandwich plates and the comparison of the USPT to the TSDT. The motivation for this paper is driven by the author's research on the theory of elastic plates, in particular his inability to find the limitations of the USPT with respect to core thickness in terms of natural frequency of vibration and damping predictions and his fruitless desire to find an analytical solution for the cantilever plate.

The true impetus for wanting to know the limitations for the USPT is a result of the requirement of the finite element package ANSYS that the core thickness be $5/6$ the total thickness of the plate to use an element based on classic sandwich plate theory. From the formulation of the USPT it is suspected that the USPT would only be valid for relatively thin cores and not suitable for the analysis of relatively thick cores. The first portion of results of this paper directly compares the USPT and TSDT with each other and FEA conducted in ANSYS to establish the performance and limitations of both theories with respect to geometric and material properties for the free vibration of simply supported boundary conditions.

The motivation for the second portion of this paper is due to the initial request of my thesis advisor Dr. Ghoneim to solve for the cantilever plate. This does not currently appear possible by conventional mathematics however the work of Gorman [13] solves for the free vibration of the cantilever plate modeled using CPT semi-analytically; obtaining a series solution that exactly satisfied the boundary conditions of the plate term by term. The creativity of this solution method is the inspiration for the second portion of this paper. A new method of solution for the free vibration of the cantilever sandwich plate based on the superposition method of Gorman is developed and presented for both the USPT and TSDT.

In short, the contribution of this paper is the comparison and analysis of the two competing methods of analysis for sandwich plates with viscoelastic cores and the introduction of a new method of solving for the free vibration of cantilever sandwich plates.

2 Basic Mechanics

2.1 Introduction

This section is an overview of some of underlining principles and tools involved in developing the theories of sandwich plates. Readers with experience in continuum mechanics and variational methods in applied mechanics can skip this section.

2.2 Conventions

In tensor analysis extensive use of indices is made. It is convenient to abbreviate a summation of terms by understanding that a repeated index means summation over all values of that index. Consider the component form of a vector $\mathbf{A}$

$$A = a_1 e_1 + a_2 e_2 + a_3 e_3$$

where (e_1, e_2, e_3) are basis vectors and (a_1, a_2, a_3) are constants, can be written as

$$A = \sum_{i=1}^{3} a_i e_i$$

However will introduce the summation convention and write the above equation as

$$A = a_i e_i$$

The repetition of an index in a term will simply denote a summation of the index over its range. The range of the index i in the case of $\mathbf{A}$ is from 1 to 3. An index that is summed over is called a dummy index and it is immaterial of what symbol is used; one that is not summed over is called a free index. Because we will be working in three dimensional Euclidian space the summation will be from 1 to 3 throughout this paper unless otherwise specified and the component forms are for rectangular Cartesian coordinate systems unless otherwise stated.

The following notation for differentiation will be used when possible for simplicity of notation, if the derivative of a function u is taken with respect to x a spatial variable we have $\frac{du}{dx}$ which can be represented as $u_{,x}$. All subscript variables following a comma will represent a partial derivative with respect to that spatial variable.

$$\frac{\partial \oplus}{\partial \otimes} = \oplus_{,\otimes}$$

The distinction is made for differentiation with respect to spatial variables because differentiation with respect to time t will be represented as

$$\frac{\partial \oplus}{\partial t} = \dot{\oplus}$$

At this time it is also important to introduce the special tensor known as the Kronecker delta defined as

$$\delta_{ij} = \begin{cases} = 0 & when \ i \neq j \\ = 1 & when \ i = j \end{cases} \tag{2.2.1}$$

These conventions and notations will be used extensively in this paper to simplify notation.

2.3 Deformation and Strain

We will adopt the continuum concept of matter, meaning that we will regard the material to be continuously distributed throughout its volume and to completely fill the space it occupies. In broader terms the individual behavior of a molecule is of no concern to us and only the behavior of the material as a whole is important. In the kinematics of continua a point will be considered a place in space and a particle is a small part of a material continuum. At any instant of time t, a continuum having a volume Ω and boundary surface Γ occupy a certain region R of physical space. The identification of particles of the continuum with the points of the space it occupies at time t by reference to a suitable set of coordinate axes species the configuration C of the continuum at that instant.

Deformation refers to a change in the shape of the continuum between some initially undeformed configuration C^0 and the deformed configuration. No attention is given to the intermediate configurations or the sequence of configurations; we are only concerned with the initial and final configurations.

In Figure 2.1 a material continuum at time $t = 0$ with the undeformed configuration C^0 is shown together with the deformed configuration C^t of the same continuum at time $t = t$. We will now superimpose the rectangular Cartesian coordinate systems $OX_1X_2X_3$ and $ox_1x_2x_3$ for the sake of simplicity.

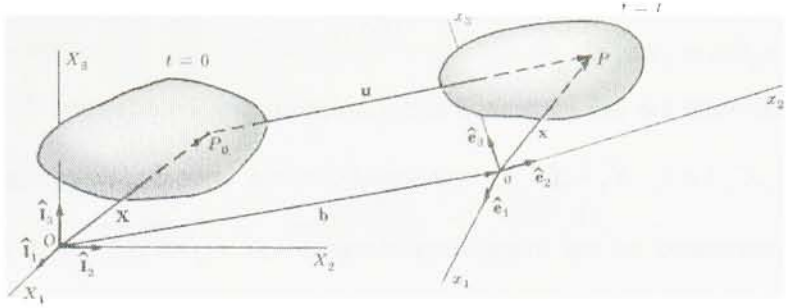

Figure 2.1

At the initial configuration a representative particle of the continuum occupies a point P_0 in space and has the position vector $\mathbf{X} = X_i e_i$, where e_i is the unit base vector along the X_i-direction. The particle originally at P_0 is now located at the point P in the deformed configuration with the position vector $\mathbf{x} = x_i e_i$, where e_i is the unit base vector along the x_i-direction. The displacement of the particle is now given by

$$\mathbf{u} = \mathbf{x} - \mathbf{X} \quad \text{or} \quad u_i = x_i - X_i \tag{2.3.1}$$

At this point it is worth noting that as a continuum undergoes deformation the particles of the continuum move along various paths in space, this motion can be expressed in two forms. The *Lagrangian* formulation

$$\mathbf{x} = \mathbf{x}(\mathbf{X}, t) \quad \text{or} \quad x_i = x_i(X_1, X_2, X_3, t) \tag{2.3.2}$$

which gives the present location x of the particle that occupied the point (X_1, X_2, X_3) at time $t = 0$. It is assumed that this mapping is one-to-one and continuous, with continuous partial derivatives to whatever order is desired. The *Eulerian* formulation

$$\mathbf{X} = \mathbf{X}(\mathbf{x}, t) \quad \text{or} \quad \mathrm{X_i} = X_i(x_1, x_2, x_3, t) \tag{2.3.3}$$

which gives the tracing of the particle to its undeformed position from the position it currently occupies. If mapping (2.3.3) is also one-to-one and continuous with continuous partial derivatives, like (2.3.2), then the two mappings are unique inverses of one another. The necessary and sufficient condition for the inverse functions to exist is that the Jacobian (2.3.4) does not equal zero.

$$J = \left| \frac{\partial x_i}{\partial X_j} \right| \neq 0 \tag{2.3.4}$$

Now consider the two particles p and q which occupy the positions $P_0(X_1, X_2, X_3)$ and $Q_0(X_1 + dX_1, X_2 + dX_2, X_3 + dX_3)$, respectively, in the undeformed configuration C^0. The particles are separated by the infinitesimal distance $dS = \sqrt{dX_i dX_i}$ and $d\mathbf{X}$ is the vector connecting the position of P_0 to Q_0. These two particles move to positions $P(x_1, x_2, x_3)$ and $Q(x_1 + dx_1, x_2 + dx_2, x_3 + dx_3)$, respectively, in the deformed configuration. The two particles are now separated by a distance $ds = \sqrt{dx_i dx_i}$ in C^t and $d\mathbf{x}$ is the vector connecting P to Q.

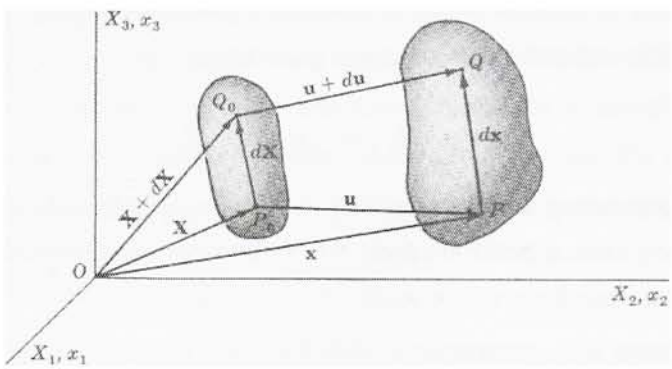

Figure 2.2

The deformation of a body is measured in terms of a strain tensor which is defined such that it gives the change of the square of the length of $d\mathbf{X}$. Since $\mathbf{x}$ is a function of $\mathbf{X}$ the total differential is given by using the chain rule of differentiation on (2.3.2)

$$dx_i = \frac{\partial x_i}{\partial X_i} dX_j$$

so the square of the length $ds = (d\mathbf{x})^2$ may be written

$$dx_i dx_i = \frac{\partial x_i}{\partial X_j} \frac{\partial x_i}{\partial X_k} dX_j dX_k$$

now the difference of the squares of the length is

$$ds^2 - dS^2 = \frac{\partial x_i}{\partial X_j}\frac{\partial x_i}{\partial X_k} dX_j dX_k - dX_k dX_k \quad \text{but} \quad \delta_{jk} dX_j dX_k = dX_k dX_k$$

so finally we have

$$ds^2 - dS^2 = \left(\frac{\partial x_i}{\partial X_j}\frac{\partial x_i}{\partial X_k} - \delta_{jk} \right) dX_j dX_k$$

where we define the *Lagrangian* (or Green's) *finite strain tensor*

$$E_{jk} = \frac{1}{2}\left(\frac{\partial x_i}{\partial X_j}\frac{\partial x_i}{\partial X_k} - \delta_{jk} \right) \quad \text{so that} \quad ds^2 - dS^2 = 2E_{jk} dX_j dX_k \tag{2.3.5}$$

similarly we define the *Eulerian* (or Almansi's) *finite strain tensor*

$$e_{jk} = \frac{1}{2}\left(\frac{\partial X_i}{\partial x_j}\frac{\partial X_i}{\partial x_k} - \delta_{jk} \right) \quad \text{so that} \quad ds^2 - dS^2 = 2e_{jk} dx_j dx_k \tag{2.3.6}$$

The tensors E_{jk} and e_{jk} are symmetric and are defined in the coordinate systems X_i and x_i, respectively. These tensors describe the strain at a point in the continuum at a time t, and are called the finite strain components because no assumption concerning the smallness compared to unity of the strains is made.

In order to express the strains in terms of the displacements we use (2.3.1) to write

$$\frac{\partial x_i}{\partial X_j} = \frac{\partial u_i}{\partial X_j} + \delta_{ij}$$

then the Largrangian strain tensor reduces to the simple form

$$\begin{aligned} E_{jk} &= \frac{1}{2}\left[\left(\frac{\partial u_i}{\partial X_j} + \delta_{ij} \right)\left(\frac{\partial u_i}{\partial X_k} + \delta_{ik} \right) - \delta_{jk} \right] \\ &= \frac{1}{2}\left[\frac{\partial u_i}{\partial X_j}\frac{\partial u_i}{\partial X_k} + \delta_{ij}\delta_{ik} + \frac{\partial u_i}{\partial X_j}\delta_{ik} + \frac{\partial u_i}{\partial X_k}\delta_{ij} - \delta_{jk} \right] \\ &= \frac{1}{2}\left[\frac{\partial u_k}{\partial X_j} + \frac{\partial u_j}{\partial X_k} + \frac{\partial u_i}{\partial X_j}\frac{\partial u_i}{\partial X_k} \right] \end{aligned} \tag{2.3.7}$$

similarly the Eulerian strain tensor can we expressed in terms of the displacements in the form

$$e_{jk} = \frac{1}{2}\left[\frac{\partial u_k}{\partial x_j} + \frac{\partial u_j}{\partial x_k} - \frac{\partial u_i}{\partial x_j}\frac{\partial u_i}{\partial x_k}\right] \tag{2.3.8}$$

If the components of the displacement u_i are small and such that the displacement gradient components are small compared to unity the product terms are negligible and the strain tensors reduce to Cauchy's *infinitesimal strain tensor*

$$\varepsilon_{jk} = \frac{1}{2}\left(\frac{\partial u_k}{\partial x_j} + \frac{\partial u_j}{\partial x_k}\right) \tag{2.3.9}$$

and the distinction between the Lagrangian and Eulerian strain tensor vanishes, since it is immaterial whether the displacement gradients are calculated at the position of a point before or after deformation.

For the remainder of this paper we will be using the infinitesimal strain tensor because we will be dealing small displacements, but it is worth noting that for large deformations the Lagrangian strain tensor should be used to reference back to the originally un-deformed configuration of the continuum being studied. In the special case for plates of small displacements but moderate rotations (i.e. $10^\circ - 15^\circ$) then the *von Kármám strains* [1] should be used.

2.4 Stress Tensor

The stress at a point in a continuum can also be expressed as a tensor similar to the strain tensor. Stress at a point is defined as the measure of force per unit area, the force $\Delta\mathbf{F}$ acting on an area element ΔA of the deformed continuum is called the *stress vector* $\mathbf{T}$. This vector depends on the force vector (magnitude and direction) and the area it acts on, which is dependent on the orientation of the plane defining the surface with respect to the coordinates of the deformed body. It is assumed that as ΔA goes to zero, the ratio of $\Delta\mathbf{F}/\Delta A$ goes to a definite limit $d\mathbf{F}/dA$ and that the moment of the forces acting on the surface dA about any point within the area vanish in the limit. The limiting vector is defined as the stress vector $\overset{\hat{\mathbf{n}}}{\mathbf{T}}$, where $\hat{\mathbf{n}}$ is the normal of the plane acted on by the stress vector.

The state of stress at a at a point P inside a deformed continuum can be expressed in terms of stress vectors on three mutually orthogonal planes, which can be taken to be perpendicular to the rectangular coordinate system $ox_1x_2x_3$. Let $\overset{i}{\mathbf{T}}$ define the stress vector at P on the plane perpendicular to the x_i-axis which has the corresponding unit outer normal

vector $\hat{\mathbf{n}}^{(i)}$ as show in Figure 2.3. The vectors $\overset{i}{\mathbf{T}}$ $(i=1,2,3)$ can be defined in terms of components in the coordinate system

$$\overset{i}{\mathbf{T}} = \sigma_{ij} e_j \tag{2.4.1}$$

where σ_{ij} are components of the stress vector $\overset{i}{\mathbf{T}}$ at P along the x_j-direction, and e_i is the unit base vector along the x_j-direction. There are nine stress components σ_{ij}, $(i,j=1,2,3)$ and they can be represented by the square matrix

$$\sigma = \begin{bmatrix} \sigma_{11} & \sigma_{12} & \sigma_{13} \\ \sigma_{21} & \sigma_{22} & \sigma_{23} \\ \sigma_{31} & \sigma_{32} & \sigma_{33} \end{bmatrix} \tag{2.4.2}$$

which can be represented graphically on the dimensionless point cube in Figure 2.3.

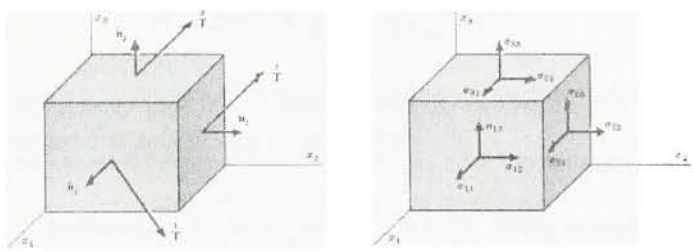

Figure 2.3

If the stress components σ_{ij} are know it can be show (Newton's second law of motion) that the stress vector $\overset{k}{\mathbf{T}}$ acting on *any* surface with the unit outer normal vector $\hat{\mathbf{n}}^{(k)}$ is given by

$$\overset{k}{\mathbf{T}}_i = \hat{\mathbf{n}}_j^{(k)} \sigma_{ij} \tag{2.4.3}$$

where it is understood that $\overset{k}{\mathbf{T}}_i$ are the components of the stress vector on the surface defined by the unit outer normal vector $\hat{\mathbf{n}}^{(k)}$, this relation is know as *Cauchy's formula*. This formula assures us that the stress components σ_{ij} are necessary and sufficient to define the stress

vector on any surface in the continuum. Therefore the state of stress in the continuum is defined by σ_{ij}.

From Cauchy's formula it also follows that σ_{ij} is a tensor, and it is known as *Cauchy stress tensor*. It can be shown (i.e. equilibrium equations) that in the absence of distributed external moments the *stress tensor is symmetric*, as will be the case in our analysis.

The stress components σ_{ij} are measured in the deformed configuration C^t and refer to the deformed coordinate system (Eulerian) in the deformed body. This is a suitable strain tensor to use with the infinitesimal strain tensor ε_{ij}. If the finite deformation is being considered and the Lagrangian strain tensor is being used then the Piola-Kirchhoff stress tensor should be used. It is measured in the deformed body but refers to the material coordinates (Lagrangian). For small deformation the difference between the two measures of stress disappears.

2.5 Constitutive Equations

Having defined the stress and strain tensors the generalized Hooke's law is introduced in the form of

$$\sigma_{ij} = C_{ijkl}\varepsilon_{kl} \quad (i,j,k,l = 1,2,3) \tag{2.5.1}$$

where C_{ijkl} are the elastic coefficients of the material of the continuum and as previously stated ε_{ij} is the infinitesimal strain tensor and σ_{ij} is the Cauchy stress tensor. In general C_{ijkl} has 81 material coefficients, however given $\varepsilon_{kl} = \varepsilon_{lk}$ and $\sigma_{ij} = \sigma_{ji}$ it follows that

$$C_{ijkl} = C_{ijlk} \qquad C_{ijkl} = C_{jikl} \tag{2.5.2}$$

and without any loss in generality there are only 36 independent elastic material coefficients. For a linear elastic material it is assumed that material behavior is isothermal (i.e. the continuum after forces causing deformation are removed goes from C^t to C^0 under isothermal conditions) and their exists a quadratic strain energy function W,

$$W = \frac{1}{2} C_{ijkl}\varepsilon_{ij}\varepsilon_{kl} \tag{2.5.3}$$

with the property

$$\frac{\partial W}{\partial \varepsilon_{ij}} = \sigma_{ij}$$

resulting in a linear relationship between stress and strain for which the *principle of superposition* is valid, this will be important later. Given the symmetry of (2.5.3) as a result of the symmetry of infinitesimal strain tensor it follows that

$$C_{ijkl} = C_{klij} \tag{2.5.4}$$

and the number of independent elastic material coefficients can be reduced to 21.

We will now introduce the *contracted notation* which utilizes single index notation for the stress and strain, and a double index for the elastic material coefficients. The contracted notation is defined as follows

Index Contraction	Stress Contraction	Strain Contraction
$11 \to 1$	$\sigma_{11} \to \sigma_1$	$\varepsilon_{11} \to \varepsilon_1$
$22 \to 2$	$\sigma_{22} \to \sigma_2$	$\varepsilon_{22} \to \varepsilon_2$
$33 \to 3$	$\sigma_{33} \to \sigma_3$	$\varepsilon_{33} \to \varepsilon_3$
$23 \to 4$	$\sigma_{23} \to \sigma_4$	$\varepsilon_{23} \to 2\varepsilon_4$
$13 \to 5$	$\sigma_{13} \to \sigma_5$	$\varepsilon_{13} \to 2\varepsilon_5$
$12 \to 6$	$\sigma_{12} \to \sigma_6$	$\varepsilon_{12} \to 2\varepsilon_6$

(2.5.5)

and this results in the generalized Hooke's Law in the form

$$\sigma_i = C_{ij}\varepsilon_j \quad (i, j = 1,2,3,4,5,6). \tag{2.5.6}$$

In addition to index contraction it is important to note that the strains in (2.5.5) that are not normal to the x_i-direction (i.e. shear strains) are multiplied by a factor of 2, these strains are commonly knows as *engineering shear strains*, the reason for the factor will become apparent when the general virtual energy statements for a continuum are developed. Having established the general Hooke's Law for a linear elastic material in contracted notation for a continuum, further simplifications of the elastic coefficients C_{ij} will depend on the properties of the material that makes up the continuum.

When the elastic coefficients at a point remain unchanged for every pair of coordinate systems which are mirror images of each other in a plane then the plane is called a *plane of material symmetry*. The elastic coefficients are invariant after a coordinate transformation to a mirror image coordinate system in a plane of material symmetry providing a relationship between elastic coefficients reducing the number of independent coefficients.

2.5.1 Orthotropic Material

When three mutually orthogonal planes of material symmetry exist the material is called *orthotropic* and the number of independent elastic material coefficients reduces to 9. The stress-strain relationship for an orthotropic material is given by

$$\begin{Bmatrix} \sigma_1 \\ \sigma_2 \\ \sigma_3 \\ \sigma_4 \\ \sigma_5 \\ \sigma_6 \end{Bmatrix} = \begin{bmatrix} C_{11} & C_{12} & C_{13} & 0 & 0 & 0 \\ C_{12} & C_{22} & C_{23} & 0 & 0 & 0 \\ C_{13} & C_{23} & C_{33} & 0 & 0 & 0 \\ 0 & 0 & 0 & C_{44} & 0 & 0 \\ 0 & 0 & 0 & 0 & C_{55} & 0 \\ 0 & 0 & 0 & 0 & 0 & C_{66} \end{bmatrix} \begin{Bmatrix} \varepsilon_1 \\ \varepsilon_2 \\ \varepsilon_3 \\ \varepsilon_4 \\ \varepsilon_5 \\ \varepsilon_6 \end{Bmatrix} \tag{2.5.7}$$

where the coordinate system used is with respect to the planes of material symmetries and they will in general differ from the coordinates used later in the elastic material coefficient transformations between the material coordinates and the plate coordinates (see **2.5.3**).

Plates and layers of sandwich (or more generally laminated) plates are thin and are assumed to experience a state of *plane stress*. A state of plane stress is one in which the transverse stresses are considered negligible. Both plate theories used for analysis assume that the transverse normal strain is zero which results in the transverse normal stress not appearing in the virtual strain energy statement (see **2.7**) and although it is not identically zero it is neglected. Therefore it is safe to make the reduction of the general elastic material constants to the *plane stress reduced stiffnesses*. The reduction based on the fact that the transverse normal stress is negligible and therefore zero, but the transverse shear strains are included because they are the motivation for the TSDT, and they also occur in the core layer of the USPT. The plane stress reduced stiffness stress-strain relation for an orthotropic material in terms of the engineering constants is

$$\begin{Bmatrix} \bar{\sigma}_1 \\ \bar{\sigma}_2 \\ \bar{\sigma}_6 \\ \bar{\sigma}_4 \\ \bar{\sigma}_5 \end{Bmatrix} = \begin{bmatrix} \bar{Q}_{11} & \bar{Q}_{12} & 0 & 0 & 0 \\ \bar{Q}_{12} & \bar{Q}_{22} & 0 & 0 & 0 \\ 0 & 0 & \bar{Q}_{66} & 0 & 0 \\ 0 & 0 & 0 & \bar{Q}_{44} & 0 \\ 0 & 0 & 0 & 0 & \bar{Q}_{55} \end{bmatrix} \begin{Bmatrix} \bar{\varepsilon}_1 \\ \bar{\varepsilon}_2 \\ \bar{\varepsilon}_6 \\ \bar{\varepsilon}_4 \\ \bar{\varepsilon}_5 \end{Bmatrix}$$

$$\bar{Q}_{11} = \frac{E_1}{1-\nu_{12}\nu_{21}} \qquad \bar{Q}_{12} = \frac{\nu_{12}E_2}{1-\nu_{12}\nu_{21}} \qquad \bar{Q}_{22} = \frac{E_2}{1-\nu_{12}\nu_{21}} \tag{2.5.8}$$

$$\bar{Q}_{66} = G_{12} \qquad \bar{Q}_{44} = G_{23} \qquad \bar{Q}_{55} = G_{13}$$

with the reciprocal relation

$$\frac{\nu_{ij}}{E_i} = \frac{\nu_{ji}}{E_j} \quad (\text{no sum on } i, j) \tag{2.5.9}$$

where the bar denotes that the coordinate system is the material coordinate system $(\overline{x}_1, \overline{x}_2, \overline{x}_3) = (\overline{x}, \overline{y}, \overline{z})$ and E_i is modulus of elasticity (Young's modulus) in the material direction i, G_{ij} is the shear modulus between the i and j material directions and ν_{ij} is Poisson's Ratio defined as the ratio of the extension strain of the material direction j over the extension strain of the material direction i. The material coordinates refer to the principal material directions in which for fiber reinforced materials the fibers direction is parallel to the $\overline{x}_1$-axis. The reader should again note that the subscripts on the engineering constants refer material coordinates and not the layer number of the plate, which is the notation used in Chapter 3 for the USPT as a matter of convenience.

2.5.2 Isotropic Material

When an infinite number of planes of material symmetry exist (i.e. there is no preferred directions in the material) the material is called *isotropic* and the number of independent material constants is 2. The stress-strain relationship of the general isotropic material takes the same form as (2.5.7) where the coordinate system is arbitrary due to the infinite planes of material symmetry. The plane stress reduced stiffness stress-strain relation for an isotropic material in terms of the engineering constants is

$$\begin{Bmatrix} \overline{\sigma}_1 \\ \overline{\sigma}_2 \\ \overline{\sigma}_6 \\ \overline{\sigma}_4 \\ \overline{\sigma}_5 \end{Bmatrix} = \begin{bmatrix} \overline{Q}_{11} & \overline{Q}_{12} & 0 & 0 & 0 \\ \overline{Q}_{12} & \overline{Q}_{22} & 0 & 0 & 0 \\ 0 & 0 & \overline{Q}_{66} & 0 & 0 \\ 0 & 0 & 0 & \overline{Q}_{44} & 0 \\ 0 & 0 & 0 & 0 & \overline{Q}_{55} \end{bmatrix} \begin{Bmatrix} \overline{\varepsilon}_1 \\ \overline{\varepsilon}_2 \\ \overline{\varepsilon}_6 \\ \overline{\varepsilon}_4 \\ \overline{\varepsilon}_5 \end{Bmatrix}$$

$$\begin{aligned} &\overline{Q}_{11} = \overline{Q}_{22} = \frac{E}{1-\nu^2} \quad \overline{Q}_{12} = \nu \overline{Q}_{11} \\ &\overline{Q}_{66} = \overline{Q}_{44} = \overline{Q}_{55} = G \end{aligned} \tag{2.5.10}$$

with

$$G = \frac{E}{2(1+\nu)} \tag{2.5.11}$$

where the bar once again denotes the material coordinates but as stated earlier the coordinate system is arbitrary for an isotropic material so the stress strain relationship is identical for the material and plate coordinate systems.

2.5.3 Transformation of Elastic Material Coefficients

In the formulation of the theories of sandwich plates (or laminated plates) all of the variables and coefficients of the governing equations must be described in the same coordinate system. The rectangular Cartesian coordinate system that is used for the problem formulation is the plate coordinates defined as $(x_1, x_2, x_3) = (x, y, z)$. Therefore it is necessary that the elastic material coefficients be transformed from the material coordinates to the plate coordinates.

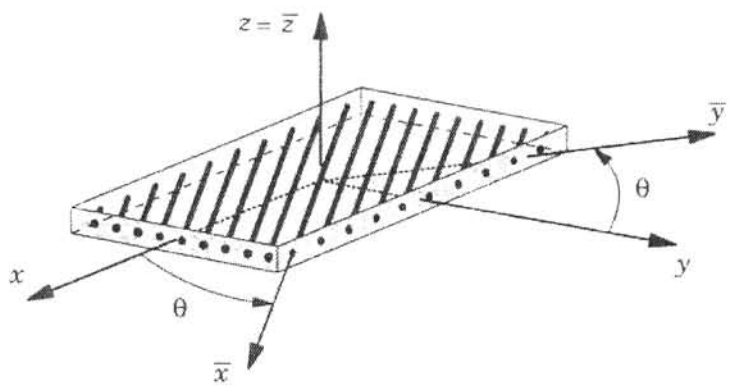

Figure 2.4

Given the laminate configuration in Figure 2.4, the transformation matrix from material coordinates to the plate coordinates for the reduced notation, plane stress reduced elastic material coefficients (reduced plate stiffnesses) of an orthotropic material (2.5.8) is easily show to be

$$[T] = \begin{bmatrix} c^2 & s^2 & cs & 0 & 0 \\ s^2 & c^2 & -cs & 0 & 0 \\ -2cs & 2cs & c^2 - s^2 & 0 & 0 \\ 0 & 0 & 0 & c & s \\ 0 & 0 & 0 & -s & c \end{bmatrix} \tag{2.5.12}$$

such that

$$Q_{ij} = T_{ik}\bar{Q}_{kj} \quad (k = 1,2,6,4,5) \tag{2.5.13}$$

where $c = \cos\theta$ and $s = \sin\theta$, where θ is measured from the x-axis of the plate coordinates positive counterclockwise to the $\bar{x}$-axis of the material coordinates as shown in Figure 2.4. So we now have the following stress-strain relations

Material Coordinates $(\bar{x}_1, \bar{x}_2, \bar{x}_3) = (\bar{x}, \bar{y}, \bar{z})$ Plate Coordinates $(x_1, x_2, x_3) = (x, y, z)$

$$\bar{\sigma}_i = \bar{Q}_{ij}\bar{\varepsilon}_j \quad (i, j = 1,2,6,4,5) \qquad \sigma_i = Q_{ij}\varepsilon_j \quad (i, j = 1,2,6,4,5)$$

$$Q_{ij} = T_{ik}\bar{Q}_{kj} \quad (k = 1,2,6,4,5)$$

with the understanding that the transverse normal stress and strain are considered negligible and in the contracted notation the place of the transverse normal strain and stress have been replaced in *position of appearance only* in the stress and strain vectors by the in-plane shear strains. This at first may seem unnecessary and confusing but it becomes convenient when computer programs are created and numerical results are computed.

2.6 *Linear Viscoelasticity*

An elastic material exhibits the capacity to store mechanical energy but has none for dissipating energy. An elastic material subjected to a suddenly applied load (i.e. loading state with rates that do not cause a dynamic response) that is held constant responds instantaneously with a deformation that remains constant. A material with the ability to dissipate energy and store mechanical energy while having deformation that does not respond instantaneously to a constant state, or is time dependent can be characterized as a viscoelastic material. A viscoelastic material has a stress-strain relation that depends on all previous states of stress experienced by the material with respect to time, that is the response of the material is not only determined by the current state of stress but by all previous states. It is shown in [2] that these properties can be expressed by the following stress-strain relation for a linear isothermal viscoelastic solid

$$\sigma_{ij}(t) = \int_{-\infty}^{t} C_{ijkl}(t-\tau)\frac{d\varepsilon_{kl}}{d\tau}d\tau$$

or in contracted form

$$\sigma_k(t) = \int_{-\infty}^{t} C_{kl}(t-\tau)\frac{d\varepsilon_l}{d\tau}d\tau \tag{2.6.1}$$

For a material subject to steady state harmonic motion, as is the case for free vibration (2.6.1) can be represented in complex form as a function of the frequency of vibration, not time. We first represent the harmonic strain as

$$\varepsilon_l(t) = \varepsilon_l^0 e^{i\omega t} \tag{2.6.2}$$

where $i = \sqrt{-1}$, ε_l^0 is the amplitude and ω is the frequency of vibration. Substituting (2.6.2) into (2.6.1) with the change of variables $\varsigma = t - \tau$ results in

$$\sigma_k(t) = -i\omega\varepsilon_l^0 e^{i\omega t}\int_{-\infty}^{t} C_{kl}(\varsigma)e^{-i\omega\varsigma}d\varsigma \tag{2.6.3}$$

and for steady state motion it is assumed that all transient behavior dies out after sufficient time and this can be taken at $t=\infty$ for the upper bound of the integral in (2.6.3) and the integral term can now be recognized as the complex Fourier transform of the elastic coefficients C_{kl} represented as

$$\hat{C}_{kl}(\omega) = \int_{-\infty}^{\infty} C_{kl}(\varsigma)e^{-i\omega\varsigma}d\varsigma \tag{2.6.4}$$

with the inverse

$$C_{kl}(\varsigma) = \frac{1}{2\pi}\int_{-\infty}^{\infty} \hat{C}_{kl}(\omega)e^{i\omega\varsigma}d\omega$$

Taking the frequency dependent form of the elastic coefficients and recognizing that the coefficient of the integral in (2.6.3) contains the harmonic strain, the stress-strain relation can be expressed as

$$\sigma_k(t) = C_{kl}^*(\omega)\varepsilon_l(t) \tag{2.6.5}$$

where $C_{kl}^*(\omega) = -i\omega\hat{C}_{kl}(\omega)$ are the complex elastic coefficients, and can be represented as

$$\sigma_k(t) = \left\{C_{kl}^{'}(\omega) + iC_{kl}^{"}(\omega)\right\}\varepsilon_l(t)$$

where $C_{kl}^{'}(\omega)$ is called the storage modulus and $C_{kl}^{"}(\omega)$ is referred to as the loss modulus. A form of representation with significance in physically interpreting the behavior between the stress and the strain comes from the understanding that the response to a harmonic strain applied to a linear viscoelastic continuum at steady state will oscillate harmonically but differ from the strain by a phase lag θ, therefore the stress can be represented as

$$\sigma_k(t) = \sigma_k^0 e^{i(\omega t+\theta)} \tag{2.6.6}$$

taking (2.6.2) we have

$$\frac{\sigma_k(t)}{\varepsilon_l(t)} = \frac{\sigma_k^0}{\varepsilon_l^0}e^{i\theta}$$

writing (2.6.5) in polar form and comparing to (2.6.6) we have

$$\frac{\sigma_k^0}{\varepsilon_l^0} = \left| C_{ij}^*(\omega) \right| \quad \text{and} \quad \tan\theta = \frac{\mathrm{Re}\left[C_{ij}^*(\omega) \right]}{\mathrm{Im}\left[C_{ij}^*(\omega) \right]} = \frac{C_{ij}^{'}(\omega)}{C_{ij}^{''}(\omega)}$$

and finally we have the form of the stress strain relation we will use

$$\sigma_k(t) = C_{ij}^{'}(\omega)(1+\eta i) \tag{2.6.7}$$

where η is the loss factor and is the tangent of the phase lag between the harmonic stress and strain at steady state applied to a linear viscoelastic continuum and $C_{ij}^{'}(\omega)$ is the real part of the frequency dependent elastic coefficients.

The *linear elastic-viscoelastic principle* states that for and elastic solid subjected to steady state harmonic motion (e.g. free vibration) the material coefficients of the corresponding linear viscoelastic solid can be obtained by adding a imaginary part of the real material coefficients that consists of the real coefficients times a loss factor, over a region where the material coefficients can be assumed to be constant with respect to frequency.

$$C_{ij} \rightarrow C_{ij}(1+\eta i)$$

We will make use of this principle to introduce damping in the core of the sandwich plate during for free vibration analysis.

2.7 Hamilton's Principle for a Continuum

The form of the laws of physics can take several forms in continuum mechanics; in particular for a solid continuum both energy principles and Newton's laws can be used to determine the governing equations of the continuum. The use of Newton's laws requires a free body diagram of a typical volume element; difficulty occurs for complicated systems and the appropriate boundary conditions that are to be used with the derived equations become unclear. The alternative variational methods are used to form integral statements that contain the governing equations and associated boundary conditions of the continuum. We will make use of the dynamic form of the principle of virtual displacements, Hamilton's principle to derive the equations of motion and associated boundary conditions of sandwich plates.

A continuum can take on many possible geometric configurations that are consistent with the geometric constraints of the continuum, but of all of the possible configurations only one satisfies the principle of conservation of linear momentum. This is the actual configuration of the continuum, the set of all other configurations that satisfy the geometric constraints of the continuum but do not satisfy Newton's second law $(\mathbf{F} = m\mathbf{a})$ is the *set of admissible configurations*. A system undergoes a *virtual displacement* if the true configuration is infinitesimally varied to an admissible configuration without violating geometric constraints of the

system while all the forces acting on the continuum remain at their fixed values. Therefore the virtual displacements at the boundary of the continuum at which the displacements (or geometry) are specified are necessarily zero.

The work done by an actual force $\mathbf{F}$ moving through a virtual displacement $\delta\mathbf{u}$ is called the *virtual work* given by

$$\delta W = \int_{\Omega_0} F_i \delta u_j \delta_{ij} \, d\Omega \tag{2.7.1}$$

where the reader is reminded δ_{ij} is the Kronecker delta defined by (2.2.1).

Forces acting on a continuum cause deformation, the forces acting on the continuum at a point are measured in terms of Cauchy's stress tensor σ_{ij} and the deformation is provided by the infinitesimal strain tensor ε_{ij}. The work done by particles in the continuum subjected to a stress field moving through the deformation of the strain field is called *internal work*. The internal virtual work can be computed by taking an infinitesimal volume element $d\Omega = dx_1 dx_2 dx_3$ that experiences virtual strains $\delta\varepsilon_{ij}$ due to the virtual displacements δu_i. The work done by the force due to the actual stress σ_{11} moving through its corresponding virtual displacement $\delta u_{11} = \delta\varepsilon_{11} dx_1$ is

$$\sigma_{11} dx_2 dx_3 \cdot \delta\varepsilon_{11} dx_1 = \sigma_{11} \delta\varepsilon_{11} d\Omega$$

A similar analysis can be conducted for the remaining components of σ_{ij} and its corresponding displacement $\delta u_i = \delta\varepsilon_{ij} dx_i$ which results in $dW = \sigma_{ij}\delta\varepsilon_{ij} d\Omega$, if this expression is integrated over the volume of the continuum we have an expression for the total internal virtual work of the continuum or the *virtual strain energy* given by

$$\delta U = \int_{\Omega_0} \sigma_{ij} \delta\varepsilon_{ij} \, d\Omega \tag{2.7.2}$$

which can be expressed in contracted notation as

$$\delta U = \int_{\Omega_0} \sigma_i \delta\varepsilon_i \, d\Omega \tag{2.7.3}$$

where the doubling of the shear strains in the contracted notation given by (2.5.5) and symmetry of both σ_{ij} and ε_{ij} make both statements of the virtual strain energy equivalent.

In moving through the virtual displacement $\delta\mathbf{u}$ work is also done by the inertia force $m\mathbf{a}$ as well as the work done by the internal forces stored in the body. The inertia force acting on an infinitesimal volume element $d\Omega = dx_1 dx_2 dx_3$ can be expressed as $\rho\ddot{u}_i \delta u_i d\Omega$, if this expression is integrated over the volume of the continuum we have an expression for the total virtual work done by the inertia force or the *virtual kinetic energy* given by

$$\delta K = \int_{\Omega_0} \rho \frac{\partial^2 u_i}{\partial t^2} \delta u_i \, d\Omega \tag{2.7.4}$$

where ρ is the mass density and it can be a function of position.

With expressions for the virtual kinetic and virtual strain energy of a deformable continuum we can now develop Hamilton's principle. This paper will only consider the free vibration of sandwich plates for various boundary conditions therefore the statements for the virtual work done by applied surface tractions and body forces will not be considered and consequently they will not appear in the statement of Hamilton's principle.

If the actual path $\mathbf{u} = \mathbf{u}(\mathbf{x}, t)$ of a particle at a point P_0 in the undeformed configuration C^0 to P in the deformed configuration C^t is varied consistent with the kinematic boundary conditions to $\mathbf{u} + \delta\mathbf{u}$, where $\delta\mathbf{u}$ is the admissible variation of the path, the varied path differs from the actual path except at the initial time $t_1 = 0$ and the final time $t_2 = t$, then the admissible variation $\delta\mathbf{u}$ satisfies the conditions

$$\delta\mathbf{u} = 0 \text{ on } \Gamma \text{ for all } t$$

$$\delta\mathbf{u}(\mathbf{x}, t_1) = \delta\mathbf{u}(\mathbf{x}, t_2) = 0 \text{ for all } \mathbf{x} \tag{2.7.5}$$

where Γ is the boundary of the continuum where the displacement $\mathbf{u}$ is specified, for the case of free vibration this corresponds to the entire boundary of the continuum. The total virtual work done by all forces acting on the continuum both internal and external while moving through the admissible variation $\delta\mathbf{u}$ is given by

$$\delta W = \delta K - \delta U \tag{2.7.6}$$

where δU is the virtual work done by internal forces in the body (i.e. work done by the continuum) hence it is negative.

Hamilton's principle states that of all the paths of admissible configurations $\mathbf{u} + \delta\mathbf{u}$ that the continuum can take as it goes from the initial configuration C^0 at time $t_1 = 0$ to the final

configuration C' at time $t_2 = t$ the path that satisfies Newton's second law at each instant during the interval and is therefore the actual path is the path for which the total virtual work of all the actual forces acting on the continuum in moving through the admissible variation $\delta\mathbf{u}$ is zero. Hamilton's principle for the free vibration of a continuum is then given by

$$\int_{t_1}^{t_2}(\delta K - \delta U)\,dt = 0 \tag{2.7.7}$$

where δK is the virtual kinetic energy given by (2.7.4) and δU is the virtual strain energy given by (2.7.3).

In order to obtain the differential equations of motion and the corresponding boundary conditions from the integral statement in (2.7.7) we will make use of the *fundamental lemma of calculus of variations*. The lemma can be stated as follows: If $\varphi(x)$ is an arbitrary, continuous function for all x in (a,b) then the statement

$$\int_a^b I(x)\varphi(x)\,dx = 0 \tag{2.7.8}$$

then it follows that $I(x) = 0$ in (a,b).

With the lemma and Hamilton's principle stated in terms of the virtual displacements the variationally consistent governing equations and corresponding boundary conditions for the free vibration of sandwich plates can be derived from the assumed displacement fields.

3 Theory of Unsymmetrical Sandwich Plate Theory

3.1 Introduction

The unsymmetrical sandwich plate theory, USPT is an extension of the well known sandwich beam theory and consists of two face layers modeled with classic plate theory and a core in a state of pure shear derived from enforcing the continuity of displacements at the interfaces of the core and face layers. The first full development of the theory that is not restricted with respect to the use of the classic plate theory and the thickness of the layers with respect to themselves was done by Rao and Nakra. [1], and the corresponding extension to a sandwich plate with a viscoelastic core is made in [2].

This chapter covers the derivation of the equations of motion, the solutions of the simply supported plate and the derivation of the uncoupled and non-dimensional forms of the equations of motion.

3.2 Displacement Field

The plate geometry in Figure 3.1 shows the plate in a state of positive bending and extension with respect to the rectangular Cartesian coordinate system $oxyz$. The assumptions of the USPT are:

1. Normals to the mid-plane of each layer plane before bending remain normal after bending
2. Transverse displacement of a layer is invariant with respect to the thickness
3. There is perfect continuity at all interfaces and no slip between layers occurs during deformation
4. Extension effects in the core are neglected and all stresses with exception to transverse shear are considered negligible in the core

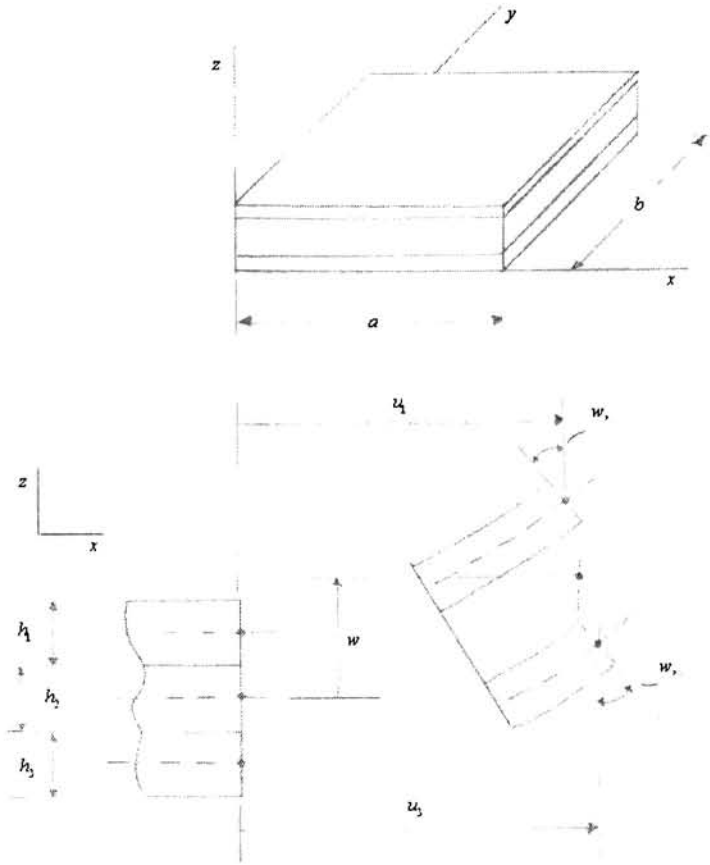

Figure 3.1

The displacements of the face layers are defined as follows, where the first subscript defines the direction, the second subscript defines the layer and z is measured from the mid-plane of each layer

$$u_{11}(x,y,t) = u_1(x,y,t) - z\frac{w(x,y,t)}{\partial x} \qquad u_{21}(x,y,t) = v_1(x,y,t) - z\frac{w(x,y,t)}{\partial y}$$

$$u_{13}(x,y,t) = u_3(x,y,t) - z\frac{w(x,y,t)}{\partial x} \qquad u_{23}(x,y,t) = v_3(x,y,t) - z\frac{w(x,y,t)}{\partial y} \qquad (3.2.1)$$

$$u_{31}(x,y,t) = w(x,y,t) \qquad u_{33}(x,y,t) = w(x,y,t)$$

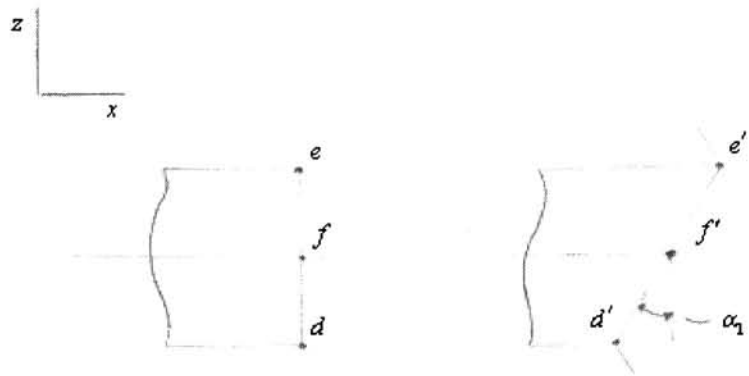

Figure 3.2

Examining Figure 3.2, which shows the displacement of the core in the $x-z$ plane, the displacements of the deformed state are obtained from (3.2.1) by enforcing the continuity of the of the displacements at the interfaces of the core and the face layers, and are given by

$$
\begin{aligned}
e' &= u_1 + \frac{h_1}{2} w_{,x} \\
d' &= u_3 - \frac{h_3}{2} w_{,x} \\
f' &= \frac{(e'+d')}{2} = \frac{1}{2}\left[u_1 + u_3 + w_{,x}\left(\frac{h_1 - h_3}{2} \right) \right] \\
\alpha_1 &= \frac{(e'-d')}{h_2} = \frac{1}{h_2}\left[u_1 - u_3 + w_{,x}\left(\frac{h_1 + h_3}{2} \right) \right]
\end{aligned}
$$

From this the displacement in the core is defined in the x direction as $u_{12} = f' + \alpha_1 z = u_2 + \alpha_1 z$ and a similar analysis is done to define the core displacement in the y direction. The resulting displacements in the core are

$$
\begin{aligned}
u_{12} &= u_2 + \alpha_1 z & \qquad u_{22} &= v_2 + \alpha_2 z \\
u_2 &= \frac{1}{2}\left[u_1 + u_3 + w_{,x}\left(\frac{h_1 - h_3}{2} \right) \right] & \qquad v_2 &= \frac{1}{2}\left[v_1 + v_3 + w_{,y}\left(\frac{h_1 - h_3}{2} \right) \right] \\
\alpha_1 &= \frac{1}{h_2}\left[u_1 - u_3 + w_{,x}\left(\frac{h_1 + h_3}{2} \right) \right] & \qquad \alpha_2 &= \frac{1}{h_2}\left[v_1 - v_3 + w_{,y}\left(\frac{h_1 + h_3}{2} \right) \right]
\end{aligned}
\tag{3.2.2}
$$

The distortion angles of the core are defined as follows, where the first subscript defines the strain in contracted form and the second subscript defines the layer

$$\varepsilon_{52} = \alpha_1 + w_{,x} \qquad \varepsilon_{42} = \alpha_2 + w_{,y}$$

$$\varepsilon_{52} = \frac{h_c}{h_2}\left[\frac{(u_1 - u_3)}{h_c} + w_{,x}\right] \qquad \varepsilon_{42} = \frac{h_c}{h_2}\left[\frac{(v_1 - v_3)}{h_c} + w_{,y}\right] \tag{3.2.3}$$

where

$$h_c = h_2 + \frac{h_1 + h_3}{2} \tag{3.2.4}$$

The strain components that correspond with the displacements in (3.2.1), obtained from (2.3.9) in the contracted notation (2.5.5) are

$$\begin{aligned}
\varepsilon_{11} &= u_{1,x} - zw_{,xx} \\
\varepsilon_{13} &= u_{3,x} - zw_{,xx} \\
\varepsilon_{21} &= v_{1,y} - zw_{,yy} \\
\varepsilon_{23} &= v_{3,y} - zw_{,yy} \\
\varepsilon_{61} &= u_{1,y} + v_{1,x} - 2zw_{,xy} \\
\varepsilon_{63} &= u_{3,y} + v_{3,x} - 2zw_{,xy}
\end{aligned} \tag{3.2.5}$$

The resulting strain components for each layer of the sandwich plate are kinematically consistent with the assumed displacement field. It should be noted that as a result of the displacement field transverse strains in the face layers are identically zero, as a result the transverse shear stresses are zero for any face layers made of an orthotropic (or layers of orthotropic, if the theory is to be extended to an equivalent single layer theory for the face layers) material. However the transverse normal stress is not necessarily zero but as stated in **2.5.1** it can be neglected and a state of plane stress is assumed.

A final note on the displacement field concerns the choice to neglect the normals strains in the core, which can be formulated based on the core displacements. This assumption is not valid for extremely stiff cores [3], which contradicts the basis of the theory. The TSDT includes the effect of normal strain in the core without the cumbersome additional derivation needed in the USPT and in **5.2.4** we will see how minimal the effects are.

3.3 Constitutive Equations

The face layers of the sandwich plate are in a state of plane stress as a result of the assumed displacement field. We will restrict our analysis to that of sandwich plates with isotropic layers therefore the stress components in terms of the strain are

$$\sigma_{1n} = \frac{E_n}{1-\nu_n^2}\left(\varepsilon_{1n} + \nu_n \varepsilon_{2n}\right)$$
$$\sigma_{2n} = \frac{E_n}{1-\nu_n^2}\left(\varepsilon_{2n} + \nu_n \varepsilon_{1n}\right) \tag{3.3.1}$$
$$\sigma_{6n} = \frac{E_n}{2\left(1+\nu_n\right)}\varepsilon_{6n}$$

where $n = 1,3$ corresponding to the face layers, and the shear stress components in the core are

$$\sigma_{42} = G_2 \varepsilon_{42}$$
$$\sigma_{52} = G_2 \varepsilon_{52} \tag{3.3.2}$$

where E_n is the modulus of elasticity (Young's modulus) and ν_n is Poisson's ratio of the layer denoted by n and the shear modulus for the face layers has been replaced by its equivalent expression for an isotropic material $G = E/\left(2\left(1+\nu\right)\right)$.

3.4 Equations of Motion

Making use of Hamilton's Principle for free vibration of a deformable continuum,

$$\int_{t_1}^{t_2}\left(\delta K - \delta U\right)dt = 0 \tag{3.4.1}$$

the equations of motion for the USPT are derived. The virtual strain energy, δU and the virtual kinetic energy, δK are given by

$$\delta U = \sum_{n=1}^{3}\int_{S_0}\int_{Z}\sigma_{in}\delta\varepsilon_{in}dzdS \qquad i = 1,2,3,4,5,6$$
$$\delta K = \sum_{n=1}^{3}\int_{S_0}\int_{Z}\rho_n \ddot{u}_{jn}\delta u_{jn}dzdS + \int_{S_0}\sum_{n=1}^{3}\left(\rho_n h_n\right)\ddot{w}\delta w dS \qquad j = 1,2 \tag{3.4.2}$$

where ρ_n is the density of the layer denoted by n, S_0 is denotes the mid-plane of each layer of the plate, Z denotes the thickness of each layer and components (3.4.2) are

$$\delta\varepsilon_{11} = \delta u_{1},_{x} - z\delta w,_{xx}$$
$$\delta\varepsilon_{21} = \delta v_{1},_{y} - z\delta w,_{yy}$$
$$\delta\varepsilon_{61} = \delta u_{1},_{y} + \delta v_{1},_{x} - 2z\delta w,_{xy}$$
$$\delta\varepsilon_{42} = \frac{h_c}{h_2}\left[\frac{\left(\delta v_1 - \delta v_3\right)}{h_c} + \delta w,_{y}\right]$$
$$\delta\varepsilon_{52} = \frac{h_c}{h_2}\left[\frac{\left(\delta u_1 - \delta u_3\right)}{h_c} + \delta w,_{x}\right]$$
$$\delta\varepsilon_{13} = \delta u_{3},_{x} - z\delta w,_{xx}$$
$$\delta\varepsilon_{23} = \delta v_{3},_{y} - z\delta w,_{yy}$$
$$\delta\varepsilon_{63} = \delta u_{3},_{y} + \delta v_{3},_{x} - 2z\delta w,_{xy}$$

$$\delta u_{11} = \delta u_1 - z\delta w,_{x}$$
$$\delta u_{21} = \delta v_1 - z\delta w,_{y}$$
$$\delta u_{12} = \frac{1}{2}\left[\delta u_1 + \delta u_3 + \delta w,_{x}\left(\frac{h_1 - h_3}{2}\right)\right] + z\frac{1}{h_2}\left[\delta u_1 - \delta u_3 + \delta w,_{x}\left(\frac{h_1 + h_3}{2}\right)\right]$$
$$\delta u_{22} = \frac{1}{2}\left[\delta v_1 + \delta v_3 + \delta w,_{y}\left(\frac{h_1 - h_3}{2}\right)\right] + z\frac{1}{h_2}\left[\delta v_1 - \delta v_3 + \delta w,_{y}\left(\frac{h_1 + h_3}{2}\right)\right]$$
$$\delta u_{13} = \delta u_3 - z\delta w,_{x}$$
$$\delta u_{23} = \delta v_3 - z\delta w,_{y}$$

$$\ddot{u}_{11} = \ddot{u}_1 - z\ddot{w},_{x}$$
$$\ddot{u}_{21} = \ddot{v}_1 - z\ddot{w},_{y}$$
$$\ddot{u}_{12} = \frac{1}{2}\left[\ddot{u}_1 + \ddot{u}_3 + \ddot{w},_{x}\left(\frac{h_1 - h_3}{2}\right)\right] + z\frac{1}{h_2}\left[\ddot{u}_1 - \ddot{u}_3 + \ddot{w},_{x}\left(\frac{h_1 + h_3}{2}\right)\right]$$
$$\ddot{u}_{22} = \frac{1}{2}\left[\ddot{v}_1 + \ddot{v}_3 + \ddot{w},_{y}\left(\frac{h_1 - h_3}{2}\right)\right] + z\frac{1}{h_2}\left[\ddot{v}_1 - \ddot{v}_3 + \ddot{w},_{y}\left(\frac{h_1 + h_3}{2}\right)\right]$$
$$\ddot{u}_{13} = \ddot{u}_3 - z\ddot{w},_{x}$$
$$\ddot{u}_{23} = \ddot{v}_3 - z\ddot{w},_{y}$$

Substituting (3.4.2) into (3.4.1) and integrating by parts and collecting coefficients of $\delta u_1, \delta v_1, \delta u_3, \delta v_3, \delta w$ the following equations of motion for a rectangular plate are obtained

$$\delta \mathbf{u_1}: \quad \theta_1\left(\frac{\partial^2 u_1}{\partial x^2}+\overline{\nu}_1\frac{\partial^2 v_1}{\partial x\partial y}+\overline{\nu}_1^*\frac{\partial^2 u_1}{\partial y^2}\right)-\frac{\theta_2}{h_c}\left(u_1-u_3+h_c\frac{\partial w}{\partial x}\right)=\left(h_1\rho_1+4I_2\right)\ddot{u}_1+2I_2\ddot{u}_3+K_1\frac{\partial \ddot{w}}{\partial x}$$

$$\delta \mathbf{u_3}: \quad \theta_3\left(\frac{\partial^2 u_3}{\partial x^2}+\overline{\nu}_3\frac{\partial^2 v_3}{\partial x\partial y}+\overline{\nu}_3^*\frac{\partial^2 u_3}{\partial y^2}\right)+\frac{\theta_2}{h_c}\left(u_1-u_3+h_c\frac{\partial w}{\partial x}\right)=\left(h_3\rho_3+4I_2\right)\ddot{u}_3+2I_2\ddot{u}_1+K_3\frac{\partial \ddot{w}}{\partial x}$$

$$\delta \mathbf{v_1}: \quad \theta_1\left(\frac{\partial^2 v_1}{\partial y^2}+\overline{\nu}_1\frac{\partial^2 u_1}{\partial x\partial y}+\overline{\nu}_1^*\frac{\partial^2 v_1}{\partial x^2}\right)-\frac{\theta_2}{h_c}\left(v_1-v_3+h_c\frac{\partial w}{\partial y}\right)=\left(h_1\rho_1+4I_2\right)\ddot{v}_1+2I_2\ddot{v}_3+K_1\frac{\partial \ddot{w}}{\partial y}$$

$$\delta \mathbf{v_3}: \quad \theta_3\left(\frac{\partial^2 v_3}{\partial y^2}+\overline{\nu}_3\frac{\partial^2 u_3}{\partial x\partial y}+\overline{\nu}_3^*\frac{\partial^2 v_3}{\partial x^2}\right)+\frac{\theta_2}{h_c}\left(v_1-v_3+h_c\frac{\partial w}{\partial y}\right)=\left(h_1\rho_1+4I_2\right)\ddot{v}_3+2I_2\ddot{v}_1+K_3\frac{\partial \ddot{w}}{\partial y}$$

$$\delta \mathbf{w}: \quad \left(D_1+D_3\right)\nabla^4 w-\theta_2\left\{\frac{\partial}{\partial x}\left(u_1-u_3\right)+\frac{\partial}{\partial y}\left(v_1-v_3\right)+h_c\nabla^2 w\right\}=-I_0\ddot{w}+J_0\nabla^2\ddot{w}$$
$$+K_1\left(\frac{\partial \ddot{u}_1}{\partial x}+\frac{\partial \ddot{v}_1}{\partial y}\right)+K_3\left(\frac{\partial \ddot{u}_3}{\partial x}+\frac{\partial \ddot{v}_3}{\partial y}\right)$$

(3.4.3)

The corresponding boundary conditions are

along $x=0$ and $x=a$

$$\theta_1\left(\frac{\partial u_1}{\partial x}+\nu_1\frac{\partial v_1}{\partial y}\right)=0 \text{ or } u_1 \text{ is specified}$$

$$\theta_3\left(\frac{\partial u_3}{\partial x}+\nu_3\frac{\partial v_3}{\partial y}\right)=0 \text{ or } u_3 \text{ is specified}$$

$$\theta_1\overline{\nu}_1^*\left(\frac{\partial v_1}{\partial x}+\frac{\partial u_1}{\partial y}\right)=0 \text{ or } v_1 \text{ is specified}$$

$$\theta_3\overline{\nu}_3^*\left(\frac{\partial v_3}{\partial x}+\frac{\partial u_3}{\partial y}\right)=0 \text{ or } v_3 \text{ is specified}$$

$$D_1\left(\frac{\partial^2 w}{\partial x^2}+\nu_1\frac{\partial^2 w}{\partial y^2}\right)+D_3\left(\frac{\partial^2 w}{\partial x^2}+\nu_3\frac{\partial^2 w}{\partial y^2}\right)=0 \text{ or } \frac{\partial w}{\partial x} \text{ is specified}$$

$$D_1\left(\frac{\partial^3 w}{\partial x^3}+\left(2-\nu_1\right)\frac{\partial^3 w}{\partial x\partial y^2}\right)-D_3\left(\frac{\partial^3 w}{\partial x^3}+\left(2-\nu_3\right)\frac{\partial^3 w}{\partial x\partial y^2}\right)-\theta_2\left(u_1-u_3+h_c\frac{\partial w}{\partial x}\right)=J_0\frac{\partial \ddot{w}}{\partial x}+K_1\ddot{u}_1+K_3$$

or w is specified

(3.4.4)

along $y=0$ and $y=b$

$$\theta_1\left(\frac{\partial v_1}{\partial y}+\nu_1\frac{\partial u_1}{\partial x}\right)=0 \text{ or } v_1 \text{ is specified}$$

$$\theta_3\left(\frac{\partial v_3}{\partial y}+\nu_3\frac{\partial u_3}{\partial x}\right)=0 \text{ or } v_3 \text{ is specified}$$

$$\theta_1\overline{\nu}_1^*\left(\frac{\partial v_1}{\partial x}+\frac{\partial u_1}{\partial y}\right)=0 \text{ or } u_1 \text{ is specified}$$

$$\theta_3\overline{\nu}_3^*\left(\frac{\partial v_3}{\partial x}+\frac{\partial u_3}{\partial y}\right)=0 \text{ or } u_3 \text{ is specified}$$

$$D_1\left(\frac{\partial^2 w}{\partial y^2}+\nu_1\frac{\partial^2 w}{\partial x^2}\right)+D_3\left(\frac{\partial^2 w}{\partial y^2}+\nu_3\frac{\partial^2 w}{\partial x^2}\right)=0 \text{ or } \frac{\partial w}{\partial y} \text{ is specified}$$

$$D_1\left(\frac{\partial^3 w}{\partial y^3}+(2-\nu_1)\frac{\partial^3 w}{\partial y\partial x^2}\right)-D_3\left(\frac{\partial^3 w}{\partial y^3}+(2-\nu_3)\frac{\partial^3 w}{\partial y\partial x^2}\right)-\theta_2\left(\nu_1-\nu_3+h_c\frac{\partial w}{\partial y}\right)=J_0\frac{\partial\ddot{w}}{\partial y}+K_1\ddot{v}_1+K_3\ddot{v}_3$$

or w is specified

(3.4.5)

and for the free edge reaction at the corner

$$\left\{D_1(1-\nu_1)+D_3(1-\nu_3)\right\}\frac{\partial^2 w}{\partial x\partial y}=0 \tag{3.4.6}$$

where

$$D_1=\frac{E_1h_1^3}{12(1-\nu_1^2)} \qquad D_3=\frac{E_3h_3^3}{12(1-\nu_3^2)}$$

$$I_1=\frac{\rho_1h_1^3}{12} \qquad I_3=\frac{\rho_3h_3^3}{12}$$

$$\theta_1=\frac{E_1h_1}{(1-\nu_1^2)} \qquad \theta_3=\frac{E_3h_3}{(1-\nu_3^2)}$$

$$\overline{\nu}_1=\frac{(1+\nu_1)}{2} \qquad \overline{\nu}_3=\frac{(1+\nu_3)}{2} \tag{3.4.7}$$

$$\overline{\nu}_1^*=\frac{(1-\nu_1)}{2} \qquad \overline{\nu}_3^*=\frac{(1+\nu_3)}{2}$$

$$\theta_2=\frac{h_c}{h_2}G_2 \qquad I_2=\frac{\rho_2h_2}{12}$$

$$K_1=I_2(2h_1-h_3) \qquad K_3=I_2(h_1-2h_3)$$

$$J_0=I_2h_1^2-I_2h_1h_3+I_2h_3^2+I_1+I_3 \qquad I_0=\rho_1h_1+\rho_2h_2+\rho_3h_3$$

with the understanding that $\nabla^2=\frac{\partial^2}{\partial x^2}+\frac{\partial^2}{\partial y^2}$ and $\nabla^4=\left(\nabla^2\right)^2$.

3.5 Simply Supported Plate Solution

The analytical solution of the partial differential equations in (3.4.3) for a general sandwich plate with arbitrary boundary conditions is not possible. But for the simply supported boundary conditions the Navier solution procedure are used to examine the solution of (3.4.3). The boundary conditions where all edges of the plate are simply supported from (3.4.4) and (3.4.5) are

along $x = 0$ and $x = a$

I. $\theta_1 \left(u_{1,x} + \nu_1 v_{1,y} \right) = 0$

II. $\theta_3 \left(u_{3,x} + \nu_3 v_{3,y} \right) = 0$

III. $v_1 = 0$

IV. $v_3 = 0$

V. $D_1 \left(w_{,xx} + \nu_1 w_{,yy} \right) + D_3 \left(w_{,xx} + \nu_3 w_{,yy} \right) = 0$

VI. $w = 0$

(3.5.1)

along $y = 0$ and $y = b$

I. $u_1 = 0$

II. $u_3 = 0$

III. $\theta_1 \left(v_{1,y} + \nu_1 u_{1,x} \right) = 0$

IV. $\theta_3 \left(v_{3,y} + \nu_3 u_{3,x} \right) = 0$

V. $D_1 \left(w_{,yy} + \nu_1 w_{,xx} \right) + D_3 \left(w_{,yy} + \nu_3 w_{,xx} \right) = 0$

VI. $w = 0$

(3.5.2)

Following the Navier solution procedure the following form of spatial variation of $\left(u_1, v_1, u_3, v_3, w \right)$ satisfies (3.5.1) and (3.5.2)

$$
\begin{aligned}
u_1 &= \sum_{m=1}^{\infty} \sum_{n=1}^{\infty} U_{1mn}(t) \cos \alpha x \sin \beta y \\
u_3 &= \sum_{m=1}^{\infty} \sum_{n=1}^{\infty} U_{3mn}(t) \cos \alpha x \sin \beta y \\
v_1 &= \sum_{m=1}^{\infty} \sum_{n=1}^{\infty} V_{1mn}(t) \sin \alpha x \cos \beta y \\
v_3 &= \sum_{m=1}^{\infty} \sum_{n=1}^{\infty} V_{3mn}(t) \sin \alpha x \cos \beta y \\
w &= \sum_{m=1}^{\infty} \sum_{n=1}^{\infty} W_{mn}(t) \sin \alpha x \sin \beta y
\end{aligned}
\qquad (3.5.3)
$$

where $\alpha = m\pi / a$ and $\beta = n\pi / b$.

Substituting (3.5.3) into (3.4.3) and collecting the coefficients the following equation is obtained

$$
\left[\hat{m} \right] \underline{\ddot{u}} + \left[\hat{s} \right] \underline{u} = \underline{0} \qquad (3.5.4)
$$

$$\underline{u} = \begin{Bmatrix} U_{1mn} \\ U_{3mn} \\ V_{1mn} \\ V_{3mn} \\ W_{mn} \end{Bmatrix} \quad [\hat{m}] = \begin{Bmatrix} \hat{m}_{11} & \hat{m}_{12} & 0 & 0 & \hat{m}_{15} \\ \hat{m}_{21} & \hat{m}_{22} & 0 & 0 & \hat{m}_{25} \\ 0 & 0 & \hat{m}_{33} & \hat{m}_{34} & \hat{m}_{35} \\ 0 & 0 & \hat{m}_{43} & \hat{m}_{44} & \hat{m}_{45} \\ \hat{m}_{51} & \hat{m}_{52} & \hat{m}_{53} & \hat{m}_{54} & \hat{m}_{55} \end{Bmatrix} \quad [\hat{s}] = \begin{Bmatrix} \hat{s}_{11} & \hat{s}_{12} & \hat{s}_{13} & 0 & \hat{s}_{15} \\ \hat{s}_{21} & \hat{s}_{22} & 0 & \hat{s}_{24} & \hat{s}_{25} \\ \hat{s}_{31} & 0 & \hat{s}_{33} & \hat{s}_{34} & \hat{s}_{35} \\ 0 & \hat{s}_{42} & \hat{s}_{43} & \hat{s}_{44} & \hat{s}_{45} \\ \hat{s}_{51} & \hat{s}_{52} & \hat{s}_{53} & \hat{s}_{54} & \hat{s}_{55} \end{Bmatrix}$$

For the case of free vibration the solution of (3.5.4) can be converted to a standard eigenvalue problem if $\underline{u}(x,y,t) = \underline{U}(x,y)e^{i\omega t}$ then

$$[D - \lambda I]\underline{U} = \underline{0} \tag{3.5.5}$$

where D the dynamic matrix is $[D] = [\hat{m}]^{-1}[\hat{s}]$, I is the identity matrix and $\lambda = \omega^2$ which is the square of the corresponding frequency of vibration. Where the $\hat{m}_{ij}$ and $\hat{s}_{ij}$ are given by

$$
\begin{aligned}
\hat{m}_{11} &= -h_1\rho_1 - 4I_2 \\
\hat{m}_{12} &= -2I_2 \\
\hat{m}_{15} &= -\alpha K_1 \\
\hat{m}_{21} &= -2I_2 \\
\hat{m}_{22} &= -h_3\rho_3 - 4I_2 \\
\hat{m}_{25} &= -\alpha K_3 \\
\hat{m}_{33} &= -h_1\rho_1 - 4I_2 \\
\hat{m}_{34} &= -2I_2 \\
\hat{m}_{35} &= -\beta K_1 \\
\hat{m}_{43} &= -2I_2 \\
\hat{m}_{44} &= -h_3\rho_3 - 4I_2 \\
\hat{m}_{45} &= -\beta K_3 \\
\hat{m}_{51} &= \alpha K_1 \\
\hat{m}_{52} &= \alpha K_3 \\
\hat{m}_{53} &= \beta K_1 \\
\hat{m}_{54} &= \beta K_3 \\
\hat{m}_{55} &= I_0 + J_0\left(\alpha^2 + \beta^2\right)
\end{aligned}
\qquad (3.5.6)
$$

$$
\begin{aligned}
\hat{s}_{11} &= -\theta_1\alpha^2 - \theta_1\overline{\nu}_1^*\beta^2 - \theta_2/h_c \\
\hat{s}_{12} &= \theta_2/h_c \\
\hat{s}_{13} &= -\theta_1\overline{\nu}_1\alpha\beta \\
\hat{s}_{15} &= -\theta_2\alpha \\
\hat{s}_{21} &= \theta_2/h_c \\
\hat{s}_{22} &= -\theta_3\alpha^2 - \theta_3\overline{\nu}_3^*\beta^2 - \theta_2/h_c \\
\hat{s}_{24} &= -\theta_3\overline{\nu}_3\alpha\beta \\
\hat{s}_{25} &= \theta_2\alpha \\
\hat{s}_{31} &= -\theta_1\overline{\nu}_1\alpha\beta \\
\hat{s}_{33} &= -\theta_1\beta^2 - \theta_1\overline{\nu}_1^*\alpha^2 - \theta_2/h_c \\
\hat{s}_{34} &= \theta_2/h_c \\
\hat{s}_{35} &= -\theta_2\beta \\
\hat{s}_{42} &= -\theta_3\overline{\nu}_3\alpha\beta \\
\hat{s}_{43} &= \theta_2/h_c \\
\hat{s}_{44} &= -\theta_3\beta^2 - \theta_3\overline{\nu}_1^*\alpha^2 - \theta_2/h_c \\
\hat{s}_{45} &= \theta_2\beta \\
\hat{s}_{51} &= \theta_2\alpha \\
\hat{s}_{52} &= -\theta_2\alpha \\
\hat{s}_{53} &= \theta_2\beta \\
\hat{s}_{54} &= -\theta_2\beta \\
\hat{s}_{55} &= \left(D_1 + D_3\right)\left(\alpha^4 + 2\alpha^2\beta^2 + \beta^4\right) + h_c\theta_2\left(\alpha^2 + \beta^2\right)
\end{aligned}
\qquad (3.5.7)
$$

3.6 *Uncoupled Equations of Motion*

Following the method in [4], two additional assumptions can be made to the USPT and the extension-bending coupling is removed from the equations of motion allowing for a simplified set of equations for considering transverse vibration only. Making the following assumptions

5. Although the material of the face layers may be different, the value of their Poisson ratios are approximated as equal, $\nu_1 \approx \nu_2 \approx \nu$
6. The in-plane and rotary inertia effects of the plate are neglected and only the transverse inertia effects are considered

Now we introduce the following variables

$$\hat{U} = \frac{1}{(\theta_1 + \theta_3)}(\theta_1 u_1 + \theta_3 u_3)$$
$$\hat{V} = \frac{1}{(\theta_1 + \theta_3)}(\theta_1 v_1 + \theta_3 v_3)$$
$$\psi_x = \frac{1}{h_c}(u_1 - u_3) \qquad (3.6.1)$$
$$\psi_y = \frac{1}{h_c}(v_1 - v_3)$$

where $\hat{U}$ and $\hat{V}$ can be considered the weighted mean in-plane displacements, ψ_x and ψ_y are the rotations of a line connecting the two corresponding points on the mid-plane of the face layers after bending.

Taking the equations of motion corresponding to δu_1 and δu_3 in (3.4.3) while neglecting the terms involving derivatives with respect to time and adding the resulting equations then substituting in $\hat{U}$ and $\hat{V}$ we get

$$\hat{U}_{,xx} + \bar{\nu}\hat{V}_{,xy} + \bar{\nu}^*\hat{U}_{,yy} = 0$$

Once again taking the equations of motion corresponding to δu_1 and δu_3 in (3.4.3) while neglecting the terms involving derivatives with respect to time and dividing the equations by θ_1 and θ_3 respectively then subtracting the resulting equations and substituting in ψ_x and ψ_y we get

$$\psi_{x,xx} + \bar{\nu}\psi_{y,xy} + \bar{\nu}^*\psi_{x,yy} - \hat{g}_1(\psi_x + w_{,x}) = 0$$

By repeating the above steps for the equations of motion corresponding to δv_1 and δv_3 in (3.4.3) and by directly substituting ψ_x and ψ_y in the equation of motion corresponding to δw in (3.4.3) with only the transverse inertia considered, three more equations are obtained. Therefore the uncoupled equations of motion for USPT are

$$
\begin{aligned}
&\hat{U}_{,xx}+\overline{\nu}\hat{V}_{,xy}+\overline{\nu}^{*}\hat{U}_{,yy}=0\\
&\hat{V}_{,yy}+\overline{\nu}\hat{U}_{,xy}+\overline{\nu}^{*}\hat{V}_{,xx}=0\\
&\psi_{x,xx}+\overline{\nu}\psi_{y,xy}+\overline{\nu}^{*}\psi_{x,yy}-\hat{g}_1\left(\psi_x+w_{,x}\right)=0\\
&\psi_{y,yy}+\overline{\nu}\psi_{x,xy}+\overline{\nu}^{*}\psi_{y,xx}-\hat{g}_1\left(\psi_y+w_{,y}\right)=0\\
&\nabla^4 w-\hat{g}_2\left(\psi_{x,x}+\psi_{y,y}+\nabla^2 w\right)+\hat{g}_0\ddot{w}=0
\end{aligned}
\qquad (3.6.2)
$$

where

$$
\hat{g}_1=\frac{\theta_2}{h_c}\overline{\theta}\qquad \hat{g}_2=\frac{\theta_2 h_c}{\left(D_1+D_3\right)}\qquad \hat{g}_0=\frac{I_0}{\left(D_1+D_3\right)}\qquad \overline{\theta}=\frac{\theta_1+\theta_3}{\theta_1\theta_3}
\qquad (3.6.3)
$$

Using the same steps taken to arrive at the uncoupled equations of motion on the boundary conditions for each of the corresponding virtual displacements the following conditions are found for a rectangular sandwich plate

along $x=0$ and $x=a$

$$
\begin{aligned}
&\frac{1}{\theta_1}\left(\hat{U}_{,x}+\nu\hat{V}_{,y}\right)=0 \text{ or } \hat{U} \text{ is specified}\\
&\frac{\overline{\nu}^{*}}{\overline{\theta}}\left(\hat{U}_{,y}+\hat{V}_{,x}\right)=0 \text{ or } \hat{V} \text{ is specified}\\
&h_c\left(\psi_{x,x}+\nu\psi_{y,y}\right)=0 \text{ or } \psi_x \text{ is specified}\\
&\overline{\nu}^{*}h_c\left(\psi_{x,y}+\psi_{y,x}\right)=0 \text{ or } \psi_y \text{ is specified}\\
&\left(D_1+D_3\right)\left(w_{,xx}+\nu w_{,yy}\right)=0 \text{ or } w_{,x} \text{ is specified}\\
&\hat{g}_2\left(\psi_x+w_{,x}\right)-\left(w_{,xxx}+\left(2-\nu\right)w_{,xyy}\right)=0 \text{ or } w \text{ is specified}
\end{aligned}
\qquad (3.6.4)
$$

along $y=0$ and $y=b$

$$
\begin{aligned}
&\frac{1}{\theta_1}\left(\hat{V}_{,y}+\nu\hat{U}_{,x}\right)=0 \text{ or } \hat{V} \text{ is specified}\\
&\frac{\overline{\nu}^{*}}{\overline{\theta}}\left(\hat{U}_{,y}+\hat{V}_{,x}\right)=0 \text{ or } \hat{U} \text{ is specified}\\
&h_c\left(\psi_{y,y}+\nu\psi_{x,x}\right)=0 \text{ or } \psi_y \text{ is specified}\\
&\overline{\nu}^{*}h_c\left(\psi_{x,y}+\psi_{y,x}\right)=0 \text{ or } \psi_x \text{ is specified}\\
&\left(D_1+D_3\right)\left(w_{,yy}+\nu w_{,xx}\right)=0 \text{ or } w_{,y} \text{ is specified}
\end{aligned}
$$

$$\hat{g}_2\left(\psi_y + w_{,y}\right) - \left(w_{,yyy} + (2-\nu)w_{,yxx}\right) = 0 \text{ or } w \text{ is specified} \tag{3.6.5}$$

and for the free edge reaction at the corner

$$\left(D_1 + D_3\right)(1-\nu)w_{,xy} = 0 \tag{3.6.6}$$

The simplified equations of motion in (3.6.2) are uncoupled with respect to extension and bending and now if the assumption that the in-plane rigid body motion of the plate is suppressed, the first two equations (3.6.2) involving $\hat{U}$ and $\hat{V}$ can be neglected and the three remaining equations of motion can be used to investigate the transverse vibration of the sandwich plate, in particular the cantilever sandwich plate.

3.7 Non-Dimensional Transverse Simplified USPT

To make numerical calculations less demanding the uncoupled bending equations of motion will be nondimensionalized with respect to a, the length of an edge of the plate in the x direction. We will soon see that various Lévy solutions for plates are in the form of hyperbolic and trigonometric functions that can create problems with computer under and overflow, the non-dimensional form aims at minimizing the magnitude of the arguments of these functions. We will now introduce the following dimensionless variables

$$\xi = \frac{x}{a} \qquad \eta = \frac{y}{b} \qquad W = \frac{w}{a} \qquad \psi_\xi = \psi_x \qquad \psi_\eta = \psi_y \tag{3.7.1}$$

where ξ is defined on the interval $[0,1]$ and η is defined on the interval $[0,\phi]$ with $\phi = b/a$.

By applying the chain rule the following relationships for derivation are established

$$\frac{\partial}{\partial x} = \frac{\partial \zeta}{\partial x}\frac{\partial}{\partial \zeta} \qquad \frac{\partial \zeta}{\partial x} = \frac{\partial}{\partial x}\left(\frac{x}{a}\right) = \frac{1}{a} \qquad \frac{\partial}{\partial x} = \frac{1}{a}\frac{\partial}{\partial \zeta}$$

in general

$$\frac{\partial^n}{\partial x^n} = \frac{1}{a^n}\frac{\partial^n}{\partial \zeta^n} \qquad \frac{\partial^n}{\partial y^n} = \frac{1}{a^n}\frac{\partial^n}{\partial \eta^n} \tag{3.7.2}$$

now we substitute (3.7.1) into (3.6.2) and the resultant non-dimensional equations are

$$\begin{aligned}
&\psi_{\xi,\xi\xi} + \bar{\nu}\psi_{\eta,\xi\eta} + \bar{\nu}^*\psi_{\xi,\eta\eta} - g_1\left(\psi_\xi + W_{,\xi}\right) = 0 \\
&\psi_{\eta,\eta\eta} + \bar{\nu}\psi_{\xi,\xi\eta} + \bar{\nu}^*\psi_{\eta,\xi\xi} - g_1\left(\psi_\eta + W_{,\eta}\right) = 0 \\
&\nabla^4 W - g_2\left(\psi_{\xi,\xi} + \psi_{\eta,\eta} + \nabla^2 W\right) + g_0\ddot{W} = 0
\end{aligned} \tag{3.7.3}$$

where

$$g_1 = a^2 \hat{g}_1 \qquad g_2 = a^2 \hat{g}_2 \qquad g_0 = a^4 g_0 \tag{3.7.4}$$

with the understanding that the differential operators ∇^4 and ∇^2 are with respect to the non-dimensional variables ξ, η.

Then taking dimensionless variables of the form

$$\begin{aligned} W &= W(\xi,\eta)e^{i\omega t} \\ \psi_\xi &= \psi_\xi(\xi,\eta)e^{i\omega t} \\ \psi_\eta &= \psi_\eta(\xi,\eta)e^{i\omega t} \end{aligned} \tag{3.7.5}$$

where ω is the circular frequency of free vibration. By substituting into (3.7.3) we now have the non-dimensional equations of motion as functions of the spatial variables for a given frequency

$$\begin{aligned} &\psi_{\xi,\xi\xi} + \bar{\nu}\psi_{\eta,\xi\eta} + \bar{\nu}^*\psi_{\xi,\eta\eta} - g_1\left(\psi_\xi + W_{,\xi}\right) = 0 \\ &\psi_{\eta,\eta\eta} + \bar{\nu}\psi_{\xi,\xi\eta} + \bar{\nu}^*\psi_{\eta,\xi\xi} - g_1\left(\psi_\eta + W_{,\eta}\right) = 0 \\ &\nabla^4 W - g_2\left(\psi_{\xi,\xi} + \psi_{\eta,\eta} + \nabla^2 W\right) - \omega^2 g_0 W = 0 \end{aligned} \tag{3.7.6}$$

The corresponding boundary conditions are

$\xi = 0$ and $\xi = 1$

$$\frac{h_c}{a}\left(\psi_{\xi,\xi} + \nu\psi_{\eta,\eta}\right) = 0 \text{ or } \psi_\xi \text{ is specified}$$

$$\bar{\nu}^* \frac{h_c}{a}\left(\psi_{\xi,\eta} + \psi_{\eta,\xi}\right) = 0 \text{ or } \psi_\eta \text{ is specified}$$

$$\frac{(D_1 + D_3)}{a}\left(W_{,\xi\xi} + \nu W_{,\eta\eta}\right) = 0 \text{ or } W_{,\xi} \text{ is specified}$$

$$g_2\left(\psi_\xi + W_{,\xi}\right) - \left(W_{,\xi\xi\xi} + (2-\nu)W_{,\xi\eta\eta}\right) = 0 \text{ or } W \text{ is specified}$$

(3.7.7)

$\eta = 0$ and $\eta = \phi$

$$\frac{h_c}{a}\left(\psi_{\eta,\eta} + \nu\psi_{\xi,\xi}\right) = 0 \text{ or } \psi_\eta \text{ is specified}$$

$$\bar{\nu}^* \frac{h_c}{a}\left(\psi_{\xi,\eta} + \psi_{\eta,\xi}\right) = 0 \text{ or } \psi_\xi \text{ is specified}$$

$$\frac{(D_1 + D_3)}{a}\left(W_{,\eta\eta} + \nu W_{,\xi\xi}\right) = 0 \text{ or } W_{,\eta} \text{ is specified}$$

$$g_2\left(\psi_\eta + W_{,\eta}\right) - \left(W_{,\eta\eta\eta} + (2-\nu)W_{,\eta\xi\xi}\right) = 0 \text{ or } W \text{ is specified} \tag{3.7.8}$$

and for the free edge reaction at the corner

$$\frac{(D_1 + D_3)}{a}(1-\nu)W_{,\xi\eta} = 0 \tag{3.7.9}$$

4 Third Order Plate Theory of Reddy

4.1 Introduction

The motivation for the third order plate theory of Reddy (or third order shear deformation theory, TSDT), is to account for transverse shear strains for materials whose elastic modulus to shear modulus ratios are very large instead of the 2.6 for typical isotropic materials [1]. The classical theory of plates, which assumes normals to the mid-plane before deformation remain normal and straight after deformation, neglects transverse shear strains.

The first order shear deformation plate theory, FSDT, incorporates transverse shear strain by relaxing the requirement on the deformation of normals to the mid-plane. The normals do not have to remain perpendicular to the mid-plane after deformation. This introduces two independent variables that are the rotations of the normals with respect the x and y axes. Since FSDT results in the transverse shear strains being represented as constants through the thickness of the plate, it follows that the transverse shear stresses will also be constant. On the top and bottom surfaces of the plate FSDT does not satisfy the condition of zero transverse stress.

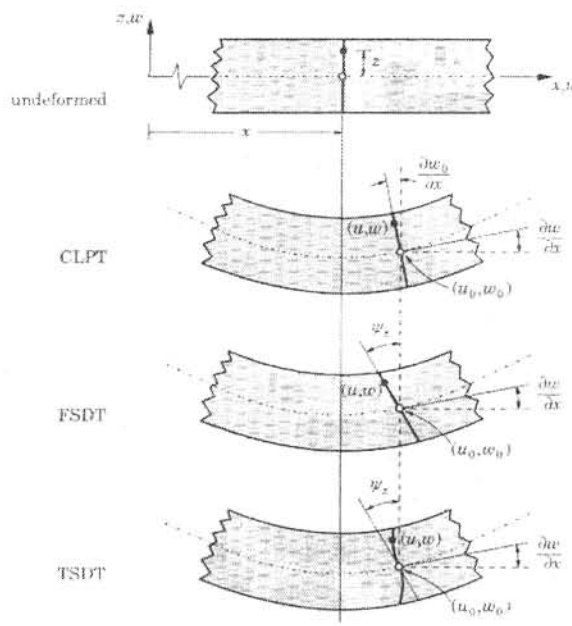

Figure 4.1

From the well know theory of beams the transverse shear stress varies parabolically through the beam thickness satisfying the zero stress condition on the free surfaces. The discrepancy between the constant state of stress and the actual state of stress is dealt with by use of shear correction factors. These factors are calculated such that the strain energy due to transverse stresses from FSDT equals the true strain energy predicted by three-dimensional elastic theory [2].

The advantage of TSDT is its ability to incorporate transverse shear strains and maintain the condition of zero transverse shear stress on the top and bottom of the plate. For our application it is necessary to incorporate the transverse shear strains to predict the damping effects of the viscoelastic layer.

4.2 Displacement Field

The present theory assumes a displacement field that satisfies the condition that the transverse shear stresses vanish on the free surfaces of the plate and are nonzero elsewhere. This requires a displacement field where the inplane displacements are expanded as cubic functions of the thickness coordinate and the transverse deflection is constant through the plate thickness. Since the transverse normal stress is of the order of the square of the ratio of the thickness of the plate to the length of the plate times the in-plane normal stresses, the assumption that the transverse displacement is not a function of the thickness is justified [1]. The presentation of the derivation of the resulting strains of TSDT is identical to that of [1] with only slight elaboration on matters of theoretical importance.

We begin with the displacement field

$$\begin{aligned} u_1(x,y,z,t) &= u(x,y,t) + z\psi_x(x,y,t) + z^2\xi_x(x,y,t) + z^3\zeta_x(x,y,t) \\ u_2(x,y,z,t) &= v(x,y,t) + z\psi_y(x,y,t) + z^2\xi_y(x,y,t) + z^3\zeta_y(x,y,t) \\ u_3(x,y,t) &= w(x,y,t) \end{aligned} \tag{4.2.1}$$

where u, v and w denote the displacement of a point (x,y) on the midplane with u and v being the inplane displacements and w being the transverse displacement. ψ_x and ψ_y are the rotations of the normals to the midplane about the x and y axis respectively. The functions ξ_x, ξ_y, ζ_x and ζ_y are determined using the condition that the transverse shear stresses vanish on the free surfaces (i.e. top and bottom) of the plate.

$$\sigma_5\left(x,y,\pm\frac{h}{2}\right) = 0, \quad \sigma_4\left(x,y,\pm\frac{h}{2}\right) = 0$$

For isotropic plates (or orthotropic and plates composed of orthotropic layers), these conditions are equivalent to the requirement that the corresponding strains be zero on the surfaces. Using the contracted small deformation theory of elasticity we have

$$\varepsilon_5 = \frac{\partial u_1}{\partial z} + \frac{\partial u_3}{\partial x} = \psi_x + 2z\xi_x + 3z^2\zeta_x + \frac{\partial w}{\partial x}$$
$$\varepsilon_4 = \frac{\partial u_2}{\partial z} + \frac{\partial u_3}{\partial y} = \psi_y + 2z\xi_y + 3z^2\zeta_y + \frac{\partial w}{\partial y}$$

setting $\varepsilon_5\left(x, y, \pm h/2\right) = \varepsilon_4\left(x, y, h/2\right) = 0$, we obtain

$$\psi_x + h\xi_x + \frac{3}{4}h^2\zeta_x + \frac{\partial w}{\partial x} = 0$$
$$\psi_x + h\xi_x + \frac{3}{4}h^2\zeta_x + \frac{\partial w}{\partial x} = 0$$
$$\psi_y + h\xi_y + \frac{3}{4}h^2\zeta_y + \frac{\partial w}{\partial y} = 0$$
$$\psi_y - h\xi_y + \frac{3}{4}h^2\zeta_y + \frac{\partial w}{\partial y} = 0$$

from this it is apparent that $\xi_x = \xi_y = 0$ and

$$\zeta_x = -\frac{4}{3h^2}\left(\frac{\partial w}{\partial x} + \psi_x\right)$$
$$\zeta_y = -\frac{4}{3h^2}\left(\frac{\partial w}{\partial y} + \psi_y\right)$$

the displacement field in (4.2.1) becomes

$$u_1 = u + z\psi_x - \frac{4}{3h^2}z^3\left(\psi_x + \frac{\partial w}{\partial x}\right)$$
$$u_2 = v + z\psi_y - \frac{4}{3h^2}z^3\left(\psi_y + \frac{\partial w}{\partial y}\right)$$
$$u_3 = w \qquad (4.2.2)$$

The strains associated with the displacement in (4.2.2) are

$$\varepsilon_1 = \varepsilon_1^0 + z\kappa_1^1 + z^3\kappa_1^3$$
$$\varepsilon_2 = \varepsilon_2^0 + z\kappa_2^1 + z^3\kappa_2^3$$
$$\varepsilon_3 = 0$$
$$\varepsilon_4 = \varepsilon_4^0 + z^2\kappa_4^2$$

$$\varepsilon_5 = \varepsilon_5^0 + z^2\kappa_5^2$$
$$\varepsilon_6 = \varepsilon_6^0 + z\kappa_6^1 + z^3\kappa_6^3 \tag{4.2.3}$$

where

$$\varepsilon_1^0 = u_{,x} \quad \kappa_1^1 = \psi_{x,x} \quad \kappa_1^3 = -\frac{4}{3h^2}\left(\psi_{x,x} + w_{,xx}\right)$$
$$\varepsilon_2^0 = v_{,y} \quad \kappa_2^1 = \psi_{y,y} \quad \kappa_2^3 = -\frac{4}{3h^2}\left(\psi_{y,y} + w_{,yy}\right)$$
$$\varepsilon_4^0 = \psi_y + w_{,y} \quad \kappa_4^2 = -\frac{4}{h^2}\left(\psi_y + w_{,y}\right)$$
$$\varepsilon_5^0 = \psi_x + w_{,x} \quad \kappa_5^2 = -\frac{4}{h^2}\left(\psi_x + w_{,x}\right)$$
$$\varepsilon_6^0 = u_{,y} + v_{,x} \quad \kappa_6^1 = \psi_{x,y} + \psi_{y,x} \quad \kappa_6^3 = -\frac{4}{3h^2}\left(\psi_{x,y} + \psi_{y,x} + 2w_{,xy}\right) \tag{4.2.4}$$

4.3 Equations of Motion

Making use of Hamilton's Principle for free vibration of a deformable continuum,

$$\int_{t_1}^{t_2}\left(\delta K - \delta U\right)dt = 0 \tag{4.3.1}$$

the equations of motion for the third-order theory are derived. The virtual strain energy, δU and the virtual kinetic energy, δK are given by

$$\delta U = \int_{S_0}\int_{Z}\Big\{\sigma_1\left(\delta\varepsilon_1^0 + z\delta\kappa_1^1 + z^3\delta\kappa_1^3\right) + \sigma_2\left(\delta\varepsilon_2^0 + z\delta\kappa_2^1 + z^3\delta\kappa_2^3\right)$$
$$+\sigma_4\left(\delta\varepsilon_4^0 + z^2\delta\kappa_4^2\right) + \sigma_5\left(\delta\varepsilon_5^0 + z^2\delta\kappa_5^2\right) + \sigma_6\left(\delta\varepsilon_6^0 + z\delta\kappa_6^1 + z^3\delta\kappa_6^3\right)\Big\}dzdS$$

$$\delta U = \int_{S_0}\Big\{N_1\delta\varepsilon_1^0 + M_1\delta\kappa_1^1 + P_1\delta\kappa_1^3 + N_2\delta\varepsilon_2^0 + M_2\delta\kappa_2^1 + P_2\delta\kappa_2^3$$
$$+Q_4\delta\varepsilon_4^0 + R_4\delta\kappa_4^2 + Q_5\delta\varepsilon_5^0 + R_5\delta\kappa_5^2 + N_6\delta\varepsilon_6^0 + M_6\delta\kappa_6^1 + P_6\delta\kappa_6^3\Big\}\,dS \tag{4.3.2}$$

$$\delta K = \int_{S_0}\int_{Z}\hat{\rho}\Big\{\left(\ddot{u} + z\ddot{\psi}_x - c_1z^3\ddot{\phi}_x\right)\left(\delta u + z\delta\psi_x - c_1z^3\delta\phi_x\right)$$
$$+\left(\ddot{v} + z\ddot{\psi}_y - c_1z^3\ddot{\phi}_y\right)\left(\delta v + z\delta\psi_y - c_1z^3\delta\phi_y\right) + \left(\ddot{w}\right)\delta w\Big\}\,dzdS$$

$$\delta K = \int_{S_0} \Big\{ \left(I_0 \ddot{u} + I_1 \ddot{\psi}_x - c_1 I_3 \ddot{\phi}_x \right) \delta u + \left(I_1 \ddot{u} + I_2 \ddot{\psi}_x - c_1 I_4 \ddot{\phi}_x \right) \delta \psi_x$$
$$- c_1 \left(I_3 \ddot{u} + I_4 \ddot{\psi}_x - c_1 I_6 \ddot{\phi}_x \right) \delta \phi_x + \left(I_0 \ddot{v} + I_1 \ddot{\psi}_y - c_1 I_3 \ddot{\phi}_y \right) \delta v \qquad (4.3.3)$$
$$+ \left(I_1 \ddot{v} + I_2 \ddot{\psi}_y - c_1 I_4 \ddot{\phi}_y \right) \delta \psi_y - c_1 \left(I_3 \ddot{v} + I_4 \ddot{\psi}_y - c_1 I_6 \ddot{\phi}_y \right) \delta \phi_y + \left(I_0 \ddot{w} \right) \delta w \Big\} dS$$

where $c_1 = \dfrac{4}{3h^2}$, $c_2 = 3c_1$, $\phi_x = \psi_x + w_{,x}$ and $\phi_y = \psi_y + w_{,y}$. S_0 denotes the midplane of the plate, and the stress resultants N_i, M_i, P_i, Q_i and R_i are defined by

$$\left(N_i, M_i, P_i \right) = \int_z \sigma_i \left(1, z, z^3 \right) dz \qquad i = 1,2,6 \qquad (4.3.4)$$

$$\left(Q_i, R_i \right) = \int_z \sigma_i \left(1, z^2 \right) dz \qquad i = 4,5 \qquad (4.3.5)$$

The inertias I_i are defined by

$$I_i = \int_z \hat{\rho} \left(z \right)^i dz \qquad i = 0,1,2,3,4,6 \qquad (4.3.6)$$

where $\left(z \right)^i$ denotes z raised to the i power, and $\hat{\rho}$ is the density as a function of the z coordinate.

Substituting (4.3.2) and (4.3.3) into (4.3.1), integrating by parts and collecting coefficients of δu, δv, $\delta \psi_x$, $\delta \psi_y$ and δw the following equations of motion for a rectangular plate are obtained

$$\delta \mathbf{u}: \quad \frac{\partial N_1}{\partial x}+\frac{\partial N_6}{\partial y}=I_0\ddot{u}+\left(I_1-c_1I_3\right)\ddot{\psi}_x-c_1I_3\frac{\partial \ddot{w}}{\partial x}$$

$$\delta \mathbf{v}: \quad \frac{\partial N_2}{\partial y}+\frac{\partial N_6}{\partial x}=I_0\ddot{v}+\left(I_1-c_1I_3\right)\ddot{\psi}_y-c_1I_3\frac{\partial \ddot{w}}{\partial y}$$

$$\delta \boldsymbol{\psi}_x: \quad \frac{\partial}{\partial x}\left(M_1-c_1P_1\right)+\frac{\partial}{\partial y}\left(M_6-c_1P_6\right)-\left(Q_5-c_2R_5\right)=\left(I_1-c_1I_3\right)\ddot{u}+\left(I_2-2c_1I_4+c_1^2I_6\right)\ddot{\psi}_x$$
$$-c_1\left(I_4-c_1I_6\right)\frac{\partial \ddot{w}}{\partial x}$$

$$\delta \boldsymbol{\psi}_y: \quad \frac{\partial}{\partial y}\left(M_2-c_1P_2\right)+\frac{\partial}{\partial x}\left(M_6-c_1P_6\right)-\left(Q_4-c_2R_4\right)=\left(I_1-c_1I_3\right)\ddot{v}+\left(I_2-2c_1I_4+c_1^2I_6\right)\ddot{\psi}_y$$
$$-c_1\left(I_4-c_1I_6\right)\frac{\partial \ddot{w}}{\partial y}$$

$$\delta \mathbf{w}: \quad \frac{\partial}{\partial x}\left(Q_5-c_2R_5\right)+\frac{\partial}{\partial y}\left(Q_4-c_2R_4\right)+c_1\left(\frac{\partial^2P_1}{\partial x^2}+2\frac{\partial^2P_6}{\partial x\partial y}+\frac{\partial^2P_2}{\partial y^2}\right)=I_0\ddot{w}$$
$$+c_1\left[I_5\left(\frac{\partial \ddot{u}}{\partial x}+\frac{\partial \ddot{v}}{\partial y}\right)+\left(I_4-c_1I_6\right)\left(\frac{\partial \ddot{\psi}_x}{\partial x}+\frac{\partial \ddot{\psi}_y}{\partial y}\right)\right]-c_1^2I_6\left(\frac{\partial^2\ddot{w}}{\partial x^2}+\frac{\partial^2\ddot{w}}{\partial y^2}\right) \qquad (4.3.7)$$

The corresponding boundary conditions are

$x=0$ and $x=a$

$N_1=0$ or u is specified

$N_6=0$ or v is specified

$M_1-c_1P_1=0$ or ψ_x is specified

$M_6-c_1P_6=0$ or ψ_y is specified

$P_1=0$ or $\dfrac{\partial w}{\partial x}$ is specified

$$\left(Q_5-c_2R_5\right)+c_1\left(\frac{\partial P_1}{\partial x}+2\frac{\partial P_6}{\partial y}\right)-c_1I_3\ddot{u}+c_1\left(c_1I_6-I_4\right)\ddot{\psi}_x+c_1^2I_6\frac{\partial \ddot{w}}{\partial x}=0 \text{ or } w \text{ is specified} \qquad (4.3.8)$$

$y=0$ and $y=b$

$N_6=0$ or u is specified

$N_2=0$ or v is specified

$M_6-c_1P_6=0$ or ψ_x is specified

$M_2-c_1P_2=0$ or ψ_y is specified

$P_2=0$ or $\dfrac{\partial w}{\partial y}$ is specified

$$\left(Q_4 - c_2 R_4\right) + c_1\left(\frac{\partial P_2}{\partial y} + 2\frac{\partial P_6}{\partial x}\right) - c_1 I_3 \ddot{v} + c_1\left(c_1 I_6 - I_4\right)\ddot{\psi}_y + c_1^2 I_6 \frac{\partial \ddot{w}}{\partial y} = 0 \text{ or } w \text{ is specified} \tag{4.3.9}$$

and for the free edge reaction at the corner

$$-2c_1 P_6 = 0\,. \tag{4.3.10}$$

4.4 Constitutive Equations

Unlike the USPT the TSDT is independent of the number of layers and the material properties of the layer with respect to the equations of motion. The equations of motion are formulated in terms of the general stress resultants which are then determined from the material properties of the plate layers. The stress resultants are related to the strains by taking the stress-strain relation of an orthotropic layer k

$$\sigma_i^{(k)} = Q_{ij}^{(k)} \varepsilon_j \quad \left(i, j = 1,2,6,4,5\right) \tag{4.4.1}$$

and making the substitution in (4.3.4) and (4.3.5) for the appropriate indices and carrying out the integration over the thickness of the layer k; and repeating for all the layers of the plate. The *stress resultants* are given by

$$\begin{aligned} N_i &= A_{ij}\varepsilon_j^0 + B_{ij}\kappa_j^1 + E_{ij}\kappa_j^3 \\ M_i &= B_{ij}\varepsilon_j^0 + D_{ij}\kappa_j^1 + F_{ij}\kappa_j^3 \\ P_i &= E_{ij}\varepsilon_j^0 + F_{ij}\kappa_j^1 + H_{ij}\kappa_j^3 \\ &\left(i, j = 1,2,6\right) \end{aligned} \tag{4.4.2}$$

$$\begin{aligned} Q_i &= A_{ij}^s \varepsilon_j^0 + D_{ij}^s \kappa_j^2 \\ R_i &= D_{ij}^s \varepsilon_j^0 + F_{ij}^s \kappa_j^2 \\ &\left(i, j = 4,5\right) \end{aligned} \tag{4.4.3}$$

where the coefficients of the strain components in (4.4.2) are known as the *plate stiffnesses* and are defined for $i, j = 1,2,6$ and are matrices of the order 3x3, and those in (4.4.3) are defined for $i, j = 4,5$ and are matrices of the order 2x2. The coefficients in (4.4.2) and (4.4.3) given in terms of the transformed layer stiffnesses $Q_{ij}^{(k)}$ and the layer coordinates z_{k+1} and z_k are defined by

$$A_{ij}=\sum_{k=1}^{N}Q_{ij}^{(k)}\left(z_{k+1}-z_k\right) \qquad B_{ij}=\frac{1}{2}\sum_{k=1}^{N}Q_{ij}^{(k)}\left(z_{k+1}^2-z_k^2\right)$$
$$D_{ij}=\frac{1}{3}\sum_{k=1}^{N}Q_{ij}^{(k)}\left(z_{k+1}^3-z_k^3\right) \qquad E_{ij}=\frac{1}{4}\sum_{k=1}^{N}Q_{ij}^{(k)}\left(z_{k+1}^4-z_k^4\right) \tag{4.4.4}$$
$$F_{ij}=\frac{1}{5}\sum_{k=1}^{N}Q_{ij}^{(k)}\left(z_{k+1}^5-z_k^5\right) \qquad H_{ij}=\frac{1}{7}\sum_{k=1}^{N}Q_{ij}^{(k)}\left(z_{k+1}^7-z_k^7\right)$$
$$\left(i,j=1,2,6\right)$$

$$\begin{aligned} A_{ij}^{s}&=A_{ij}\\ D_{ij}^{s}&=D_{ij}\\ F_{ij}^{s}&=F_{ij}\\ \left(i,j=4,5\right)& \end{aligned} \tag{4.4.5}$$

where $Q_{ij}^{(k)}$ is the transformed plane stress reduced elastic constants from material coordinates to plate coordinates as defined in (2.5.13). It should also be noted that the coefficients of the stress resultants that correspond to the transverse shear strains (4.4.5) have a subscript s as to not confuse them with the inplane coefficients. The layer coordinates z_{k+1} and z_k for a general laminate are defined in Figure 4.2.

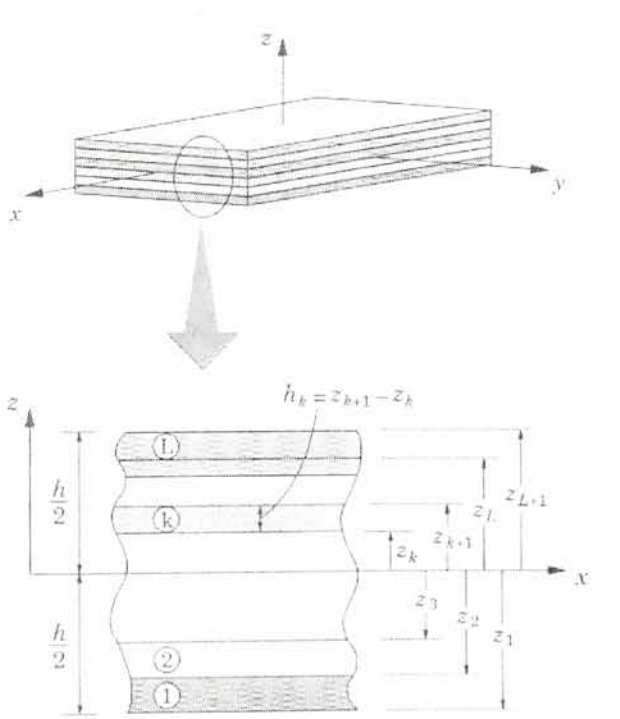

Figure 4.2

We will depart from the convention of numbering the layers from the bottom up to have the layer numbering coincide with the USPT, but will still integrate from the bottom surface to the top surface through the thickness of the plate such that for the sandwich plate the thickness vector Z is given by $Z=\{-h_3-h_2/2,\ -h_2/2,\ h_2/2,\ h_1+h_2/2\}$.

For the three layer sandwich plate all of the layer stiffnesses $Q_{ij}^{(k)}\ \ k=1,2,3$ will take the form of (2.5.10) with the only exception being that core in general does not obey the isotropic relation between the modulus of elasticity and the shear modulus given in (2.5.11). The core will have a specific value for the shear modulus unlike the face layers which will be considered isotropic. We will not make use of the ability to use orthotropic layers, in particular fiber reinforced layers but the TSDT is presented in full generality so the extension can easily be made by the reader.

4.5 Simply Supported Plate Solution

The analytical solution of the partial differential equations in (4.3.7) for a general laminate with arbitrary boundary conditions is not possible. But for the simply supported boundary conditions the Navier solution procedure can be used to examine the solution of (4.3.7) for antisymmetric cross-ply laminates as well as angle-ply laminates.

Cross-ply laminates are such that the material coordinates of each orthotropic layer are related by angles that are multiples of 90 degrees (this is arbitrary for isotropic layers and thus for our analysis) and angle-ply laminates are composed of layers such that at least one of the material coordinates is at angle that is not a multiple of 90 degrees. The two types of laminate require different Navier solutions and boundary condition formulation [3]. We will restrict our analysis to cross-ply laminates because we want to analyze the sandwich plate composed of three isotropic layers to make the comparison to the USPT.

The boundary conditions when all edges of the cross-ply plate are simply supported from (4.3.8) and (4.3.9) are

along $x=0$ and $x=a$

I. $N_1=0$
II. $v=0$
III. $\left(M_1-c_1P_6\right)=0$
IV. $\psi_y=0$
V. $P_1=0$
VI. $w=0$

(4.5.1)

along $y=0$ and $y=b$

I. $u=0$
II. $N_2=0$
III. $\psi_x=0$
IV. $\left(M_2-c_1P_2\right)=0$
V. $P_2=0$
VI. $w=0$

(4.5.2)

Following the Navier solution procedure for cross-ply laminates the following form of spatial variation of $(u, v, \psi_x, \psi_y, w)$ satisfies the conditions (4.5.1) and (4.5.2)

$$
\begin{aligned}
u &= \sum_{m=1}^{\infty}\sum_{n=1}^{\infty} U_{mn}(t)\cos\alpha x \sin\beta y \\
v &= \sum_{m=1}^{\infty}\sum_{n=1}^{\infty} V_{mn}(t)\sin\alpha x \cos\beta y \\
\psi_x &= \sum_{m=1}^{\infty}\sum_{n=1}^{\infty} X_{mn}(t)\cos\alpha x \sin\beta y \\
\psi_y &= \sum_{m=1}^{\infty}\sum_{n=1}^{\infty} Y_{mn}(t)\sin\alpha x \cos\beta y \\
w &= \sum_{m=1}^{\infty}\sum_{n=1}^{\infty} W_{mn}(t)\sin\alpha x \sin\beta y
\end{aligned}
\tag{4.5.3}
$$

where $\alpha = m\pi/a$ and $\beta = n\pi/b$.

Substituting (4.5.3) into (4.3.7) and collecting the coefficients the following equation is obtained

$$
[\hat{m}]\underline{\ddot{u}} + [\hat{s}]\underline{u} = \underline{0} \tag{4.5.4}
$$

$$
\underline{u} = \begin{Bmatrix} U_{mn} \\ V_{mn} \\ X_{mn} \\ Y_{mn} \\ W_{mn} \end{Bmatrix}
\quad
[\hat{m}] = \begin{Bmatrix} \hat{m}_{11} & 0 & \hat{m}_{13} & 0 & \hat{m}_{15} \\ 0 & \hat{m}_{22} & 0 & \hat{m}_{24} & \hat{m}_{25} \\ \hat{m}_{31} & 0 & \hat{m}_{33} & 0 & \hat{m}_{35} \\ 0 & \hat{m}_{42} & 0 & \hat{m}_{44} & \hat{m}_{45} \\ \hat{m}_{51} & \hat{m}_{52} & \hat{m}_{53} & \hat{m}_{54} & \hat{m}_{55} \end{Bmatrix}
\quad
[\hat{s}] = \begin{Bmatrix} \hat{s}_{11} & \hat{s}_{12} & \hat{s}_{13} & \hat{s}_{14} & \hat{s}_{15} \\ \hat{s}_{21} & \hat{s}_{22} & \hat{s}_{23} & \hat{s}_{24} & \hat{s}_{25} \\ \hat{s}_{31} & \hat{s}_{32} & \hat{s}_{33} & \hat{s}_{34} & \hat{s}_{35} \\ \hat{s}_{41} & \hat{s}_{42} & \hat{s}_{43} & \hat{s}_{44} & \hat{s}_{45} \\ \hat{s}_{51} & \hat{s}_{52} & \hat{s}_{53} & \hat{s}_{54} & \hat{s}_{55} \end{Bmatrix}
$$

For the case of free vibration the solution of (4.5.4) is converted to a standard eigenvalue problem if $\underline{u}(x, y, t) = \underline{U}(x, y)e^{i\omega t}$ then

$$
[D - \lambda I]\underline{U} = \underline{0}
$$

where $\mathbf{D}$, the dynamic matrix is $[D] = [\hat{m}]^{-1}[\hat{s}]$, $\mathbf{I}$ is the identity matrix and $\lambda = \omega^2$ which is the square of the corresponding frequency of vibration. Where the $\hat{m}_{ij}$ and $\hat{s}_{ij}$ are given by

$$\hat{m}_{11} = -I_0 \qquad \hat{m}_{13} = -I_1 + c_1 I_3$$
$$\hat{m}_{15} = \alpha c_1 I_3 \qquad \hat{m}_{22} = -I_0$$
$$\hat{m}_{24} = -I_1 + c_1 I_3 \qquad \hat{m}_{25} = \beta c_1 I_3$$
$$\hat{m}_{33} = -I_2 + 2c_1 I_4 - c_1^2 I_6 \qquad \hat{m}_{35} = \alpha c_1 I_4 - \alpha c_1^2 I_6$$
$$\hat{m}_{44} = -I_2 + 2c_1 I_4 - c_1^2 I_6 \qquad \hat{m}_{45} = \beta c_1 I_4 - \beta c_1^2 I_6$$
$$\hat{m}_{55} = -I_0 - \alpha^2 c_1^2 I_6 - \beta^2 c_1^2 I_6$$

(4.5.5)

$$\hat{s}_{11} = -\alpha^2 A_{11} - \beta^2 A_{66} \qquad \hat{s}_{12} = -\alpha\beta\left(A_{12} + A_{66}\right)$$
$$\hat{s}_{13} = -\alpha^2\left(B_{11} - c_1 E_{11}\right) - \beta^2\left(B_{66} - c_1 E_{66}\right) \qquad \hat{s}_{14} = -\alpha\beta\left[\left(B_{12} + B_{66}\right) + c_1\left(E_{12} + E_{66}\right)\right]$$
$$\hat{s}_{15} = \alpha c_1\left(\alpha^2 E_{11} + \beta^2 E_{12} + 2\beta^2 E_{66}\right) \qquad \hat{s}_{22} = -\beta^2 A_{22} - \alpha^2 A_{66}$$
$$\hat{s}_{23} = \hat{s}_{14} \qquad \hat{s}_{24} = -\beta^2\left(B_{11} - c_1 E_{11}\right) - \alpha^2\left(B_{66} - c_1 E_{66}\right)$$
$$\hat{s}_{25} = \beta c_1\left(\beta^2 E_{22} + \alpha^2 E_{21} + 2\alpha^2 E_{66}\right)$$
$$\hat{s}_{33} = -A_{55}^s + 2c_2 D_{55}^s - c_2^2 F_{55}^s - \alpha^2\left(D_{11} - 2c_1 F_{11} + c_1^2 H_{11}\right) - \beta^2\left(D_{66} - 2c_1 F_{66} + c_1^2 H_{66}\right)$$
$$\hat{s}_{34} = -\alpha\beta\left[D_{11} + D_{66} + 2c_1\left(F_{12} + F_{66}\right) - c_1^2\left(H_{12} + H_{66}\right)\right]$$
$$\hat{s}_{35} = -\alpha\left(A_{55}^s - 2c_2 D_{55}^s + c_2^2 F_{55}^s\right) + \alpha c_1\left(\alpha^2 F_{11} + \beta^2 F_{12} + 2\beta^2 F_{66}\right) - \alpha c_1^2\left(\alpha^2 H_{11} + \beta^2 H_{12} + 2\beta^2 H_{66}\right)$$
$$\hat{s}_{44} = -A_{44}^s + 2c_2 D_{44}^s - c_2^2 F_{44}^s - \beta^2\left(D_{22} - 2c_1 F_{22} + c_1^2 H_{22}\right) - \alpha^2\left(D_{66} - 2c_1 F_{66} + c_1^2 H_{66}\right)$$
$$\hat{s}_{45} = -\beta\left(A_{44}^s - 2c_2 D_{44}^s + c_2^2 F_{44}^s\right) + \beta c_1\left(\beta^2 F_{22} + \alpha^2 F_{12} + 2\alpha^2 F_{66}\right) - \beta c_1^2\left(\beta^2 H_{22} + \alpha^2 H_{12} + 2\alpha^2 H_{66}\right)$$
$$\hat{s}_{55} = -\alpha^2\left(A_{55}^s - 2c_2 D_{55}^s + c_2^2 F_{55}^s\right) - \beta^2\left(A_{44}^s - 2c_2 D_{44}^s + c_2^2 F_{44}^s\right) - c_1^2\left[\alpha^4 H_{11} + 2\alpha^2\beta^2\left(H_{12} + 2H_{66}\right) + \beta^4 H_{22}\right]$$

(4.5.6)

4.6 *Uncoupled Equations of Motion*

For the extension and bending effects in the equations of motion for the TSDT to be uncoupled the plate stiffnesses (stress resultant coefficients) B_{ij} and E_{ij} defined in (4.4.4) must be zero. For a laminate composed of orthotropic layers this occurs for laminates that are symmetric about the midplane of the plate, and because we are restricting ourselves to cross-ply laminates composed of orthotropic layers the inplane and out of plane components of the plate stiffnesses are also uncoupled, so the following plate stiffnesses are identically zero for the uncoupled equations of motion

$$\begin{aligned} &B_{ij} = E_{ij} = 0 \quad \left(i, j = 1, 2, 6, 4, 5\right) \\ &A_{16} = A_{26} = D_{16} = D_{26} = F_{16} = F_{26} = H_{16} = H_{26} = 0 \\ &A_{45}^s = D_{45}^s = F_{45}^s = 0 \end{aligned} \tag{4.6.1}$$

Having uncoupled the equations of motion we focus on the transverse equations of motion, and as a result of the complicated nature of the TSDT and given that we seek to obtain the equations of motion in terms of the displacements, only the uncoupled transversely simplified equations will be presented.

Along with the restriction made in **4.5** for the simply supported plate solution we added an additional restriction such that the TSDT is held to the restrictions

1. The laminate is a cross-ply laminate (i.e. the material coordinates of each layer is related by angles that are multiples of 90 degrees)
2. The laminate is symmetric about the midplane of the laminate (with respect to thickness)

and we make the additional *assumption*

3. The in-plane and rotary inertia effects of the plate can be neglected and only the transverse inertia effects are considered

This results in the following transversely simplified equations of motion

$$\begin{aligned}
&\frac{\partial}{\partial x}\left(M_1 - c_1 P_1\right) + \frac{\partial}{\partial y}\left(M_6 - c_1 P_6\right) - \left(Q_5 - c_2 R_5\right) = 0 \\
&\frac{\partial}{\partial y}\left(M_2 - c_1 P_2\right) + \frac{\partial}{\partial x}\left(M_6 - c_1 P_6\right) - \left(Q_4 - c_2 R_4\right) = 0 \\
&\frac{\partial}{\partial x}\left(Q_5 - c_2 R_5\right) + \frac{\partial}{\partial y}\left(Q_4 - c_2 R_4\right) + c_1\left(\frac{\partial^2 P_1}{\partial x^2} + 2\frac{\partial^2 P_6}{\partial x \partial y} + \frac{\partial^2 P_2}{\partial y^2}\right) = I_0 \ddot{w}
\end{aligned} \tag{4.6.2}$$

The corresponding boundary conditions are

$x = 0$ and $x = a$

$M_1 - c_1 P_1 = 0$ or ψ_x is specified

$M_6 - c_1 P_6 = 0$ or ψ_y is specified

$P_1 = 0$ or $\dfrac{\partial w}{\partial x}$ is specified

$\left(Q_5 - c_2 R_5\right) + c_1\left(\dfrac{\partial P_1}{\partial x} + 2\dfrac{\partial P_6}{\partial y}\right) = 0$ or w is specified

(4.6.3)

$y = 0$ and $y = b$

$M_6 - c_1 P_6 = 0$ or ψ_x is specified

$M_2 - c_1 P_2 = 0$ or ψ_y is specified

$$P_2 = 0 \text{ or } \frac{\partial w}{\partial y} \text{ is specified}$$

$$\left(Q_4 - c_2 R_4\right) + c_1\left(\frac{\partial P_2}{\partial y} + 2\frac{\partial P_6}{\partial x}\right) = 0 \text{ or } w \text{ is specified} \tag{4.6.4}$$

and for the free edge reaction at the corner

$$-2c_1 P_6 = 0\,. \tag{4.6.5}$$

utilizing (4.6.1) the stress resultants in terms of the displacements are given by

$$\begin{aligned}
M_1 &= \left(D_{11} - c_1 F_{11}\right)\psi_{x,x} + \left(D_{12} - c_1 F_{12}\right)\psi_{y,y} + \left(-c_1 F_{11}\right) w_{,xx} + \left(-c_1 F_{12}\right) w_{,yy} \\
M_2 &= \left(D_{12} - c_1 F_{12}\right)\psi_{x,x} + \left(D_{22} - c_1 F_{22}\right)\psi_{y,y} + \left(-c_1 F_{12}\right) w_{,xx} + \left(-c_1 F_{22}\right) w_{,yy} \\
M_6 &= \left(D_{66} - c_1 F_{66}\right)\psi_{x,y} + \left(D_{66} - c_1 F_{66}\right)\psi_{y,x} + \left(-c_1 F_{66}\right) w_{,xy} \\
P_1 &= \left(F_{11} - c_1 H_{11}\right)\psi_{x,x} + \left(F_{12} - c_1 H_{12}\right)\psi_{y,y} + \left(-c_1 H_{11}\right) w_{,xx} + \left(-c_1 H_{12}\right) w_{,yy} \\
P_2 &= \left(F_{12} - c_1 H_{12}\right)\psi_{x,x} + \left(F_{22} - c_1 H_{22}\right)\psi_{y,y} + \left(-c_1 H_{12}\right) w_{,xx} + \left(-c_1 H_{22}\right) w_{,yy} \\
P_6 &= \left(F_{66} - c_1 H_{66}\right)\psi_{x,y} + \left(F_{66} - c_1 H_{66}\right)\psi_{y,x} + \left(-c_1 H_{66}\right) w_{,xy} \\
Q_4 &= \left(A^s_{44} - c_2 D^s_{44}\right)\psi_y + \left(A^s_{44} - c_2 D^s_{44}\right) w_{,y} \\
Q_5 &= \left(A^s_{55} - c_2 D^s_{55}\right)\psi_x + \left(A^s_{55} - c_2 D^s_{55}\right) w_{,x} \\
R_4 &= \left(D^s_{44} - c_2 F^s_{44}\right)\psi_y + \left(D^s_{44} - c_2 F^s_{44}\right) w_{,y} \\
R_5 &= \left(D^s_{55} - c_2 F^s_{55}\right)\psi_x + \left(D^s_{55} - c_2 F^s_{55}\right) w_{,x}
\end{aligned} \tag{4.6.6}$$

substituting (4.6.6) into (4.6.2) we obtain

$$\begin{aligned}
&\hat{\Theta}_1\psi_y + \hat{\Theta}_2\psi_{y,yy} + \hat{\Theta}_3\psi_{y,xx} + \hat{\Theta}_4\psi_{x,xy} + \hat{\Theta}_5 w_{,y} + \hat{\Theta}_6 w_{,yyy} + \hat{\Theta}_7 w_{,yxx} = 0 \\
&\hat{\Theta}_8\psi_x + \hat{\Theta}_9\psi_{x,xx} + \hat{\Theta}_{10}\psi_{x,yy} + \hat{\Theta}_{11}\psi_{y,xy} + \hat{\Theta}_{12} w_{,x} + \hat{\Theta}_{13} w_{,xxx} + \hat{\Theta}_{14} w_{,xyy} = 0 \\
&\hat{\Theta}_{15} w_{,xxxx} + \hat{\Theta}_{16} w_{,xxyy} + \hat{\Theta}_{17} w_{,yyyy} + \hat{\Theta}_{18}\psi_{x,xxx} + \hat{\Theta}_{19}\psi_{x,xyy} + \hat{\Theta}_{20}\psi_{y,yyy} + \hat{\Theta}_{21}\psi_{y,yxx} \\
&+ \hat{\Theta}_{22}\psi_{x,x} + \hat{\Theta}_{23}\psi_{y,y} + \hat{\Theta}_{24} w_{,xx} + \hat{\Theta}_{25} w_{,yy} = \hat{g}_0 \ddot{w}
\end{aligned} \tag{4.6.7}$$

where

$$\begin{aligned}
\hat{\Theta}_1 &= -A^s_{44} + 2c_2 D^s_{44} - c_2^2 F^s_{44} & \hat{\Theta}_2 &= D_{22} - 2c_1 F_{22} + c_1^2 H_{22} \\
\hat{\Theta}_3 &= D_{66} - 2c_1 F_{66} + c_1^2 H_{66} & \hat{\Theta}_4 &= \hat{\Theta}_3 + \left(D_{12} - 2c_1 F_{12} + c_1^2 H_{12}\right) \\
\hat{\Theta}_5 &= \hat{\Theta}_1 & \hat{\Theta}_6 &= -c_1 F_{22} + c_1^2 H_{22} \\
\hat{\Theta}_7 &= -c_1 F_{12} + c_1^2 H_{12} - 2c_1 F_{66} + 2c_1^2 H_{66} & \hat{\Theta}_8 &= -A^s_{55} + 2c_2 D^s_{55} - c_2^2 F^s_{55} \\
\hat{\Theta}_9 &= D_{11} - 2c_1 F_{11} + c_1^2 H_{11} & \hat{\Theta}_{10} &= \hat{\Theta}_3
\end{aligned}$$

$$\hat{\Theta}_{11} = \hat{\Theta}_4 \qquad \hat{\Theta}_{12} = \hat{\Theta}_8$$
$$\hat{\Theta}_{13} = -c_1 F_{11} + c_1^2 H_{11} \qquad \hat{\Theta}_{14} = \hat{\Theta}_7$$
$$\hat{\Theta}_{15} = -c_1^2 H_{11} \qquad \hat{\Theta}_{16} = -2c_1^2 H_{12} - 4c_1^2 H_{66}$$
$$\hat{\Theta}_{17} = -c_1^2 H_{22} \qquad \hat{\Theta}_{18} = -\hat{\Theta}_{13}$$
$$\hat{\Theta}_{19} = -\hat{\Theta}_7 \qquad \hat{\Theta}_{20} = -\hat{\Theta}_6$$
$$\hat{\Theta}_{21} = \hat{\Theta}_{19} \qquad \hat{\Theta}_{22} = -\hat{\Theta}_8$$
$$\hat{\Theta}_{23} = -\hat{\Theta}_1 \qquad \hat{\Theta}_{24} = \hat{\Theta}_{22}$$
$$\hat{\Theta}_{25} = \hat{\Theta}_{23} \qquad \hat{g}_0 = I_0$$

(4.6.8)

and the corresponding boundary conditions are

$x = 0$ and $x = a$

$\hat{\Xi}_1 \psi_{x,x} + \hat{\Xi}_2 \psi_{y,y} + \hat{\Xi}_3 w_{,xx} + \hat{\Xi}_4 w_{,yy} = 0$ or ψ_x is specified

$\hat{\Xi}_9 \psi_{x,y} + \hat{\Xi}_{10} \psi_{y,x} + \hat{\Xi}_{11} w_{,xy} = 0$ or ψ_y is specified

$\hat{\Xi}_{26} \psi_{x,x} + \hat{\Xi}_{27} \psi_{y,y} + \hat{\Xi}_{28} w_{,xx} + \hat{\Xi}_{29} w_{,yy} = 0$ or $w_{,x}$ is specified

$\hat{\Xi}_{12} \psi_x + \hat{\Xi}_{13} \psi_{x,xx} + \hat{\Xi}_{14} \psi_{x,yy} + \hat{\Xi}_{15} \psi_{y,xy} + \hat{\Xi}_{16} w_{,x} + \hat{\Xi}_{17} w_{,xxx} + \hat{\Xi}_{18} w_{,xyy} = 0$ or w is specified

(4.6.9)

$y = 0$ and $y = b$

$\hat{\Xi}_9 \psi_{x,y} + \hat{\Xi}_{10} \psi_{y,x} + \hat{\Xi}_{11} w_{,xy} = 0$ or ψ_x is specified

$\hat{\Xi}_5 \psi_{y,y} + \hat{\Xi}_6 \psi_{x,x} + \hat{\Xi}_7 w_{,yy} + \hat{\Xi}_8 w_{,xx} = 0$ or ψ_y is specified

$\hat{\Xi}_{30} \psi_{y,y} + \hat{\Xi}_{31} \psi_{x,x} + \hat{\Xi}_{32} w_{,yy} + \hat{\Xi}_{33} w_{,xx} = 0$ or $w_{,y}$ is specified

$\hat{\Xi}_{19} \psi_y + \hat{\Xi}_{20} \psi_{y,yy} + \hat{\Xi}_{21} \psi_{y,xx} + \hat{\Xi}_{22} \psi_{x,xy} + \hat{\Xi}_{23} w_{,y} + \hat{\Xi}_{24} w_{,yyy} + \hat{\Xi}_{25} w_{,yxx} = 0$ or w is specified

(4.6.10)

where

$$\hat{\Xi}_1 = \hat{\Theta}_9 \qquad \hat{\Xi}_2 = \hat{\Theta}_4 - \hat{\Theta}_3$$
$$\hat{\Xi}_3 = \hat{\Theta}_{13} \qquad \hat{\Xi}_4 = -c_1 F_{12} + c_1^2 H_{12}$$
$$\hat{\Xi}_5 = \hat{\Theta}_2 \qquad \hat{\Xi}_6 = \hat{\Xi}_2$$
$$\hat{\Xi}_7 = \hat{\Theta}_6 \qquad \hat{\Xi}_8 = \hat{\Xi}_4$$
$$\hat{\Xi}_9 = \hat{\Theta}_3 \qquad \hat{\Xi}_{10} = \hat{\Theta}_3$$
$$\hat{\Xi}_{11} = \hat{\Theta}_7 - \hat{\Xi}_4 \qquad \hat{\Xi}_{12} = -\hat{\Theta}_8$$
$$\hat{\Xi}_{13} = \hat{\Theta}_{18} \qquad \hat{\Xi}_{14} = -\hat{\Xi}_{11}$$
$$\hat{\Xi}_{15} = \hat{\Theta}_{19} \qquad \hat{\Xi}_{16} = \hat{\Xi}_{12}$$

$$
\begin{aligned}
\hat{\Xi}_{17} &= \hat{\Theta}_{15} & \hat{\Xi}_{18} &= -c_1^2 H_{12} - 4c_1^2 H_{66} \\
\hat{\Xi}_{19} &= -\hat{\Theta}_{1} & \hat{\Xi}_{20} &= \hat{\Theta}_{20} \\
\hat{\Xi}_{21} &= \hat{\Xi}_{14} & \hat{\Xi}_{22} &= \hat{\Xi}_{15} \\
\hat{\Xi}_{23} &= \hat{\Xi}_{19} & \hat{\Xi}_{24} &= \hat{\Theta}_{17} \\
\hat{\Xi}_{25} &= \hat{\Xi}_{18} & \hat{\Xi}_{26} &= \frac{\hat{\Theta}_{13}}{-c_1} \\
\hat{\Xi}_{27} &= \frac{\hat{\Xi}_{4}}{-c_1} & \hat{\Xi}_{28} &= \frac{\hat{\Theta}_{15}}{c_1} \\
\hat{\Xi}_{29} &= -c_1 H_{12} & \hat{\Xi}_{30} &= \frac{\hat{\Theta}_{6}}{-c_1} \\
\hat{\Xi}_{31} &= \hat{\Xi}_{27} & \hat{\Xi}_{32} &= \frac{\hat{\Theta}_{17}}{c_1} \\
\hat{\Xi}_{33} &= \hat{\Xi}_{29}
\end{aligned}
\qquad (4.6.11)
$$

The extension and bending effects are uncoupled and now the transversely simplified equations of motion in (4.6.7) can be used to investigate the free vibration of the symmetric cross-ply laminate cantilever plate.

4.7 Non-Dimensional Transverse Simplified TSDT

Following the same procedure for the USPT in **3.7** the transverse simplified equations of motion and corresponding boundary conditions will be non-dimensionalized by introducing the following dimensionless variables

$$
\xi = \frac{x}{a} \qquad \eta = \frac{y}{b} \qquad W = \frac{w}{a} \qquad \psi_\xi = \psi_x \qquad \psi_\eta = \psi_y \qquad (4.7.1)
$$

where ξ is defined on the interval $[0,1]$ and η is defined on the interval $[0,\phi]$ with $\phi = b/a$.

Now we can substitute (4.7.1) into (4.6.7) and the resultant non-dimensional equations of motion are

$$
\begin{aligned}
&\Theta_1\psi_\eta + \Theta_2\psi_{\eta,\eta\eta} + \Theta_3\psi_{\eta,\xi\xi} + \Theta_4\psi_{\xi,\xi\eta} + \Theta_5 W_{,\eta} + \Theta_6 W_{,\eta\eta\eta} + \Theta_7 W_{,\eta\xi\xi} = 0 \\
&\Theta_8\psi_\xi + \Theta_9\psi_{\xi,\xi\xi} + \Theta_{10}\psi_{\xi,\eta\eta} + \Theta_{11}\psi_{\eta,\xi\eta} + \Theta_{12} W_{,\xi} + \Theta_{13} W_{,\xi\xi\xi} + \Theta_{14} W_{,\xi\eta\eta} = 0 \\
&\Theta_{15} W_{,\xi\xi\xi\xi} + \Theta_{16} W_{,\xi\xi\eta\eta} + \Theta_{17} W_{,\eta\eta\eta\eta} + \Theta_{18}\psi_{\xi,\xi\xi\xi} + \Theta_{19}\psi_{\xi,\xi\eta\eta} + \Theta_{20}\psi_{\eta,\eta\eta\eta} + \Theta_{21}\psi_{\eta,\eta\xi\xi} \\
&+\Theta_{22}\psi_{\xi,\xi} + \Theta_{23}\psi_{\eta,\eta} + \Theta_{24} w_{,\xi\xi} + \Theta_{25} w_{,\eta\eta} = g_0 \ddot{w}
\end{aligned}
\qquad (4.7.2)
$$

where

$$\Theta_i = \begin{cases} i = (1,5,8,12,22,23,24,25) & \Theta_i = a^2\hat{\Theta}_i \\ i \neq (1,5,8,12,22,23,24,25) & \Theta_i = \hat{\Theta}_i \end{cases} \quad (i = 1,2,3,...,21)$$
$$g_0 = a^4 \hat{g}_0 \tag{4.7.3}$$

Then taking dimensionless variables of the form

$$\begin{aligned} W &= W(\xi,\eta)e^{i\omega t} \\ \psi_\xi &= \psi_\xi(\xi,\eta)e^{i\omega t} \\ \psi_\eta &= \psi_\eta(\xi,\eta)e^{i\omega t} \end{aligned} \tag{4.7.4}$$

where ω is the circular frequency of free vibration, and substituting into (4.7.2) we now have the non-dimensional equations of motion as functions of the spatial variables for a given frequency

$$\begin{aligned} &\Theta_1\psi_\eta + \Theta_2\psi_{\eta,\eta\eta} + \Theta_3\psi_{\eta,\xi\xi} + \Theta_4\psi_{\xi,\xi\eta} + \Theta_5 W_{,\eta} + \Theta_6 W_{,\eta\eta\eta} + \Theta_7 W_{,\eta\xi\xi} = 0 \\ &\Theta_8\psi_\xi + \Theta_9\psi_{\xi,\xi\xi} + \Theta_{10}\psi_{\xi,\eta\eta} + \Theta_{11}\psi_{\eta,\xi\eta} + \Theta_{12}W_{,\xi} + \Theta_{13}W_{,\xi\xi\xi} + \Theta_{14}W_{,\xi\eta\eta} = 0 \\ &\Theta_{15}W_{,\xi\xi\xi\xi} + \Theta_{16}W_{,\xi\xi\eta\eta} + \Theta_{17}W_{,\eta\eta\eta\eta} + \Theta_{18}\psi_{\xi,\xi\xi\xi} + \Theta_{19}\psi_{\xi,\xi\eta\eta} + \Theta_{20}\psi_{\eta,\eta\eta\eta} + \Theta_{21}\psi_{\eta,\eta\xi\xi} \\ &+ \Theta_{22}\psi_{\xi,\xi} + \Theta_{23}\psi_{\eta,\eta} + \Theta_{24}w_{,\xi\xi} + \Theta_{25}w_{,\eta\eta} + \omega^2 g_0 W = 0 \end{aligned} \tag{4.7.5}$$

The corresponding boundary conditions are

$\xi = 0$ and $\xi = 1$

$\Xi_1\psi_{\xi,\xi} + \Xi_2\psi_{\eta,\eta} + \Xi_3 W_{,\xi\xi} + \Xi_4 W_{,\eta\eta} = 0$ or ψ_ξ is specified

$\Xi_9\psi_{\xi,\eta} + \Xi_{10}\psi_{\eta,\xi} + \Xi_{11}W_{,\xi\eta} = 0$ or ψ_η is specified

$\Xi_{26}\psi_{\xi,\xi} + \Xi_{27}\psi_{\eta,\eta} + \Xi_{28}W_{,\xi\xi} + \Xi_{29}W_{,\eta\eta} = 0$ or $W_{,\xi}$ is specified

$\Xi_{12}\psi_\xi + \Xi_{13}\psi_{\xi,\xi\xi} + \Xi_{14}\psi_{\xi,\eta\eta} + \Xi_{15}\psi_{\eta,\xi\eta} + \Xi_{16}W_{,\xi} + \Xi_{17}W_{,\xi\xi\xi} + \Xi_{18}W_{,\xi\eta\eta} = 0$ or W is specified

(4.7.6)

$\eta = 0$ and $\eta = \phi$

$\Xi_9\psi_{\xi,\eta} + \Xi_{10}\psi_{\eta,\xi} + \Xi_{11}W_{,\xi\eta} = 0$ or ψ_ξ is specified

$\Xi_5\psi_{\eta,\eta} + \Xi_6\psi_{\xi,\xi} + \Xi_7 W_{,\eta\eta} + \Xi_8 W_{,\xi\xi} = 0$ or ψ_η is specified

$\Xi_{30}\psi_{\eta,\eta} + \Xi_{31}\psi_{\xi,\xi} + \Xi_{32}W_{,\eta\eta} + \Xi_{33}W_{,\xi\xi} = 0$ or $W_{,\eta}$ is specified

$\Xi_{19}\psi_\eta + \Xi_{20}\psi_{\eta,\eta\eta} + \Xi_{21}\psi_{\eta,\xi\xi} + \Xi_{22}\psi_{\xi,\xi\eta} + \Xi_{23}W_{,\eta} + \Xi_{24}W_{,\eta\eta\eta} + \Xi_{25}W_{,\eta\xi\xi} = 0$ or W is specified

(4.7.7)

where

$$\Xi_i = \hat{\Xi}_i \tag{4.7.8}$$

and for some i and j if $\hat{\Xi}_i = \hat{\Theta}_j$ then it directly follows that $\Xi_i = \Theta_j$ (e.g. $\Xi_{19} = -\Theta_1 = -a^2\hat{\Theta}_1$).

5 Numerical Results 1

5.1 Introduction

This chapter contains the numerical results for both the USPT and TSDT for simply supported boundary conditions along with results obtained using the finite element software package ANSYS. The prediction of the first frequency of vibration and the corresponding loss factor for the damped case are determined for variations of the geometric and material properties of the simply supported sandwich plate.

5.2 Simply Supported Plates

5.2.1 Verification

Taking the eigenvalue problem (3.5.5) formulated in **3.5** for the USPT and **4.5** for the TSDT for the simply supported (SSSS) plate and implementing the symbolic computing software *Mathematica* solutions are obtained for the modal frequency and mode shapes of a given modal number (m,n). Programs were created for the SSSS solution for the USPT and the TSDT named *USPT-SSSS.nb* and *TSDT-SSSS.nb* respectively (the program codes are not listed, and the creation of similar codes in any number of numerical computing programs should be of no trouble to the analyst). To ensure the accuracy of the investigation of rectangular sandwich plates the programs created in *Mathematica* are verified by computing previously published results.

Verification for the USPT is conducted by computing the non-dimensional frequency, λ reported in the work of Rao and Nakra [1] which is listed in Table 5.1. The non-dimensional frequency was tabulated for various modal numbers by Rao and Nakra using the following parameters

$$E_1 = E_3,\quad G_2 = 1\times10^{-5}E_1,\quad \nu_1 = \nu_3,\quad \rho_1 = \rho_3,\quad \rho_2 = \rho_1/2,\quad a = b,\quad h_3 = .0125a/\pi,$$
$$h_1 = .7h_3,\quad h_2 = 10h_3 \qquad (5.2.1)$$

Modal number		Non-dimensional frequency parameter λ for various families of modes				
m	n	I$\times 10^8$	II$\times 10^4$	III$\times 10^4$	IV$\times 10^4$	V$\times 10^3$
1	1	0.73	0.295	0.623	0.842	0.176
1	3	7.22	1.473	3.069	4.207	0.875
2	5	45.623	4.27	8.878	12.197	2.534
5	5	125.67	7.362	15.297	21.032	4.369
4	7	206.99	9.37	19.884	27.342	5.679
3	8	258.59	10.748	22.329	30.707	6.377
2	9	346.73	12.515	25.998	35.754	7.425
5	8	378.96	13.103	27.221	37.437	7.775
7	7	456.72	14.428	29.973	41.223	8.562
1	10	484.24	14.87	30.889	42.484	8.822

Table 5.1 Non-dimensional frequencies reported by Rao and Nakra [1]

Modal number		Non-dimensional frequency parameter λ for various families of modes				
m	n	I$\times 10^8$	II$\times 10^4$	III$\times 10^4$	IV$\times 10^4$	V$\times 10^3$
1	1	0.724	0.295	0.623	0.842	0.176
1	3	7.222	1.473	3.069	4.207	0.875
2	5	45.633	4.270	8.878	12.199	2.535
5	5	125.695	7.362	15.298	21.033	4.369
4	7	207.044	9.570	19.884	27.342	5.680
3	8	258.660	10.748	22.329	30.708	6.379
2	9	346.814	12.515	25.998	35.755	7.428
5	8	379.060	13.103	27.221	37.438	7.778
7	7	456.840	14.428	29.973	41.224	8.565
1	10	484.375	14.870	30.890	42.486	8.827

Table 5.2 Non-dimensional frequencies calculated using *USPT-SSSS.nb* for the parameters (5.2.1)

Modal number		% Difference between published values and USPT-*SSSS.nb* for Non-dimensional frequency parameter λ for various families of modes				
m	n	$I\times10^{8}$	$II\times10^{4}$	$III\times10^{4}$	$IV\times10^{4}$	$V\times10^{3}$
1	1	0.76%	0.06%	0.00%	0.04%	0.08%
1	3	0.03%	0.02%	0.01%	0.00%	0.04%
2	5	0.02%	0.00%	0.00%	0.02%	0.02%
5	5	0.02%	0.00%	0.01%	0.00%	0.01%
4	7	0.03%	2.13%	0.00%	0.00%	0.02%
3	8	0.03%	0.00%	0.00%	0.00%	0.04%
2	9	0.02%	0.00%	0.00%	0.00%	0.04%
5	8	0.03%	0.00%	0.00%	0.00%	0.04%
7	7	0.03%	0.00%	0.00%	0.00%	0.03%
1	10	0.03%	0.00%	0.00%	0.00%	0.05%

Table 5.3 Difference between published results of Rao and Nakra [1] and *USPT-SSSS.nb*

Table 5.3 is a clear indication that the solutions for the SSSS boundary conditions using the program *USPT-SSSS.nb* are consistent with the solutions obtained by those obtained by Rao and Nakra. This verifies that the investigation of the SSSS plate using USPT is accurate and consistent with previous work.

Verification for the TSDT is done using two sets of published results by Reddy [2, 3] for the non-dimensional frequencies $\bar{\omega}$. The first set of results [2] are calculated for an isotropic plate with the following parameters

$$a/h=10,\quad b/a=1,\quad \nu=.3 \quad \text{with } \bar{\omega}=\omega h\sqrt{\rho/G}$$

where h is the thickness of the plate.

The second set of results [3] are calculated for a $(0/90/90/0)$ cross-ply laminate as a function of the modulus ratio E_1/E_2 with the following parameters for the layered material

$$G_{12}=G_{13}=.6E_2,\quad G_{23}=.5E_2,\quad \nu_{12}=.25\quad a/h_T=[5,10]\quad (m,n)=(1,1)$$

with $\bar{\omega}=\omega\left(a^2/h_T\right)\sqrt{\rho/E_2}$, where the subscripts denote the material coordinates of the orthotropic layer and not the layer number.

Isotropic Plate [2]					$(0/90/90/0)$ cross-ply laminate with modal number $(1,1)$ [3]				
		$\bar{\omega} = \omega h\sqrt{\rho/G}$					$\bar{\omega} = \omega\left(a^2/h_T\right)\sqrt{\rho/E_2}$		
m	n	*TSDT-SSSS.nb*	Reddy	% Diff	E_1/E_2	a/h_T	*TSDT-SSSS.nb*	Reddy	% Diff
1	1	0.0930	0.0931	0.08%	3	5	6.560	6.560	0.00%
1	2	0.2220	0.2222	0.11%	3	10	7.243	7.243	0.00%
2	2	0.3406	0.3411	0.14%	10	5	8.272	8.272	0.00%
1	3	0.4151	0.4158	0.17%	10	10	9.841	9.853	0.12%
2	3	0.5208	0.5221	0.25%	20	5	9.526	9.526	0.00%
1	4	0.6525	0.6545	0.31%	20	10	12.218	12.238	0.16%
3	3	0.6840	0.6862	0.33%	30	5	10.272	10.272	0.00%
2	4	0.7454	0.7481	0.37%	30	10	13.864	13.892	0.20%
3	4	0.8908	0.8949	0.46%	40	5	10.787	10.787	0.00%
1	5	0.9187	0.923	0.47%	40	10	15.107	15.143	0.24%
2	5	1.0001	2.0053	50.13%					
4	4	1.0785	1.0847	0.58%					
3	5	1.1292	1.1361	0.61%					

Table 5.4 Comparison of results calculated using *TSDT-SSSS.nb* and results reported by Reddy [2],[3]

Table 5.4 shows that solutions for the SSSS boundary conditions are consistent with respect to the selected results obtained by Reddy. This verifies that the investigation of the SSSS plate using TSDT is accurate and consistent with previous work.

5.2.2 Initial Geometric and Material Properties

With verification of the programs created to analyze the SSSS plate a set of initial geometric and material properties are presented as a starting point. The initial geometry represents a thin plate that has a thick core with respect to the face layers.

The core thickness to total thickness ratio is $h_2/h_T = 5/6$ and the length to total thickness ratio is $a/h_T = 12.5$. The material properties of the face layer are for 2024-T4 Aluminum and the properties of core material HEREX C70.130 PVC foam at 30°C were experimentally obtained by Meunier and Shenoi [4].

The core is assumed to exhibit the properties of a linear viscoelastic solid, since we are restricting ourselves to harmonic analysis these properties can be represented by complex material coefficients, as show in **2.6**. For this portion of the analysis we will not introduce damping in the core and will later employ the linear elastic viscoelastic principle to introduce the viscoelastic behavior in the core. These initial material properties represent a sandwich plate with a "soft" shear deformable core, which is the subject of analysis.

Face Layers	Core	Dimensions
$E = 73.1$ GPa $\nu = .3$ $\rho = 2780\ \text{kg/m}^3$	$E = 113.5$ MPa $\nu = .32$ $\rho = 130\ \text{kg/m}^3$ $G = 18.86$ MPa	$a = 1.5$ m $b = a$ $h_1 = .01$ m $h_2 = .1$ m $h_3 = .01$ m

Table 5.5 Initial material and geometric properties for SSSS plate analysis

Given the initial properties in Table 5.5 the *first natural frequency* of vibration ω_{11} for the transverse deflection w which corresponds to the modal number $(m = 1,\ n = 1)$ is obtained for both theories and listed in Table 5.6. For the remained of the chapter it is understood that the first frequency denotes the modal number $(m = 1,\ n = 1)$ and all frequencies calculated correspond to the transverse deflection w, unless otherwise specified.

The reader will also notice that all frequencies reported are in rad/s and not in non-dimensional form. This is done to understand the true behavior of each theory with the variation of geometric and material properties. Depending on the parameters selected in non-dimensionalizing the frequencies the curves produced by variations of the parameters used in the non-dimensionalization are distorted. With this in mind variation of the geometric and material parameters with respect to the initial plate properties is conducted.

First frequency of vibration for the properties in Table 5.5	
TSDT	USPT
1601.66 rad/s	540.373 rad/s

Table 5.6 First frequencies for TSDT and USPT given the properties in Table 5.5

5.2.3 Geometric Variation

With the verification of the SSSS plate for both theories established the geometric properties of the plate are varied with respect to a set of initial geometric properties. All of the geometric properties of the plate are varied but of particular interest is the effect of variations on the length to total thickness and face thickness to core thickness ratios.

It should be noted that the variations are carried out over a range of values that cover values that are valid for both theories and also values that are outside of the definition of a plate.

The length to total thickness ratio should be 5 or greater for a moderately thick plate and 10 or greater for a thin plate as a rule of thumb. The extremes of the thick and thin plate are represented to see how the theories behave as they approach these limits with respect to the first frequency of the plate.

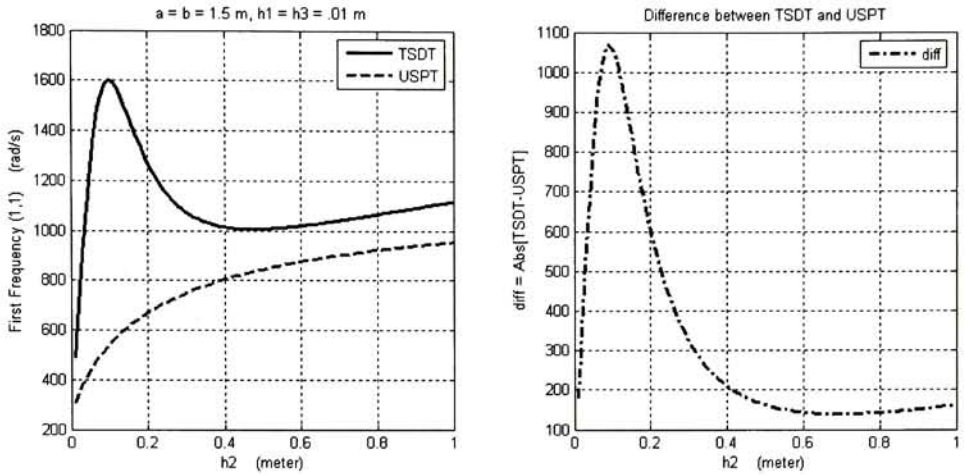

Figure 5.1 Variation of the First Frequency with Core Thickness

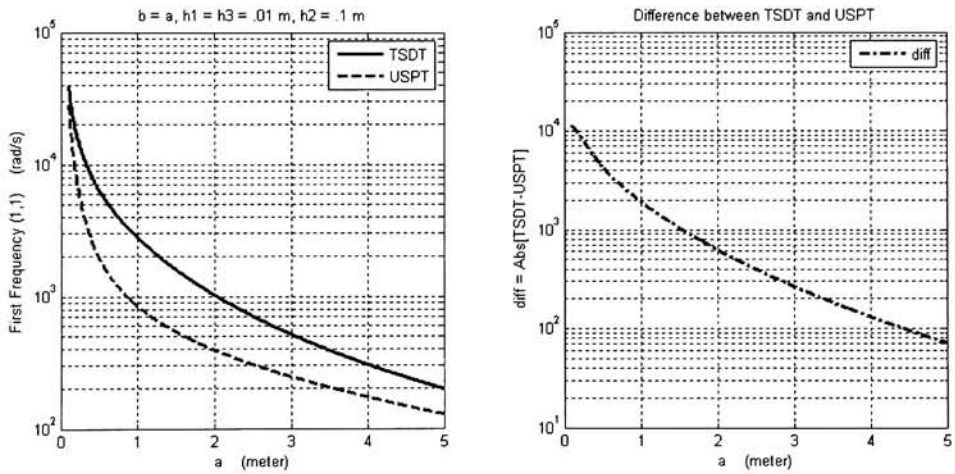

Figure 5.2 Variation of the First Frequency with the Length of a Square Plate

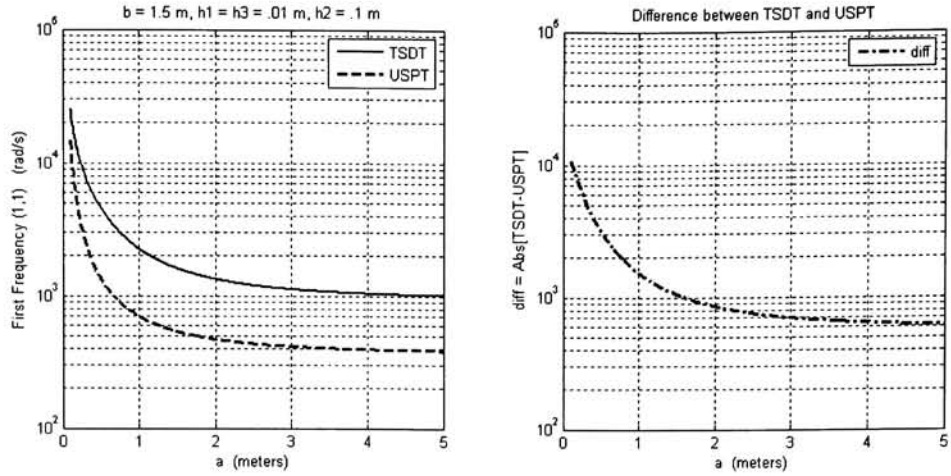

Figure 5.3 Variation of the First Frequency with the Length a in the x Direction

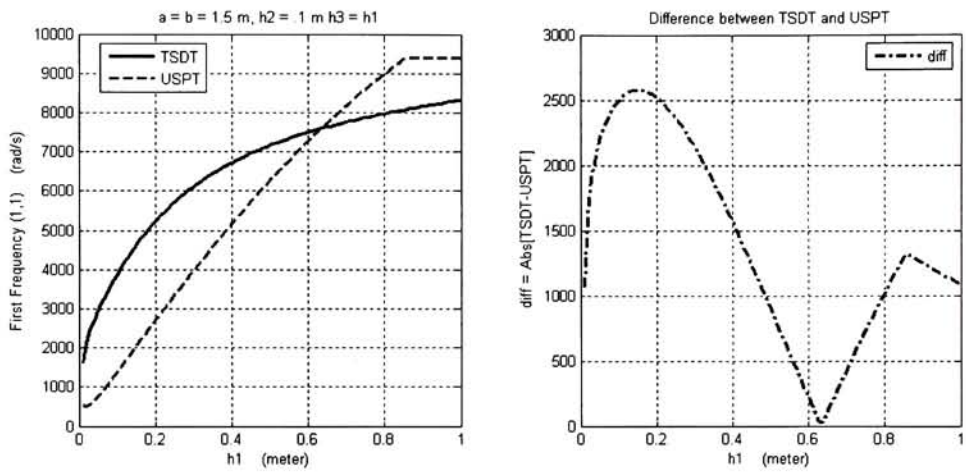

Figure 5.4 Variation of the First Frequency with Face Layer Thickness for a Symmetric Plate

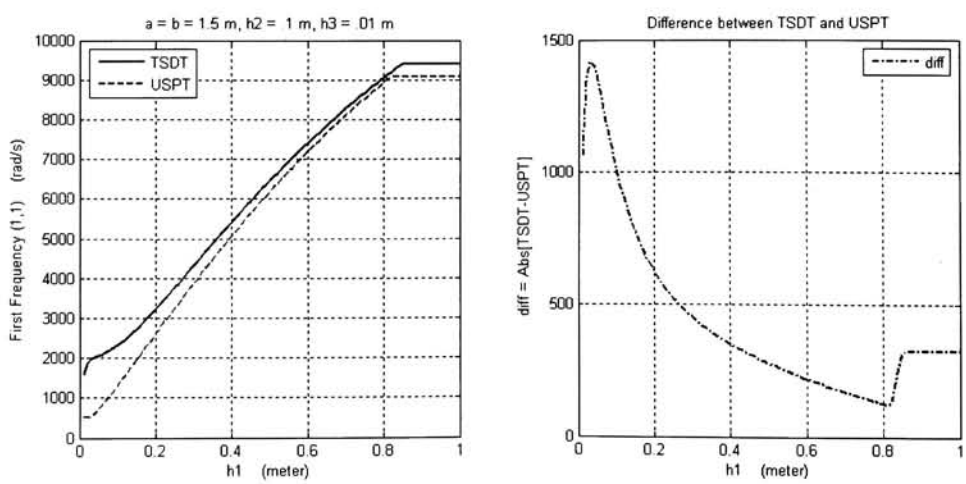

Figure 5.5 Variation of the First Frequency with the Upper Face Thickness

The geometric variations of the initial plate are shown in the above graphs which provide insight into the similarities and differences of the two theories with respect to the first frequency. Variation of the length of the rectangular and square plate show an exponential decrease in ω_{11} as the length increases for both theories (Figure 5.2, Figure 5.3). In Figure 5.5 both theories exhibit a linear increase in ω_{11} as the degree of asymmetry of the plate (increasing h_1) increases until the apparent breakdown (locking) in both theories occurs around $h_1 = .8\ m$ The variation of the asymmetry of the plate is the only geometric variation where both theories exhibit convergence as well as identical behavior.

For the variation of the core thickness (Figure 5.1) the values of ω_{11} for both theories are only close for small values of h_2, as the plate becomes moderately thick with a length to total thickness ratio still within meaningful bounds there is a large difference in the behavior of the theories is observed. This graph is particularly interesting because of the rapid increase of ω_{11} to a peak value for the TSDT. This is the only geometric variation with an extreme value (i.e. minimum or maximum); this shows a distinguished difference in behavior of the theories. It is also interesting to note the logarithmic increase of ω_{11} as h_2 increased for the USPT when a linear increasing curve that possibly locked like the face thickness variations might have been expected.

Locking of the USPT occurred in Figure 5.4 and Figure 5.5 at large values of face layer thickness for both the symmetric and asymmetric plate. The TSDT does not display locking for variation of the face layer thickness of a symmetric plate (Figure 5.4) like the asymmetric case. The logarithmic increase of ω_{11} as the face layer thickness of the symmetric plate increases for the TSDT differs from the behavior of the TSDT with respect to variations of the face layer thickness of the asymmetric plate and the variations of the core thickness.

These initial observations are specific to a distinct set of geometric properties; looking at various combinations of variations of geometric properties will determine if the behaviors are a trait of the theory with respect to certain geometric properties or just an instance of a set of particular values.

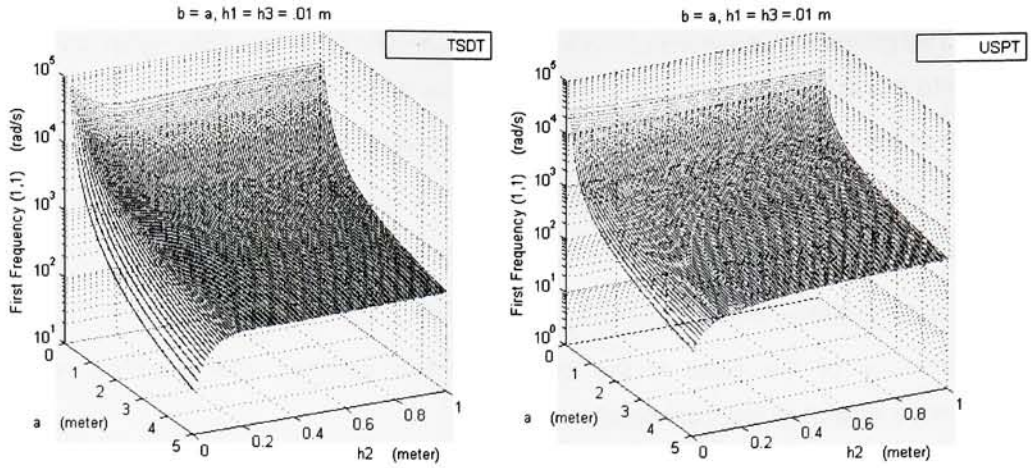

Figure 5.6 Variation of the First Frequency with the Length and Core Thickness of a Symmetric Square Plate

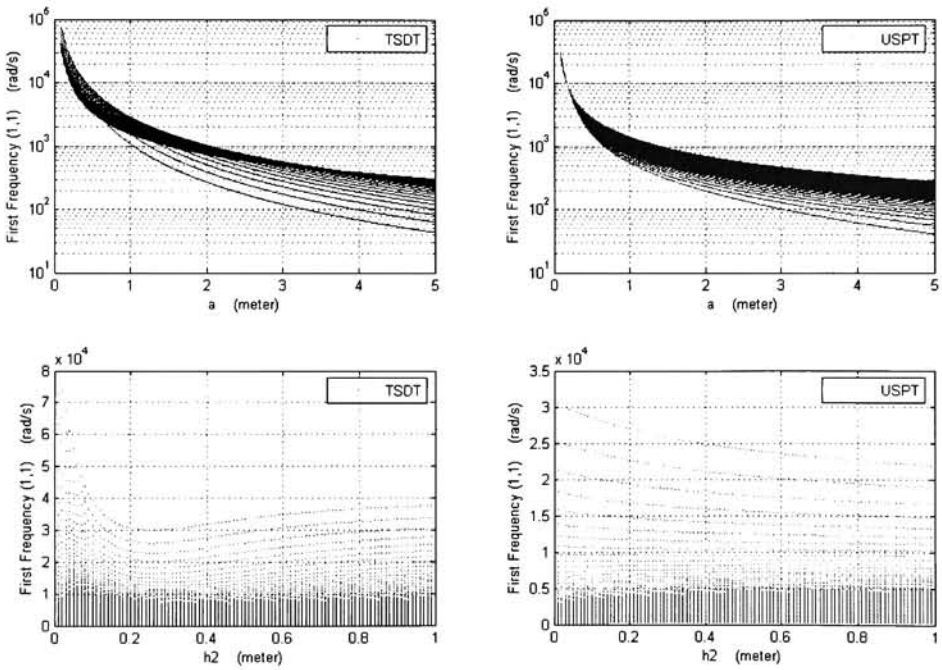

Figure 5.7 Projections of the surfaces in Figure 5.6

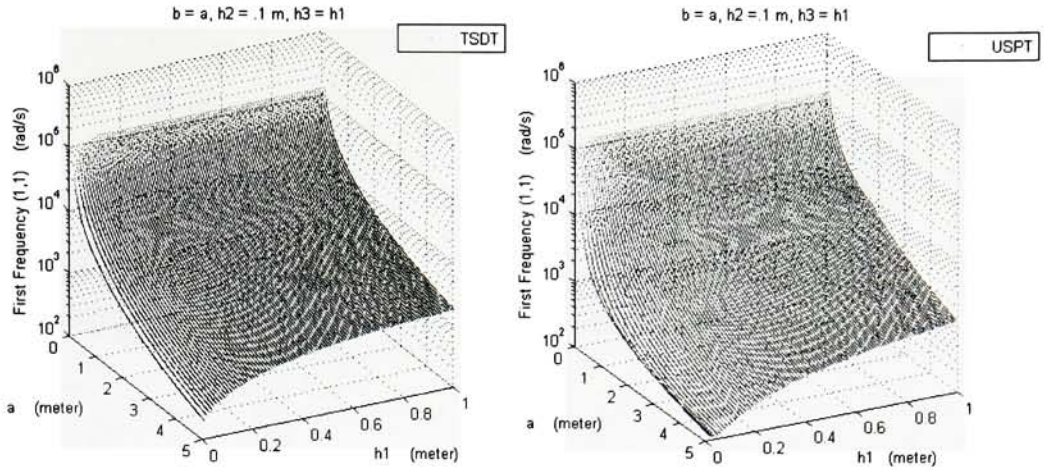

Figure 5.8 Variation of the First Frequency with the Length and Face Thickness of a Symmetric Square Plate

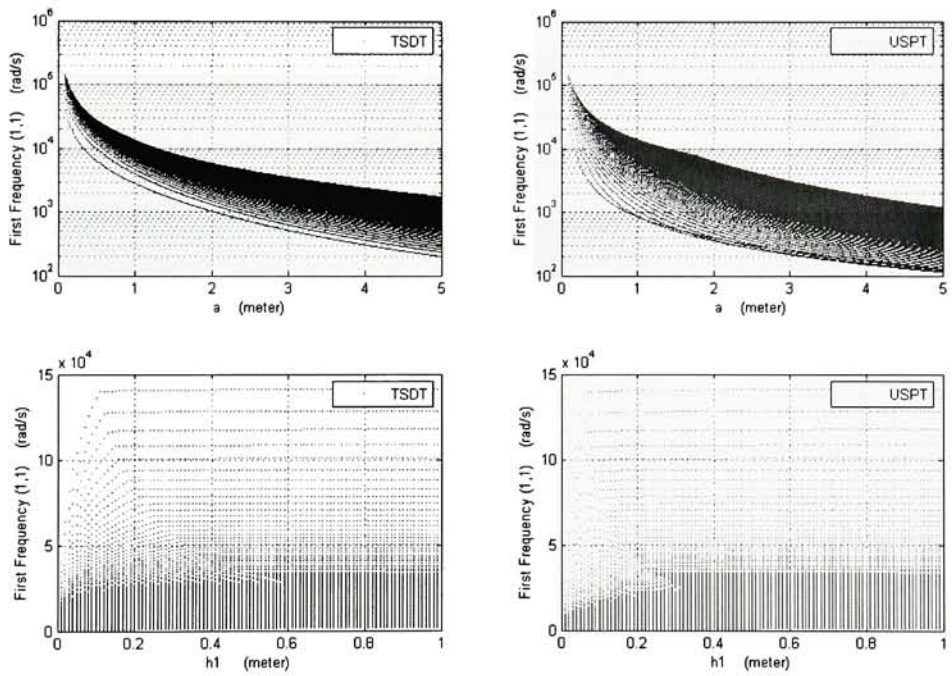

Figure 5.9 Projections of the surfaces in Figure 5.8

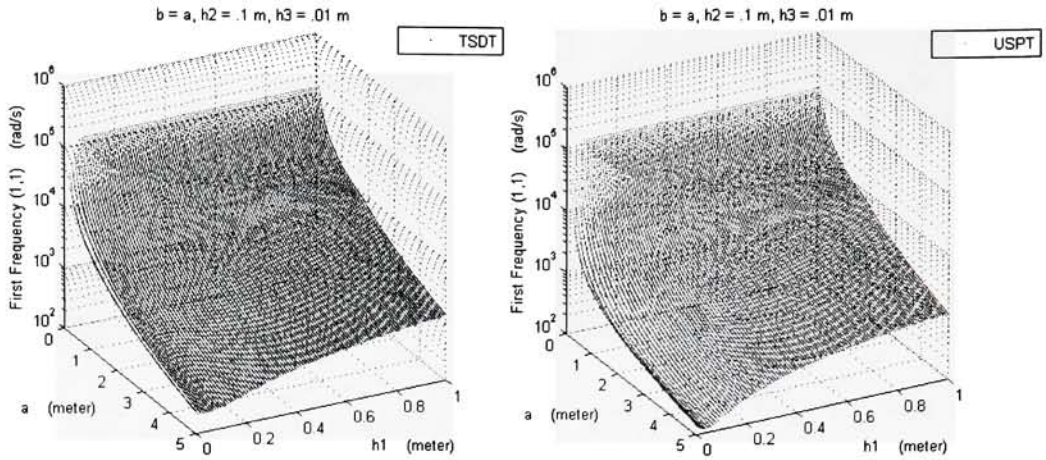

Figure 5.10 Variation of the First Frequency with the Length and Upper Face Thickness of an Unsymmetrical Square Plate

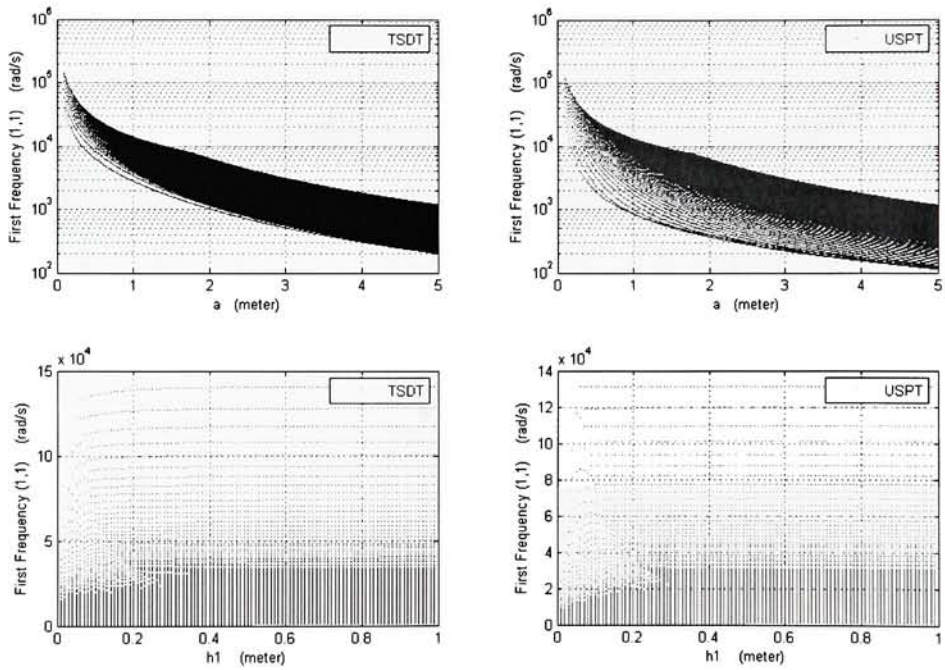

Figure 5.11 Projections of the surfaces in Figure 5.10

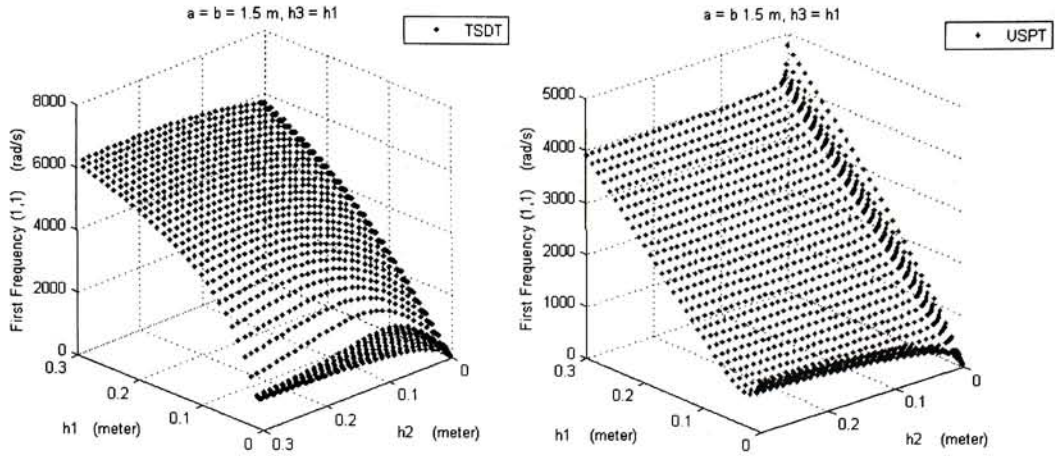

Figure 5.12 Variation of the First Frequency with the Face Thickness and Core Thickness of a Symmetric Square Plate

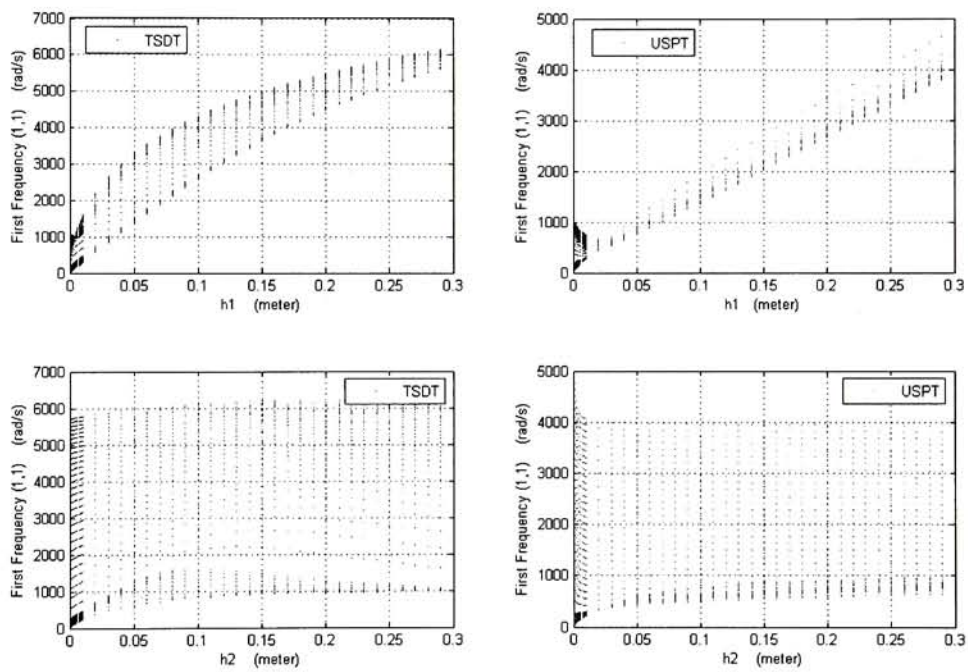

Figure 5.13 Projections of the surfaces in Figure 5.12

The combinations of geometric variations offer a better understanding of the behavior of both theories with respect to how and to what degree changes in the geometry of the rectangular sandwich plate effect the first frequency of vibration. It is clear from Figure 5.6 through Figure 5.11 that as the length of the plate increases there is an exponential decrease in the first frequency regardless of layer thicknesses and opposite edge length. The edge length is the

dominant property; variations of the thickness only have a small effect on ω_{11} as the edge length is varied.

This is clear from Figure 5.7, the dark band in the top two graphs represents the collection of variations of the length of the symmetric square plate for various values of the core thickness. The bottom graphs show a less dense set of curves representing the variation of the core thickness for various lengths of the square symmetric plate, illustrating a significant dependence of ω_{11} on the length.

The variation of h_2 with the length (Figure 5.6, Figure 5.7) and with the thickness of the face layers (Figure 5.12, Figure 5.13) for the symmetric square plate show that a peak value of ω_{11} occurs at all geometries within the specified plate range (i.e. $a/h_T \geq 5$). Figure 5.7 shows that for the TSDT the projection in the $h_2 - \omega_{11}$ plane maintains the shape of Figure 5.1. While the USPT projection repeats the characteristics of Figure 5.1 for values in the plate range (the concentrated points in the lower portion of the graph), the notable characteristic of the projection is the logarithmic shape of the curves produced.

The locking displayed with the USPT for variation of face layer thickness of the symmetric square plate can be seen in Figure 5.8 it begins around values of $a = 2$ at large values of h_1 and develops back towards the origin, where it is almost a flat line at $a = .1$ for all values of h_1. Figure 5.9 shows the locking clearly where flat lines dominate the upper portion of the $h_1 - \omega_{11}$ plane for the USPT.

The TSDT also displayed locking around the same values of the USPT and the flat surface that develops in the same region as the USPT is not as pronounced, but is still visible in Figure 5.8 and Figure 5.10. The breakdown of the TSDT for the variation of the face layer thickness of the symmetric plate did not occur for variations of the initial geometric properties (Figure 5.4), however it does occur for other initial properties. However the locking of both theories occurs for geometries that are not within the plate range.

The initial variations of the face layer thickness for both the symmetric and asymmetric plates (Figure 5.4, Figure 5.5) appeared have a linear increase in ω_{11} as the face layer thickness increased for the USPT. From examination of Figure 5.8 and Figure 5.10 the curves are actually logarithmic curves that reach the breakdown point of the theory in the apparent linear portion of the curve. As the length of the plate becomes larger the breakdown occurs for larger values of face thickness and the logarithmic curves are produced.

The length of the plate is the dominant geometric property of the sandwich plate and for the initial material properties (i.e. soft core) the next geometric property that has considerable effect on the first frequency is the face layer thickness. Figure 5.13 shows that variations with

respect the face layer thickness for a given core thickness are not as dramatically effected by changing core thickness as variations of the core thickness for a given face layer thickness.

The peak value of the first frequency for variation of the core thickness for the TSDT becomes less defined as face layer thickness is increased (Figure 5.12) but is always present for geometries in the plate range. For plates with a large initial face layer thickness corresponding to a low length to total thickness ratio variations of the core thickness do not have a peak value with respect to ω_{11}.

With the characteristics of both theories generally understood for all geometric variations, it is clear that the core thickness to face thickness ratio and the length to total thickness ratio are predominate factors in determining the difference between the TSDT and the USPT. The degree of asymmetry and the change of the major length of the plate do not generally cause differences in the theories with respect to the first frequency. The most interesting property is the peak value observed in variations of the core thickness for the TSDT which could be an effect of the soft core and is examined varying the initial material properties.

5.2.4 Material Variations

For rectangular sandwich plates consisting of identical isotropic face layers and an orthotropic core layer the material parameters of the plate are the densities, Poisson's ratios, the moduli of elasticity and the shear modulus of the core. We will only consider rectangular sandwich plates with soft (i.e. stiffness of face layers is greater than the core layer) or predominately shear deformable cores

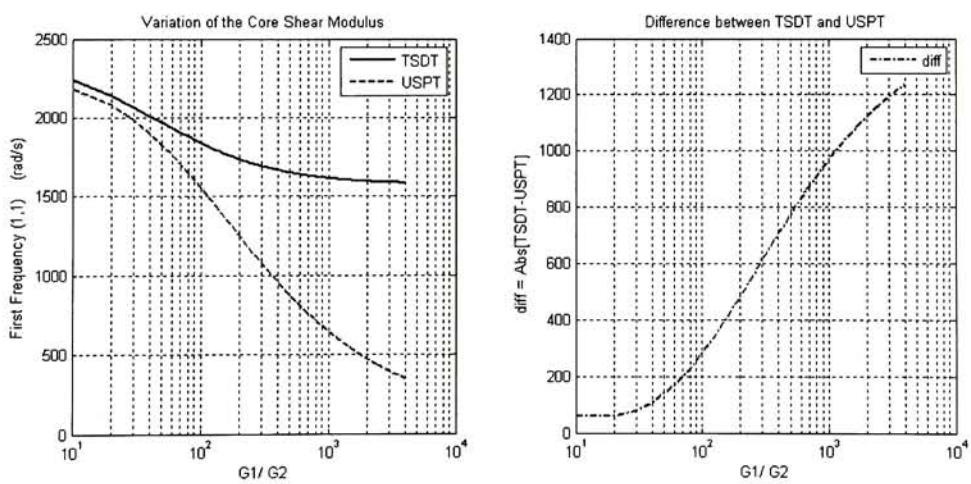

Figure 5.14 Variation of the First Frequency with the Core Shear Modulus G_2

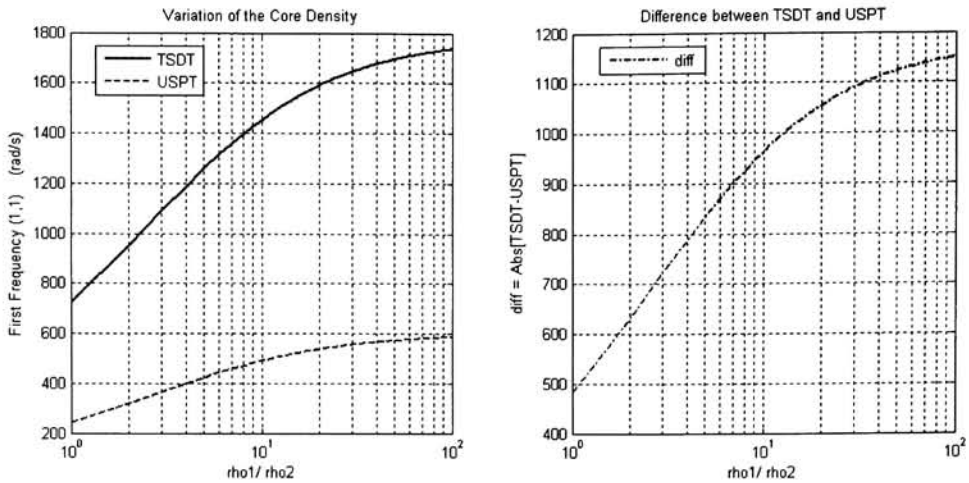

Figure 5.15 Variation of the First Frequency with the Core Density ρ_2

Figure 5.14 shows that behavior of the TSDT and USPT with the variation of the shear modulus of the core G_2 is similar with respect to the first frequency, but the TSDT levels off as the USPT continues to decrease as G_2 decreases. This can be attributed to the averaging of the material properties through the thickness of the plate for the TSDT; as G_2 decreases the average reaches a limit resulting in the no change with respect to the first frequency.

Figure 5.15 also presents similar behavior between the theories as the density of the core ρ_2 is varied with respect to the first frequency. Both theories exhibit an increase in the first frequency with a decrease in ρ_2, however the increase in the TSDT is much more drastic. Based on these variations the theories would converge for a dense (i.e. greater than aluminum) sandwich plate that has a core shear modulus on the order of magnitude of the face layer shear modulus E_1. This type of plate is dominated by inertial forces and the similarity in both theories with respect to the calculation of the equivalent inertias of the plate will result in similar first frequency predictions.

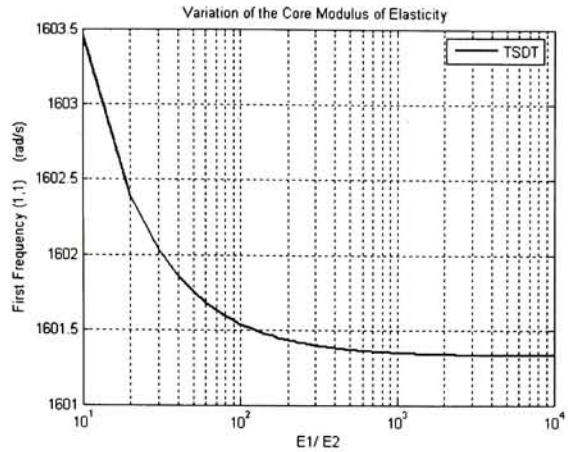

Figure 5.16 Variation of the First Frequency with the Core Modulus of Elasticity E_2 for the TSDT

Figure 5.16 shows that the total variation of the first frequency with respect to the modulus of elasticity of the core E_2 is less than 4, which indicates at the normals strains in the core have little effect on the frequency of vibration of the sandwich plate and could be considered negligible. Furthermore if E_2 is taken to be zero (i.e. neglect the normals strains in the core) there is no effect on the first frequency with respect to the initial plate properties (Table 5.5).

A peak value of ω_{11} occurs for variations of core thickness h_2 with respect to values of the plate length and face layer thickness that are within the plate range. Variation of the shear modulus of the core G_2 for the initial plate geometry and Figure 5.17 shows that peak value of the first frequency exists for a core where $G_1/G_2 \geq 100$ for the initial geometric properties. Based on geometric variations (Figure 5.1, Figure 5.6, Figure 5.7, Figure 5.12, Figure 5.13) and the material variations a simply supported rectangular sandwich plate with a "soft" shear deformable core modeled using the TSDT has a definitive maximum value for the first frequency with respect to the core thickness, while the USPT does not.

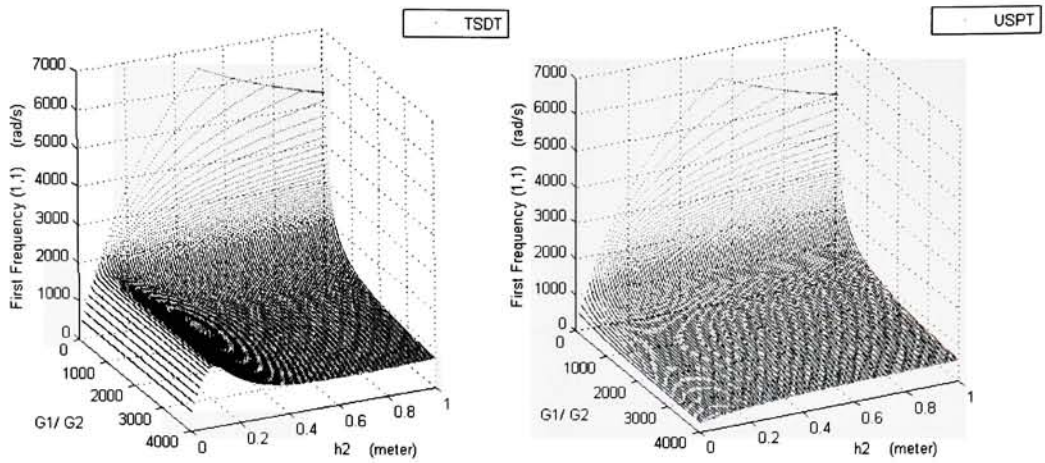

Figure 5.17 Variation of the First Frequency with the Shear Modulus and Thickness of the Core

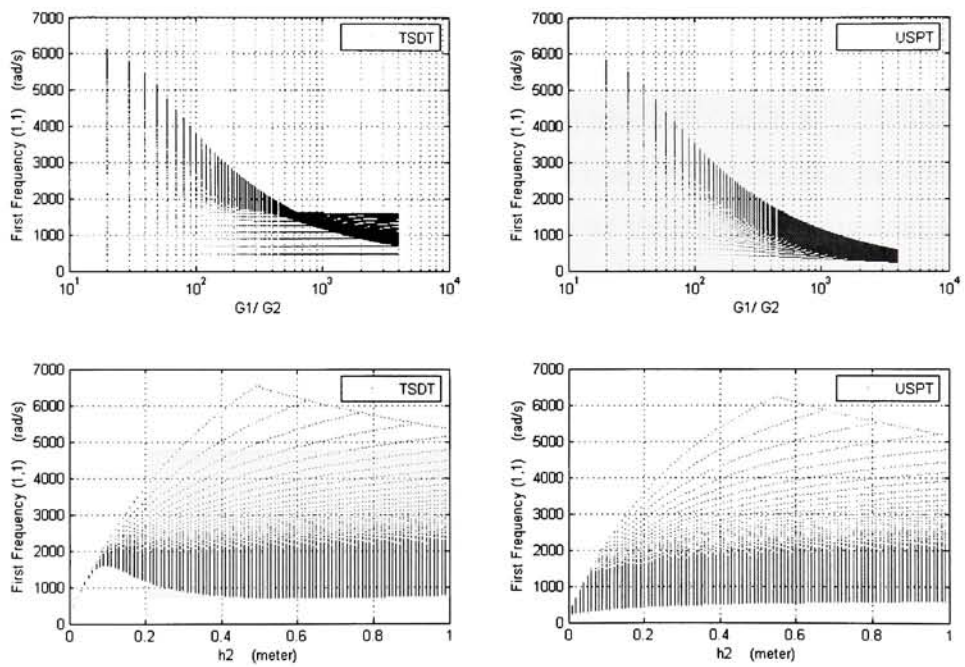

Figure 5.18 Projections of the surfaces in Figure 5.17

More importantly the top two graphs of Figure 5.18 shows that for the TSDT the prediction of the first frequency levels off around values of $G_1/G_2 \approx 500$, while the USPT continues to predict a decreasing first frequency as the ratio decreases. It is clear from intuition that if the stiffness of the core was extremely low then very frequencies would excite the sandwich plate. The averaging of the material properties through the thickness (e.g. equivalent single layer) of the TSDT appears to be limited the ability of the TSDT to predict the frequency of

vibration of the plate. For the initial plate geometry and material properties the effective shear stiffness of the plate for the TSDT is $A_{44}^s = A_{55}^s = 564\ MPa$ which is considerably stiffer than shear stiffness $G_2 = 18.86\ MPa$ used for the USPT.

This is supported by the variation of the core density (Figure 5.15) which showed if the density of the core was dramatically increased to where the inertial forces of the plate dominated the flexural forces of the plate so much so that the transverse inertia is dominant both theories would predict similar frequencies as a result of having identical formulations of the transverse inertia: $\rho_1 h_1 + \rho_2 h_2 + \rho_3 h_3$.

5.2.5 The Damped Plate

With an understanding of the behavior of the first frequency for simply supported rectangular sandwich plate with a shear deformable core for various geometric and material values, the linear elastic-viscoelastic principle is used to introduce damping to the core.

The natural frequencies and corresponding mode shapes are computer for various wave numbers (m,n) and are reported for both theories. The material properties and loss factors for the core material HEREX C70.130 PVC foam at 30°C were experimentally obtained by Meunier and Shenoi [4]. They are given in Table 5.7, and it should be noted that E_2 and its corresponding loss factor will only be used in the TSDT because it does not appear in the USPT.

Material Properties	E	η_E	G	η_G	ν	ρ
HEREX C70.130@30°C	113.5 MPa	.0288	18.86 *MPa*	.067	.32	130 kg/m^3

Table 5.7 Dynamic material properties of the core

The frequencies and corresponding modes of the transverse displacement w were tabulated for various modal numbers for the USPT and TSDT, and are listed in Table 5.8 and Table 5.9 respectively. The results of the USPT for u_1, u_3, v_1 and v_3 can be manipulated in a way similar to the method used to uncouple the equations of motion in Chapter 3 to obtain average displacements and rotations with respect to the midplane of the plate but the transverse displacement is what is of practical interest, and as noted earlier we will restrict our analysis to it.

The transverse displacement for both theories is for all layers of the sandwich plate and therefore a direct comparison can be established, however as noted the modal vectors cannot be directly compared without manipulation.

m	n	ω_{mn}	η_{mn}	U_{1mn}	$\eta_U 1_{mn}$	U_{3mn}	$\eta_U 3_{mn}$	V_{1mn}	$\eta_V 1_{mn}$	V_{3mn}	$\eta_V 3_{mn}$	W_{mn}	$\eta 5_{mn}$
1	1	540.674	0.030	-0.006	0.064	0.006	0.064	-0.006	0.064	0.006	0.064	.999	0.000
1	2	899.325	0.029	-0.002	0.066	0.002	0.066	-0.005	0.066	0.005	0.066	.999	0.000
1	3	1349.056	0.026	-0.001	0.066	0.001	0.066	-0.004	0.066	0.004	0.066	.999	0.000
1	4	1884.196	0.023	-0.001	0.067	0.001	0.067	-0.003	0.067	0.003	0.067	.999	0.000
1	5	2512.686	0.020	0.000	0.067	0.000	0.067	-0.002	0.067	0.002	0.067	.999	0.000
2	2	1180.252	0.027	-0.003	0.066	0.003	0.066	-0.003	0.066	0.003	0.066	.999	0.000
2	3	1586.368	0.025	-0.002	0.067	0.002	0.067	-0.003	0.067	0.003	0.067	.999	0.000
2	4	2098.571	0.022	-0.001	0.067	0.001	0.067	-0.002	0.067	0.002	0.067	.999	0.000
2	5	2714.652	0.019	-0.001	0.067	0.001	0.067	-0.002	0.067	0.002	0.067	.999	0.000
3	3	1956.352	0.023	-0.002	0.067	0.002	0.067	-0.002	0.067	0.002	0.067	.999	0.000
3	4	2444.715	0.020	-0.001	0.067	0.001	0.067	-0.002	0.067	0.002	0.067	.999	0.000
3	5	3046.045	0.018	-0.001	0.067	0.001	0.067	-0.002	0.067	0.002	0.067	.999	0.000
4	4	2914.164	0.018	-0.002	0.067	0.002	0.067	-0.002	0.067	0.002	0.067	.999	0.000
4	5	3502.116	0.016	-0.001	0.067	0.001	0.067	-0.001	0.067	0.001	0.067	.999	0.000
5	5	4079.458	0.015	-0.001	0.067	0.001	0.067	-0.001	0.067	0.001	0.067	.999	0.000

Table 5.8 Frequencies and mode shapes and corresponding loss factors of the transverse displacement w for various modal numbers using the USPT

m	n	ω_{mn}	η_{mn}	U_{mn}	$\eta 1_{mn}$	V_{mn}	$\eta 2_{mn}$	X_{mn}	$\eta 3_{mn}$	Y_{mn}	$\eta 4_{mn}$	W_{mn}	$\eta 5_{mn}$
1	1	1601.663	0.001	0.000	0.000	0.000	0.000	-0.436	0.005	-0.436	0.005	0.787	0.000
1	2	2994.519	0.001	0.000	0.000	0.000	0.000	0.104	-0.045	0.052	-0.045	0.993	0.000
1	3	4556.320	0.002	0.000	0.000	0.000	0.000	0.728	0.000	0.243	0.000	0.641	0.004
1	4	6156.744	0.002	0.000	0.000	0.000	0.000	0.886	0.000	0.222	0.000	0.407	0.002
1	5	7776.105	0.002	0.000	0.000	0.000	0.000	0.937	0.000	0.188	0.000	0.295	0.001
2	2	3996.072	0.002	0.000	0.000	0.000	0.000	0.447	-0.006	0.447	-0.006	0.775	0.000
2	3	5296.307	0.002	0.000	0.000	0.000	0.000	0.716	0.000	0.478	0.000	0.509	0.003
2	4	6735.766	0.002	0.000	0.000	0.000	0.000	0.835	0.000	0.418	0.000	0.358	0.002
2	5	8251.400	0.002	0.000	0.000	0.000	0.000	0.893	0.000	0.358	0.000	0.273	0.001
3	3	6354.981	0.002	0.000	0.000	0.000	0.000	0.652	0.000	0.652	0.000	0.389	0.002
3	4	7611.332	0.002	0.000	0.000	0.000	0.000	0.762	0.000	0.572	0.000	0.303	0.001
3	5	8993.507	0.002	0.000	0.000	0.000	0.000	0.831	0.000	0.499	0.000	0.245	0.001
4	4	8703.141	0.002	0.000	0.000	0.000	0.000	0.684	0.000	0.684	0.000	0.255	0.001
4	5	9950.141	0.002	0.000	0.000	0.000	0.000	0.762	0.000	0.610	0.000	0.217	0.001
5	5	11074.671	0.002	0.000	0.000	0.000	0.000	0.694	0.000	0.694	0.000	0.192	0.001

Table 5.9 Frequencies and mode shapes and corresponding loss factors of the transverse displacement w for various modal numbers using the TSDT

The various modes shapes (U_1, U_3, V_1, V_3, W) in Table 5.8 are normalized to unity and are listed with their corresponding loss factors $(\eta_U 1, \eta_U 3, \eta_V 1, \eta_V 3, \eta 5)$ along with the frequency of

vibration and its loss factor (ω_{mn}, η_{mn}). The mode shapes (U, V, X, Y, W) in Table 5.9 are also normalized to unity and are listed with their corresponding loss factors $(\eta 1, \eta 2, \eta 3, \eta 4, \eta 5)$.

The solutions for W_{mn} from Table 5.8 and utilizing the form of the transverse displacement w assumed in (4.5.3) the mode shape for various modal numbers are presented in Figure 5.19.

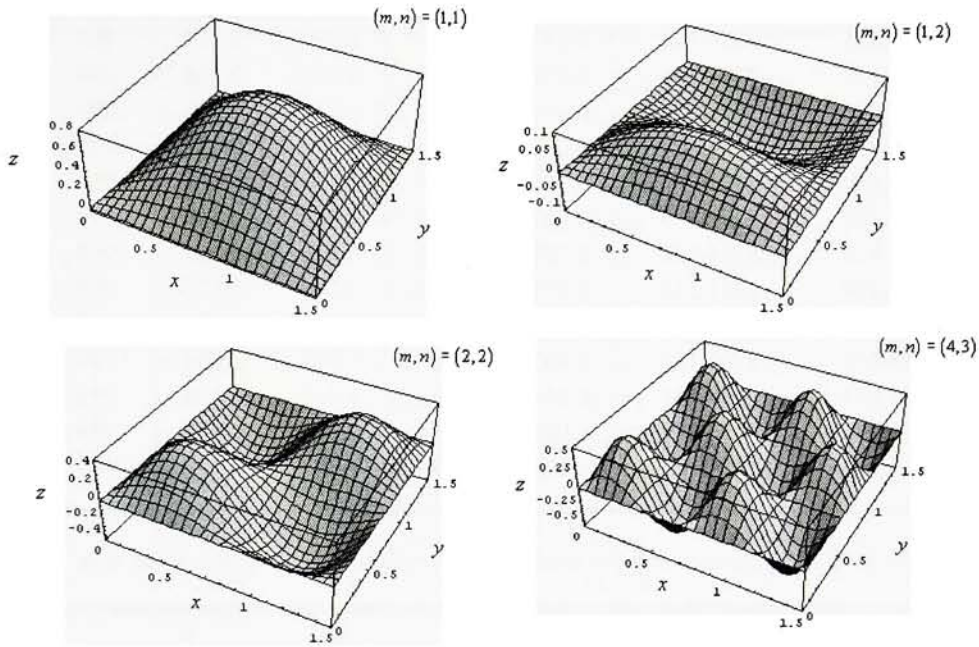

Figure 5.19 Mode shapes of the transverse displacement w calculated for various modal numbers using the TSDT

It is clear from examination of (4.5.3) and (3.5.3) that the mode shapes for both the TSDT are USPT are only going to differ by magnitude and sign for a given modal number. The intent of the simply supported solution is to evaluate the performance of the theories with respect to predictions of vibration frequencies and the corresponding energy dissipation which is represented by the loss factors.

By manipulating the modal vector components the normalized displacement magnitudes and related transverse shear strain magnitude of the core of each theory can be compared. Using the expressions (3.2.2) and (3.5.3) established from the assumed displacement field of the sandwich plate for the USPT the rotation of the normals to the mid-plane of the core (α_1, α_2) are calculated from the modal vector solutions in Table 5.8 and compared to rotations (ψ_x, ψ_y) for

the TSDT in Table 5.10. The normal displacements for the core for the USPT given in (3.2.2) are not tabulated because they are identically zero as are the values for the TSDT in Table 5.9.

m	n	ω_{mn}		α_{1mn}	X_{mn}	α_{2mn}	Y_{mn}	W_{mn}	
		USPT	TSDT					USPT	TSDT
1	1	540.373	1601.663	0.092	-0.436	0.092	-0.436	.999	0.787
1	2	898.911	2994.519	0.161	0.104	0.322	0.052	.999	0.993
1	3	1348.564	4556.320	0.185	0.728	0.555	0.243	.999	0.641
1	4	1883.675	6156.744	0.195	0.886	0.780	0.222	.999	0.407
1	5	2512.172	7776.105	0.200	0.937	1.000	0.188	.999	0.295
2	2	1179.783	3996.072	0.358	0.447	0.358	0.447	.999	0.775
2	3	1585.857	5296.307	0.381	0.716	0.572	0.478	.999	0.509
2	4	2098.049	6735.766	0.394	0.835	0.789	0.418	.999	0.358
2	5	2714.145	8251.400	0.402	0.893	1.005	0.358	.999	0.273
3	3	1955.830	6354.981	0.587	0.652	0.587	0.652	.999	0.389
3	4	2444.199	7611.332	0.599	0.762	0.799	0.572	.999	0.303
3	5	3045.552	8993.507	0.607	0.831	1.011	0.499	.999	0.245
4	4	2913.665	8703.141	0.807	0.684	0.807	0.684	.999	0.255
4	5	3501.645	9950.141	0.814	0.762	1.017	0.610	.999	0.217
5	1	2512.172	7776.105	1.000	0.188	0.200	0.937	.999	0.295
5	5	4079.015	11074.671	1.023	0.694	1.023	0.694	.999	0.192

Table 5.10 Comparison between rotation of normals to the mid-plane of the core

m	n	ω_{mn}		U_{1mn}		V_{1mn}		U_{3mn}		V_{3mn}		W_{mn}	
		TSDT	USPT	TSDT	USPT	TSDT	USPT	TSDT	USPT	TSDT	USPT	TSDT	USPT
1	1	1601.659	540.674	-0.043	-0.006	-0.043	-0.006	0.043	0.006	0.043	0.006	0.787	.999
1	2	2994.511	899.325	-0.030	-0.002	-0.060	-0.005	0.030	0.002	0.060	0.005	0.993	.999
1	3	4556.309	1349.056	-0.011	-0.001	-0.033	-0.004	0.011	0.001	0.033	0.004	0.641	.999
1	4	6156.729	1884.196	-0.004	-0.001	-0.017	-0.003	0.004	0.001	0.017	0.003	0.407	.999
1	5	7776.087	2512.686	-0.002	0.000	-0.010	-0.002	0.002	0.000	0.010	0.002	0.295	.999
2	2	3996.061	1180.252	-0.032	-0.003	-0.032	-0.003	0.032	0.003	0.032	0.003	0.775	.999
2	3	5296.293	1586.368	-0.014	-0.002	-0.021	-0.003	0.014	0.002	0.021	0.003	0.509	.999
2	4	6735.750	2098.571	-0.007	-0.001	-0.013	-0.002	0.007	0.001	0.013	0.002	0.358	.999
2	5	8251.381	2714.652	-0.003	-0.001	-0.009	-0.002	0.003	0.001	0.009	0.002	0.273	.999
3	3	6354.965	1956.352	-0.012	-0.002	-0.012	-0.002	0.012	0.002	0.012	0.002	0.389	.999
3	4	7611.314	2444.715	-0.007	-0.001	-0.009	-0.002	0.007	0.001	0.009	0.002	0.303	.999
3	5	8993.487	3046.045	-0.004	-0.001	-0.007	-0.002	0.004	0.001	0.007	0.002	0.245	.999
4	4	8703.122	2914.164	-0.006	-0.002	-0.006	-0.002	0.006	0.002	0.006	0.002	0.255	.999
4	5	9950.119	3502.116	-0.004	-0.001	-0.005	-0.001	0.004	0.001	0.005	0.001	0.217	.999
5	5	11074.647	4079.458	-0.003	-0.001	-0.003	-0.001	0.003	0.001	0.003	0.001	0.192	.999

Table 5.11 Comparison between mid-plane displacements of the face layers

Using the expressions (4.2.2) and (4.5.3) established from the assumed displacement field of the sandwich plate for the TSDT the inplane displacements of the face layers (U_1, U_3, V_1, V_3, W) are calculated from the modal vector solutions in Table 5.9 and compared to displacements for the USPT in Table 5.11.

m	n	ω_{mn}		ε_5		ε_4	
		USPT	TSDT	USPT	TSDT	USPT	TSDT
1	1	540.373	1601.663	2.187	1.211	2.187	1.211
1	2	898.911	2994.519	2.255	2.184	4.511	4.212
1	3	1348.564	4556.320	2.279	2.070	6.838	4.269
1	4	1883.675	6156.744	2.289	1.738	9.158	3.630
1	5	2512.172	7776.105	2.294	1.555	11.472	3.277
2	2	1179.783	3996.072	4.547	3.694	4.547	3.694
2	3	1585.857	5296.307	4.570	2.848	6.855	3.675
2	4	2098.049	6735.766	4.583	2.335	9.166	3.417
2	5	2714.145	8251.400	4.591	2.038	11.477	3.219
3	3	1955.830	6354.981	6.871	3.093	6.871	3.093
3	4	2444.199	7611.332	6.882	2.668	9.176	3.113
3	5	3045.552	8993.507	6.890	2.373	11.483	3.068
4	4	2913.665	8703.141	9.185	2.824	9.185	2.824
4	5	3501.645	9950.141	9.191	2.582	11.489	2.885
5	1	2512.172	7776.105	11.472	3.277	2.294	1.555
5	5	4079.015	11074.671	11.495	2.704	11.495	2.704

Table 5.12 Comparison between transverse shear strains at mid-plane of the core

It is assumed that the shear deformable core is the mechanism for energy dissipation in the sandwich plate and the magnitude of the transverse shear strain of the core $(\varepsilon_4, \varepsilon_5)$ is a way of comparing the dissipation for each theory (along with loss factors).

The magnitude of the transverse shear strains in the core are calculated using (3.2.3) for the USPT and with (4.2.3) for the TSDT with results from Table 5.10. The magnitudes of the shear strains are larger for the USPT for all of the given modal numbers in Table 5.12 when compared to the TSDT. For both theories the magnitude of the transverse strains are a function of the magnitude of the rotations of the core, the modal number and the magnitude of the transverse deflection.

From Table 5.10 there is not a large difference in the magnitude of the rotations of the core, but the magnitude of transverse deflection is large for the USPT (the modal vector is normalized to unity). The magnitude of the inplane deflections of the face layers which determines the rotations of the core for the USPT are slightly larger for the TSDT (Table 5.11). In

general the magnitude of the transverse deflection is larger for the USPT which corresponds to a larger transverse shear strain magnitudes.

The transverse shear strain in the core for the USPT is a constant value, while the shear strain is parabolically decreasing from the midplane of the core until it is zero on the free surfaces of the plate for the TSDT. Therefore if the magnitude of the shear strain is larger for the USPT the energy dissipation will undoubtedly be larger than the TSDT. This can be seen by the loss factor for each corresponding frequency of vibration listed in Table 5.8 and Table 5.9 for the USPT and TSDT, respectively. The frequency loss factors (η_{mn}) are considerably larger for the USPT which is to be expected when considering the magnitudes of the transverse shear strains. However even for modal numbers where the shear strain magnitudes are similar for both theories (e.g. $m=1$, $n=2$) the frequency loss factor is not similar which can be attributed to the averaging of the material properties by the TSDT.

With an understanding of the energy dissipation for the initial geometric and material properties of the SSSS sandwich plate, we will look at the effects of variations of the material loss factors, core thickness and plate length on the modal loss factor for the first frequency of vibration.

Figure 5.20 shows the first frequency loss factor increases rapidly with increasing core thickness for the USPT, while the TSDT has a much less dramatic increase. The first frequency loss factor has an apparent max value for the variation of the length of the square plate using the USPT, while the loss factor steadily increases for the TSDT. In both of the geometric variations the loss factor for the USPT is considerably larger than the TSDT and this is attributed to the averaged shear modulus in the TSDT.

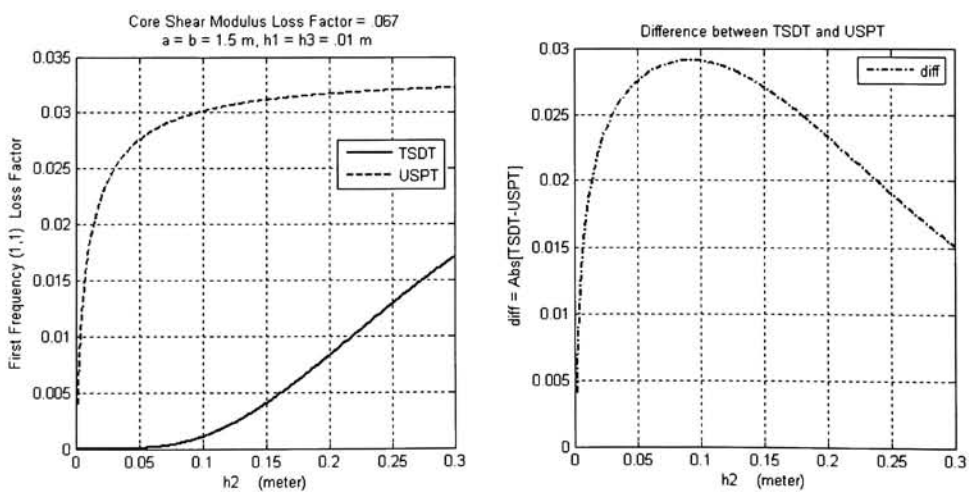

Figure 5.20 Variation of First Frequency Loss Factor with Core Thickness

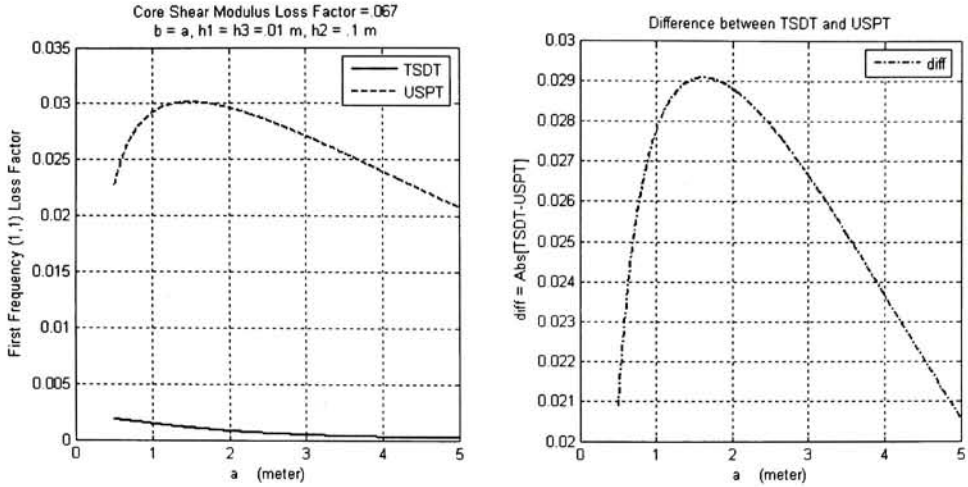

Figure 5.21 Variation of First Frequency Loss Factor with the Length of a Symmetric Square Plate

The effects of the geometric variations of the plate on the first frequency loss factor are presented in Figure 5.20 and Figure 5.21 we will now examine the effects of the material loss factors on the frequency loss factor. The normal strain in the core is neglected in the USPT but considered in the TSDT, however as seen in Figure 5.16 it can be neglected in the TSDT. As a result the damping due to loss factor of the core modulus of elasticity should also be negligible. The variation of the first frequency loss factor with the core elastic modulus loss factor (Figure 5.22) is a clear indication of this; large variations of the core elastic modulus loss factor produce minimal variations in the first frequency loss factor.

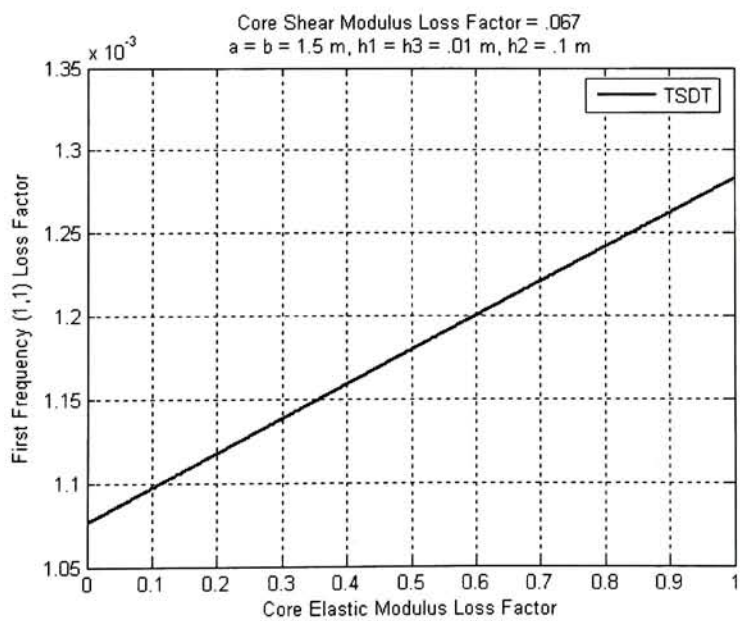

Figure 5.22 Variation of First Frequency Loss Factor with the Core Elastic Modulus Loss Factor for the TSDT

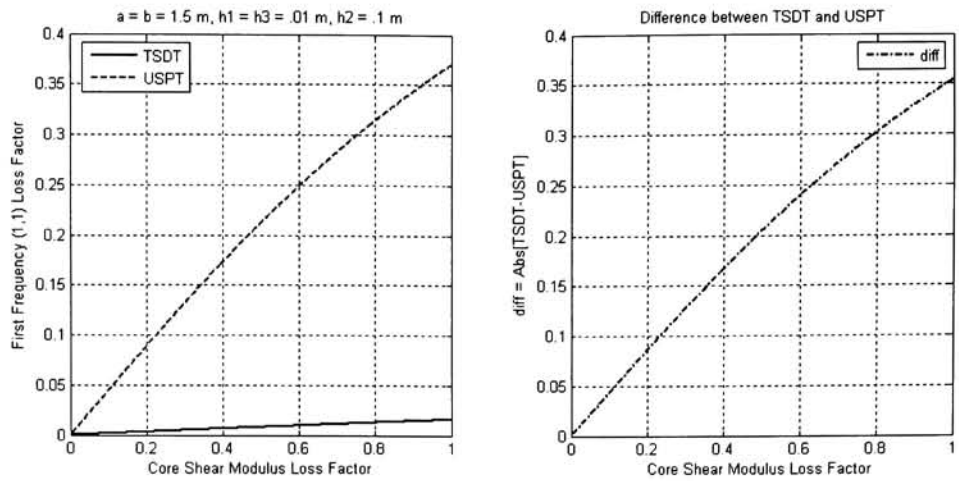

Figure 5.23 Variation of First Frequency Loss Factor with the Core Shear Modulus Loss Factor

For the initial geometric and material properties of a SSSS rectangular sandwich plate the USPT predicts a larger frequency loss factor and at a lower frequency of vibration for a given modal number when compared to the TSDT. This is due in large part to the assumption that the sandwich plate can be treated as an equivalent single layer and the averaged plate stiffnesses will process the characteristics the plate. Based on the geometric variations the both theories behaved similar, but examination of the material variations and loss factor of the core showed that the equivalent single layer appears inadequate at predicting the expected behavior which is shown by the USPT.

Based on the results of the geometric variations in **5.2.3** we will examine the energy dissipation predictions of the SSSS rectangular sandwich plate for geometric properties that both theories predict a first frequency of vibration within a difference of $10-15\ rad/s$. That is a plate with a small core to total thickness ratio and a larger length to total thickness ratio. We will use the material properties in Table 5.5 and the corresponding loss factors listed in Table 5.7 and the following geometric properties will be used for the thin plate

Dimensions
$a = 1.5$ m
$b = a$
$h_1 = .00375$ m
$h_2 = .0025$ m
$h_3 = .00375$ m

Table 5.13 Geometric properties for the thin plate analysis

The results of the analysis of the thin plate with the geometry given in Table 5.13 listed in Table 5.14 show that even though both theories predict similar first frequencies of vibration their is a large difference in the associated loss factor. The normalized magnitude of the transverse displacement W for the USPT is always very close to unity as a result it is clear that the transverse mode of vibration is essentially uncoupled from the primary displacements. The transverse mode of vibration for the TSDT is coupled with the rotations of the core and consequently the magnitude of transverse deflection is lower than the USPT.

m	n	ω_{mn}		η_{mn}		W_{mn}		ε_5		ε_4	
		TSDT	USPT	TSDT$\times 10^7$	USPT	TSDT	USPT	TSDT	USPT	TSDT	USPT
1	1	154.721	144.128	3.702	0.004	-0.320	0.999	-0.0004	0.7778	-0.0004	0.7778
1	2	386.648	330.264	3.812	0.009	-0.209	0.999	-0.0006	1.5907	-0.0012	3.1815
1	3	772.776	591.172	4.002	0.013	-0.150	0.999	-0.0009	2.4408	-0.0026	7.3225
1	4	1312.487	898.280	4.273	0.015	-0.116	0.999	-0.0011	3.1291	-0.0046	12.5163
1	5	2004.917	1240.022	4.623	0.017	-0.094	0.999	-0.0014	3.6358	-0.0071	18.1789
2	2	618.386	492.410	3.939	0.011	-0.167	0.999	-0.0016	4.3064	-0.0016	4.3064
2	3	1004.203	728.971	4.132	0.014	-0.132	0.999	-0.0020	5.5681	-0.0030	8.3522
2	4	1543.480	1017.186	4.401	0.016	-0.107	0.999	-0.0025	6.6604	-0.0050	13.3209
2	5	2235.356	1345.722	4.748	0.017	-0.089	0.999	-0.0030	7.5091	-0.0075	18.7728
3	3	1389.503	938.584	4.332	0.016	-0.112	0.999	-0.0035	9.6020	-0.0035	9.6020
3	4	1928.059	1204.031	4.603	0.017	-0.096	0.999	-0.0042	10.7755	-0.0056	14.3674
3	5	2619.014	1515.502	4.949	0.017	-0.082	0.999	-0.0049	11.7529	-0.0081	19.5882
4	4	2465.610	1448.445	4.877	0.017	-0.085	0.999	-0.0063	15.4276	-0.0063	15.4276
4	5	3155.281	1742.869	5.224	0.017	-0.075	0.999	-0.0071	16.3747	-0.0089	20.4684
5	5	3843.310	2022.417	5.572	0.017	-0.068	0.999	-0.0098	21.3053	-0.0098	21.3053

Table 5.14 Comparison of frequency of vibration damping properties

The analysis for the damped SSSS rectangular plate was conducted based on variations of an initial geometry, given the results of the geometric and material variations a thin plate was examined where the theories were in agreement with respect to the prediction of the first frequency. It is clear from the results of the analysis that the USPT theory predicts a much larger frequency loss factor when compared to the TSDT even when the predicted frequencies are similar. This can be attributed to the averaged plate stiffnesses of the TSDT, for the thin plate geometry the plate is essentially composed of a single undamped aluminum T4-2024 plate.

5.2.6 FEA comparison

In order to compare the accuracy of the theories and confirm the results of the geometric and material variations the finite element package ANSYS is used to formulate the SSSS

rectangular sandwich plate using 2-D plate elements and 3-D solid elements formulated using the theory of 3-D elasticity.

Comparison of SSSS first frequency solutions for the plate properties in Table 5.5 to various FEA solutions

TSDT $\omega_{11} = 1601.66\ rad/s$		USPT $\omega_{11} = 540.373\ rad/s$	
ANSYS ELEMENT w/ .06 m mesh	$\omega_{11}\ (rad/s)$	TSDT % Diff	USPT % Diff
SHELL91	2135.53	25.00%	74.70%
SHELL91 w/ sandwich option	476.89	235.86%	13.31%
SOLID46	534.07	199.90%	1.18%
SOLID191	1507.96	6.21%	64.17%
SOLID95 stacked	540.22	196.48%	.03%

Table 5.15 Comparison of analytical results for the first frequency of vibration for the initial plate properties to FEA solutions obtained in ANSYS

The results obtained by the various ANSYS elements for the initial plate geometries (Table 5.15) show that the SHELL91 and SOLID191 elements are in the range of the first frequency prediction of the TSDT while the SOLID46 and SHELL91 with the sandwich option elements predict frequencies similar to that of the USPT. However the most accurate finite element model composed of the SOLID95 element stacked through the thickness predicted the same frequency as the USPT for the initial plate.

The formulation of the SHELL91 element corresponds to the FSDT which in general predicts similar frequencies as the TSDT (see **4.1**) so similar results were expected. The SOLID46 element is an 8 node element, while the SOLID191 is a 20 node element and the both average the material properties of the plate through the thickness to achieve an equivalent single plate formulation similar to the TSDT. The SOLID46 is an 8 node element and therefore can produce a piecewise linear displacement through the thickness while the SOLID191 produces a piecewise quadratic displacement through the thickness. Both the SOLID46 and SOLID191 compute averaged plate stiffness through the thickness and given the displacements the agreement of the SOLID46 with the USPT and the SOLID191 with the TSDT is expected.

The FEA analysis indicates that the USPT is the more accurate theory based on a finite element model composed of the SOLID95 20 node element stacked through the thickness with 3 elements through the core and one element through each of the face layers.

6 The Cantilever Plate

6.1 *Introduction*

This section will outline the procedure for examining the rectangular sandwich plate with one clamped edge and with the remaining edges (CFFF) known as the cantilever plate. These boundary conditions present a difficult task to the analyst and an exact analytical solution is not known. It is common to use an approximate energy method (i.e. FEA, Galerkin) to solve the cantilever problem, we will use a superposition of Levy solutions for a set of building block plates developed by Gorman [1] that is exact theoretically with error introduced by numerical calculations and truncation of the Levy solutions.

In the superposition method we consider a set of appropriate plate solutions (building blocks) that we can obtain analytically and superimpose. Then by applying edge loads along the their boundaries and then adjusting the amplitudes of the loading that appear in the formulation of their boundary conditions we can satisfy the requirements of the original problems boundary conditions. We will completely develop the solution for the USPT and then by an analogous procedure present the TSDT solution in a less rigorous manor.

6.2 *UPST*

For the analysis of the cantilever plate with the USPT we will restrict ourselves to the equations of motion (3.7.6) and the corresponding boundary conditions (3.6.4) and (3.7.8). The reader should refer to sections **3.6** and **3.7** for the derivation of these equations, they are uncoupled from the rigid in-plane motions of the plate and simplified by only considering the transverse inertia of the plate.

The boundary conditions for the cantilever plate along its edges are

$\xi = 0$	$\xi = 1$
$\psi_{\xi} = 0$	$\frac{h_c}{a}\left(\psi_{\xi,\xi} + \nu\psi_{\eta,\eta}\right) = 0$
$\psi_{\eta} = 0$	$\bar{\nu}^{*}\frac{h_c}{a}\left(\psi_{\xi,\eta} + \psi_{\eta,\xi}\right) = 0$
$W_{,\xi} = 0$	$\frac{\left(D_1 + D_3\right)}{a}\left(W_{,\xi\xi} + \nu W_{,\eta\eta}\right) = 0$
$W = 0$	$g_2\left(\psi_{\xi} + W_{,\xi}\right) - \left(W_{,\xi\xi\xi} + \left(2-\nu\right)W_{,\xi\eta\eta}\right) = 0$

and

$$\eta = 0 \text{ and } \eta = \phi$$

$$\bar{\nu}^{*}\frac{h_c}{a}\left(\psi_{\xi,\eta}+\psi_{\eta,\xi}\right)=0$$

$$\frac{h_c}{a}\left(\psi_{\eta,\eta}+\nu\psi_{\xi,\xi}\right)=0$$

$$\frac{\left(D_1+D_3\right)}{a}\left(W_{,\eta\eta}+\nu W_{,\xi\xi}\right)=0$$

$$g_2\left(\psi_\eta+W_{,\eta}\right)-\left(W_{,\eta\eta\eta}+\left(2-\nu\right)W_{,\eta\xi\xi}\right)=0 \qquad (6.2.1)$$

where the plate is clamped along the edge $\xi = 0$ as shown in Figure 6.1.

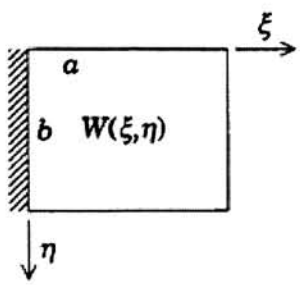

Figure 6.1 Cantilever Plate

In order to satisfy these boundary conditions it is necessary that we introduce plates with boundary conditions that can be satisfied by the Levy solution procedure and use the principle of superposition. The Levy solutions are assumed mode shapes which consist of a trigonometric series that exactly satisfy the boundary conditions of two parallel edges of the plate for each term of the series in terms of the spatial variable normal to the edges multiplied by a shape function in terms of the spatial variable tangent to the edges this results in reducing the system of partial differential equations to a system of ordinary differential equations in terms of tangent spatial variable.

To make use of this solution procedure the following distributed edge loads (forces or moments) and boundary conditions are introduced and employed in formulation the building block plates that are superimposed to satisfy the boundary conditions of the cantilever plate (6.2.1).

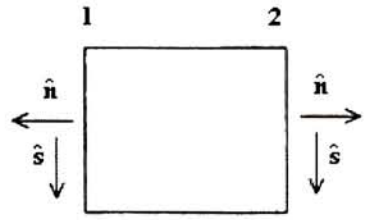

Figure 6.2 Schematic of Normal and Tangent Edge Directions of a General Plate

Variable	Distributed Edge Reactions at 1 and 2 in Figure 6.2
$\psi_{\hat{n}}$	$P_{\hat{n}} = \frac{h_c}{a}\left(\psi_{\hat{n},\hat{n}} + \nu\psi_{\hat{s},\hat{s}}\right)$
$\psi_{\hat{s}}$	$P_{\hat{n}\hat{s}} = \overline{\nu}^{*}\frac{h_c}{a}\left(\psi_{\hat{n},\hat{s}} + \psi_{\hat{s},\hat{n}}\right)$
$W_{,\hat{n}}$	$M_{\hat{n}} = \frac{\left(D_1 + D_3\right)}{a}\left(W_{,\hat{n}\hat{n}} + \nu W_{,\hat{s}\hat{s}}\right)$
W	$Q_{\hat{n}} = g_2\left(\psi_{\hat{n}} + W_{,\hat{n}}\right) - \left(W_{,\hat{n}\hat{n}\hat{n}} + (2-\nu)W_{,\hat{n}\hat{s}\hat{s}}\right)$

(6.2.2)

The non-dimensional reactions at the edges of the plate can be thought of as moments with exception to $Q_{\hat{n}}$ which can be considered a transverse force. The reason for their introduction will become clear when we introduce the building block plates. But first we will introduce the boundary conditions necessary for our analysis.

Edge Type	Conditions at 1 and 2 in Figure 6.2
Simply Supported (SS)	$W = 0,\ W_{,\hat{n}\hat{n}} = 0,\ \psi_{\hat{n},\hat{n}} = 0,\ \psi_{\hat{s}} = 0$
Free (F)	$Q_{\hat{n}} = 0,\ M_{\hat{n}} = 0,\ P_{\hat{n}} = 0,\ P_{\hat{n}\hat{s}} = 0$
Clamped (C)	$W = 0,\ W_{,\hat{n}} = 0,\ \psi_{\hat{n}} = 0,\ \psi_{\hat{s}} = 0$
Slip Shear (∘∘)	$W_{,\hat{n}\hat{n}\hat{n}} = 0,\ W_{,\hat{n}} = 0,\ \psi_{\hat{n}} = 0,\ \psi_{\hat{s},\hat{n}} = 0$

(6.2.3)

The boundary conditions are for the edges of a general plate with the spatial variable normal to the plate being $\hat{n}$ and the spatial variable tangent to the edge being $\hat{s}$. Using the boundary conditions (6.2.3) and the general forces (6.2.2) the superposition solution for the rectangular cantilever plate will now be introduced.

6.2.1 Symmetric Modes Theory

The solution for the free vibration of the cantilever can be separated into modes that are symmetric with respect to ξ-axis if it is placed in the middle of the plate for the configuration in

Figure 6.1 and those that are asymmetric. By enforcing a symmetry condition on the modes of vibration the analysis is greatly simplified along with the classification of modes.

We can take advantage of symmetry and consider only half the plate by applying the *slip shear* ($\circ\circ$) [2] boundary condition along the $\xi = 0$ edge. For the symmetric modes of vibration about the $\xi = 0$ edge the vertical edge reaction and slope normal to the edge must zero, which are the exactly the slip shear conditions given by (6.2.3). While taking advantage of symmetry we will now consider a plate of dimension $a \times 2b$ to avoid having to use $b/2$ in notation.

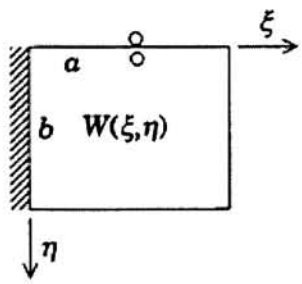

Figure 6.3 Cantilever Plate with Symmetric Modes of Vibration about the ξ-axis of Dimension $a \times 2b$

Three building blocks are used for the symmetric mode analysis to satisfy the boundary conditions of the cantilever plate and shown in Figure 6.4; it is worth noting that four blocks would be necessary if symmetry conditions are not made.

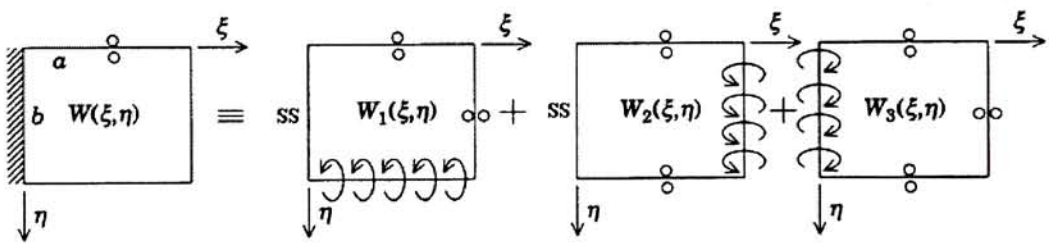

Figure 6.4 Schematic Representation of the Three Building Blocks used to Analyze the Symmetric Modes of the Cantilever Plate.

The curved arrows in Figure 6.4 represent that distributed edge loads are applied along these edges. We will later consider the total contribution of the applied loads on the cantilever boundary conditions of the superimposed solution, but first we must formulate the Levy solutions for the three building blocks

Consider the edges $\xi = 0$ and $\xi = 1$ of the first building block a Levy solution for the transverse displacement W of the form $F_m(\eta) f_m(\xi)$, where $f_m(\xi)$ is a trigonometric function, needs to satisfies the conditions

$$W = W_{,\xi\xi} = 0\Big|_{\xi=0} \qquad W_{,\xi} = W_{,\xi\xi\xi} = 0\Big|_{\xi=1} \tag{6.2.4}$$

which come from substituting ξ for the normal spatial variable $\hat{n}$ making η the tangent spatial variable $\hat{s}$ for the SS and $\circ\circ$ conditions in (6.2.3), the function that satisfies these conditions is

$$W_1(\xi,\eta) = \sum_{m=1,3,5}^{\infty} Z_m(\eta)\sin\frac{m\pi\xi}{2} \tag{6.2.5}$$

by inspection the reader can verify that (6.2.5) satisfies the conditions (6.2.4) for every term in the series. Similarly the rotation ψ_ξ must satisfy the conditions

$$\psi_{\xi,\xi} = 0\Big|_{\xi=0} \qquad \psi_\xi = 0\Big|_{\xi=1} \tag{6.2.6}$$

which is achieved by the function

$$\psi_{1\xi}(\xi,\eta) = \sum_{m=1,3,5}^{\infty} X_m(\eta)\cos\frac{m\pi\xi}{2} \tag{6.2.7}$$

and finally the rotation ψ_η must satisfy the conditions

$$\psi_\eta = 0\Big|_{\eta=0} \qquad \psi_{\eta,\xi} = 0\Big|_{\eta=\phi} \tag{6.2.8}$$

which is accomplished by the function

$$\psi_{1\eta}(\xi,\eta) = \sum_{m=1,3,5}^{\infty} Y_m(\eta)\sin\frac{m\pi\xi}{2} \tag{6.2.9}$$

and once again (6.2.7) and (6.2.9) satisfy the conditions (6.2.6) and (6.2.8) respectively for every term in the series for as many terms as desired.

Substituting (6.2.5), (6.2.7), and (6.2.9) into the equations of motion (3.7.6) the following system of ordinary differential equations with respect to η are obtained

$$\begin{aligned}
&-\alpha^2 X_{1m} + \alpha\bar{v}Y'_{1m} + \bar{v}^* X''_{1m} - g_1\left(X_{1m} + \alpha Z_{1m}\right) = 0\\
&Y'_{1m} - \alpha\bar{v}X'_{1m} - \alpha^2\bar{v}^* Y_{1m} - g_1\left(Y_{1m} + Z'_{1m}\right) = 0\\
&\alpha^4 Z_{1m} - 2\alpha^2 Z^*_{1m} + Z''''_{1m} - g_2\left(Y'_{1m} - \alpha X_{1m} + Z^*_{1m} - \alpha^2 Z_{1m}\right) - \omega^2 g_0 Z_{1m} = 0
\end{aligned} \tag{6.2.10}$$

where $f' = \dfrac{df}{d\eta}$, $\alpha = \dfrac{m\pi}{2}$ and the reader is reminded that ω is the frequency of vibration. We will represent the equations (6.2.10) in state space form, which allows us to form an analytical solution for the desired functions of η.

The following state space variables will be used for all three building blocks and the reader is responsible for being able to note what spatial variable the derivate is taken with respect to.

State Space Variables

$$\begin{aligned} Z_1 &= X_\Sigma & Z_2 &= X'_\Sigma \\ Z_2 &= Y_\Sigma & Z_4 &= Y'_\Sigma \\ Z_5 &= W_\Sigma & Z_6 &= W'_\Sigma \\ Z_7 &= W''_\Sigma & Z_8 &= W'''_\Sigma \end{aligned} \tag{6.2.11}$$

where Σ is the iterator or variable that the summation is taken over for the trigonometric series in the Levy solutions (e.g. m for the first building block). Substituting (6.2.11) into the system of differential equations (6.2.10) we obtain

$$\mathbf{Z}' = [\mathbf{C}]\mathbf{Z} \tag{6.2.12}$$

where $\mathbf{Z} = Z_i \quad (i = 1,...,8)$, and $\mathbf{Z}'$ is the derivative of $\mathbf{Z}$ with respect to η for the first building block. The solution to (6.2.12) can be obtained by letting $\mathbf{Z} = \mathbf{r}e^{\lambda y}$ then $\mathbf{Z}' = \lambda \mathbf{r}e^{\lambda y}$, but $\mathbf{Z}' = [\mathbf{C}]\mathbf{Z}$ so we have $[\mathbf{C}]\mathbf{r} = \lambda \mathbf{r}$ which is an eigenvalue problem an written in standard form as

$$[\mathbf{C} - \lambda \mathbf{I}]\mathbf{r} = \mathbf{0} \tag{6.2.13}$$

which has the general solution in component form

$$z_i = c_j r_i^{(j)} e^{\lambda_j \chi} \quad i, j = 1,...,8 \tag{6.2.14}$$

where χ is the appropriate spatial variable (i.e. ξ or η depending on the building block), λ_j is the jth eigenvalue of $\mathbf{C}$, $r_i^{(j)}$ is the ith component of the eigenvector corresponding to the jth eigenvalue and c_i are arbitrary constants that are solved for by applying the boundary conditions of the remaining two edges to (6.2.14).

For the first building block $\mathbf{C}$ is given by

$$\mathbf{C}=\begin{bmatrix} 0 & 1 & 0 & 0 & 0 & 0 & 0 & 0 \\ C_6 & 0 & 0 & C_4 & C_5 & 0 & 0 & 0 \\ 0 & 0 & 0 & 1 & 0 & 0 & 0 & 0 \\ 0 & C_1 & C_3 & 0 & 0 & C_2 & 0 & 0 \\ 0 & 0 & 0 & 0 & 0 & 1 & 0 & 0 \\ 0 & 0 & 0 & 0 & 0 & 0 & 1 & 0 \\ 0 & 0 & 0 & 0 & 0 & 0 & 0 & 1 \\ C_9 & 0 & 0 & C_8 & C_{10} & 0 & C_7 & 0 \end{bmatrix} \tag{6.2.15}$$

where

$$C_1=\alpha\bar{\nu} \qquad C_2=g_1 \qquad C_3=g_1+\alpha^2\bar{\nu}^* \qquad C_4=-\alpha\frac{\bar{\nu}}{\bar{\nu}^*} \qquad C_5=\alpha\frac{g_1}{\bar{\nu}^*}$$

$$C_6=\frac{\alpha^2+g_1}{\bar{\nu}^*} \qquad C_7=2\alpha^2+g_2 \qquad C_8=g_2 \qquad C_9=-\alpha g_2 \qquad C_{10}=\omega^2 g_0-\alpha^4-\alpha^2 g_2$$

At this point in the analysis it is clear that we cannot obtain analytical expressions for the eigenvalues and corresponding eigenvectors of $\mathbf{C}$, because it would involve an exact expression for the roots of an eighth order characteristic polynomial. We will have to use numerical methods to determine the Levy solutions via a state space approach for as many terms of the trigonometric series as required.

The eigenvalues of $\mathbf{C}$ are in general dependent on the iterator of the trigonometric series (e.g. m for the first building block) and the frequency of vibration ω. The eigenvalues of $\mathbf{C}$ can be both real and complex and we must consider how to deal will the complex eigenvalues to obtain real solutions.

When damping is *not* included in the analysis (i.e. the core is linear elastic not viscoelastic) all of the components of $\mathbf{C}$ are real making all of the coefficients of the characteristic polynomial real, therefore the complex roots of the characteristic polynomial (eigenvalues) occur in complex conjugate pairs with corresponding complex conjugate eigenvectors.

Suppose that $\lambda_1=\sigma+i\tau$ (σ and τ are real numbers and $i=\sqrt{-1}$) is an eigenvalue of $\mathbf{C}$ with the corresponding eigenvector $\mathbf{r}_2=\mathbf{s}+i\mathbf{t}$ where $\mathbf{s}$ and $\mathbf{t}$ are real constant vectors. Then $\lambda_2=\lambda_1^*$ is the conjugate of λ_1 and similarly $\mathbf{r}_2=\mathbf{r}_1^*$ therefore two linearly independent vector solutions that are part of the linear combination of all the solutions to (6.2.12) in (6.2.14) are

$$\mathbf{z}_1 = \mathbf{r}^{(1)} e^{\lambda_1 \chi} = (\mathbf{s} + i\mathbf{t}) e^{(\sigma + i\tau)\chi}$$
$$\mathbf{z}_2 = \mathbf{r}^{(2)} e^{\lambda_2 \chi} = (\mathbf{s} - i\mathbf{t}) e^{(\sigma - i\tau)\chi} \qquad (6.2.16)$$

Now we can use Euler's Formula on one of the complex vector solutions (6.2.16) to obtain two vector solutions, rewriting $\mathbf{z}_1$ as

$$\mathbf{z}_1 = \left[e^{\sigma\chi} (\mathbf{s}\cos\tau\chi - \mathbf{t}\sin\tau\chi) \right] + i \left[e^{\sigma\chi} (\mathbf{s}\sin\tau\chi + \mathbf{t}\cos\tau\chi) \right]$$
$$\mathbf{z}_1 = \mathbf{z}_{11} + i\mathbf{z}_{12}$$

and since $\mathbf{z}_1$ is a solution to (6.2.12) we have $\mathbf{z}'_{11} + i\mathbf{z}'_{12} = \mathbf{C}\mathbf{z}_{11} + i\mathbf{C}\mathbf{z}_{12}$ and by equating the real and imaginary parts we find that $\mathbf{z}_{11}$ and $\mathbf{z}_{12}$ are linearly independent real vector solutions to (6.2.12) associated with the complex conjugate eigenvalues $\sigma \pm i\tau$, therefore when we are confronted with a complex eigenvalues we will employ the following real vector solutions using the following convention

If $\lambda_j = \sigma + i\tau$	If $\lambda_j = \sigma - i\tau$
then the associated solution is	then the associated solution is
$e^{\sigma\chi} (\mathbf{s}\cos\tau\chi - \mathbf{t}\sin\tau\chi)$	$e^{\sigma\chi} (\mathbf{s}\sin\tau\chi + \mathbf{t}\cos\tau\chi)$

(6.2.17)

this enables us to have a *real* general solution consisting of a linear combination of the linearly independent solutions for both complex conjugate and real eigenvalues and their associated eigenvectors with arbitrary constants.

Having solved the system of ordinary differential equations (6.2.10) via a state space approach we now turn our attention to the two remaining edges of the first building block $\eta = 0$ and $\eta = \phi$. Along the edge $\eta = 0$ we have slip shear conditions and along $\eta = \phi$ we apply distributed loads equal to the distributed edge reactions of the rotations normal to the edge (i.e. P_η and M_η) while setting the other distributed edge reactions to zero (i.e. $P_{\eta\xi}$ and Q_η).

The applied load along $\eta = \phi$ that corresponds to the rotation $W_{1,\eta}$ and the associated edge reaction $M_{1\eta}$ is taken to be

$$M_{1\eta} = \sum_{m=1,3,5}^{\infty} E_m \sin\frac{m\pi\xi}{2} \qquad (6.2.18)$$

where E_m is the amplitude of the applied load that oscillates in phase at the same frequency ω as the plate. We substitute (6.2.5) into (6.2.2) to obtain the edge reaction using the state space variables in (6.2.11) and equate it to the applied load to get the boundary condition

$$E_m = \frac{(D_1 + D_3)}{a}\left(Z_7 - \nu\alpha^2 Z_5\right)\Big|_{\eta=\phi} \tag{6.2.19}$$

similarly the applied load equal to the edge reaction $P_{1\eta}$ associated with the rotation $\psi_{1\eta}$ is taken to be

$$P_{1\eta} = \sum_{m=1,3,5}^{\infty} O_m \sin\frac{m\pi\xi}{2} \tag{6.2.20}$$

which results in the boundary condition

$$O_m = \frac{h_c}{a}\left(Z_4 - \alpha\nu Z_1\right)\Big|_{\eta=\phi} \tag{6.2.21}$$

the remaining boundary conditions at $\eta = \phi$ are established by making the proper substitutions and obtaining the edge reactions $P_{\eta\xi}$ and Q_η in state space form and setting them to zero at $\eta = \phi$, which results in

$$\begin{aligned} &\bar{\nu}^* \frac{h_c}{a}\left(\alpha Z_3 + Z_2\right) = 0\Big|_{\eta=\phi} \\ &g_2\left(Z_3 + Z_6\right) - \left(Z_8 - \alpha^2\left(2-\nu\right)Z_6\right) = 0\Big|_{\eta=\phi} \end{aligned} \tag{6.2.22}$$

We now turn are attention to the slip shear conditions along the edge $\eta = 0$, by substituting the Levy solutions into the slip shear conditions (6.2.3), the reader can verify that the following conditions must be satisfied

$$Z_2 = Z_3 = Z_6 = Z_8 = 0\Big|_{\eta=0} \tag{6.2.23}$$

With the boundary conditions established at $\eta = 0$ and $\eta = \phi$ in terms of the Levy solutions, which by definition satisfy the boundary conditions along $\xi = 0$ and $\xi = 1$, we can apply the boundary conditions to solve for the arbitrary constants c_j in terms of the applied load amplitudes E_m and O_m for the first building block.

As noted the state space approach lends itself to numerical computation of the necessary eigenvalues and corresponding eigenvalues that are need to obtain the Levy solutions, then the arbitrary constants of the solution are solved for by applying the boundary conditions on the two edges that do not have their boundary conditions satisfied by the formulation of the Levy solutions. In terms of numerical computation this requires a routine for calculating eigenvalues, eigenvectors and a method of solving a linear system of algebraic equations to solve for the arbitrary constants.

With Levy solutions for the first building block established, we now turn our attention to the second building block. Along the edges $\eta = 0$ and $\eta = \phi$ the slip shear boundary conditions are

$$W_{,\eta} = W_{,\eta\eta\eta} = \psi_{\eta} = \psi_{\xi,\eta} = 0\big|_{\eta=0,\eta=\phi} \tag{6.2.24}$$

and the functions that satisfy these conditions are

$$\begin{aligned} W_2(\xi,\eta) &= \sum_{n=0}^{\infty} Z_n(\xi)\cos\frac{n\pi\eta}{\phi} \\ \psi_{2\xi}(\xi,\eta) &= \sum_{n=0}^{\infty} X_n(\xi)\cos\frac{n\pi\eta}{\phi} \\ \psi_{2\eta}(\xi,\eta) &= \sum_{n=0}^{\infty} Y_n(\xi)\sin\frac{n\pi\eta}{\phi} \end{aligned} \tag{6.2.25}$$

which when substituted in the equations of motion (3.7.6) and the state space variables (6.2.11), where $\Sigma = n$, are introduced we obtain $\mathbf{Z}' = [\mathbf{C}]\mathbf{Z}$, where $\mathbf{C}$ for the second building block is given by

$$[\mathbf{C}] = \begin{bmatrix} 0 & 1 & 0 & 0 & 0 & 0 & 0 & 0 \\ C_6 & 0 & 0 & C_4 & 0 & C_5 & 0 & 0 \\ 0 & 0 & 0 & 1 & 0 & 0 & 0 & 0 \\ 0 & C_1 & C_3 & 0 & C_2 & 0 & 0 & 0 \\ 0 & 0 & 0 & 0 & 0 & 1 & 0 & 0 \\ 0 & 0 & 0 & 0 & 0 & 0 & 1 & 0 \\ 0 & 0 & 0 & 0 & 0 & 0 & 0 & 1 \\ 0 & C_9 & C_8 & 0 & C_{10} & 0 & C_7 & 0 \end{bmatrix} \tag{6.2.26}$$

where $\beta = \dfrac{n\pi}{\phi}$ and

$$C_1 = \beta\frac{\overline{\nu}}{\overline{\nu}^*} \qquad C_2 = -\beta\frac{g_1}{\overline{\nu}^*} \qquad C_3 = \frac{g_1+\beta^2}{\overline{\nu}^*} \qquad C_4 = -\beta\overline{\nu} \qquad C_5 = g_1$$

$$C_6 = \beta^2\overline{\nu}^* + g_1 \qquad C_7 = 2\beta^2 + g_2 \qquad C_8 = \beta g_2 \qquad C_9 = g_2 \qquad C_{10} = \omega^2 g_0 - \beta^4 - \beta^2 g_2$$

then the solution of the system of state space equations for the second building block is given by (6.2.14) where $\chi = \xi$.

Now we must establish the boundary conditions along the edges $\xi = 0$ and $\xi = 1$. At $\xi = 1$ we apply distributed loads in the same manor as the first building block; the distributed loads are set equal to the distributed edge reactions of the rotations normal to the edge (i.e. P_ξ and M_ξ) while setting the other distributed edge reactions to zero (i.e. $P_{\xi\eta}$ and Q_ξ).

The applied load that corresponds to the rotation $W_{2,\xi}$ and the associated edge reaction $M_{2\xi}$ along $\xi = 1$ is taken to be

$$M_{2\xi} = \sum_{n=0}^{\infty} E_n \cos\frac{n\pi\eta}{\phi} \tag{6.2.27}$$

equating the applied load to the edge reaction the following boundary condition is obtained

$$E_n = \frac{(D_1 + D_3)}{a}\left(Z_7 - \nu\beta^2 Z_5\right)\Big|_{\xi=1} \tag{6.2.28}$$

similarly, if the applied load equal to the edge reaction $P_{2\xi}$ associated with the rotation $\psi_{2\xi}$ along $\xi = 1$ is taken to be

$$P_{2\xi} = \sum_{n=0}^{\infty} O_n \cos\frac{n\pi\eta}{\phi} \tag{6.2.29}$$

which results in the boundary condition

$$O_n = \frac{h_c}{a}\left(Z_2 + \beta\nu Z_3\right)\Big|_{\xi=1} \tag{6.2.30}$$

the remaining boundary conditions at $\xi = 1$ are obtained by setting the edge reactions $P_{\xi\eta}$ and Q_ξ to zero at $\xi = 1$ which results in

$$\bar{\nu}^* \frac{h_c}{a}\left(Z_4 - \beta Z_1\right) = 0\Big|_{\xi=1}$$
$$g_2\left(Z_1 - Z_6\right) - \left(Z_8 - \beta^2\left(2-\nu\right)Z_6\right) = 0\Big|_{\xi=1} \tag{6.2.31}$$

We now turn are attention to the slip shear conditions along the edge $\xi = 0$, by substituting the Levy solutions into the simply supported conditions (6.2.3), the reader can verify that the following conditions must be satisfied

$$Z_2 = Z_3 = Z_5 = Z_7 = 0\Big|_{\xi=0} \tag{6.2.32}$$

The boundary conditions are established at $\xi = 0$ and $\xi = 1$ in terms of the Levy solutions, which by definition satisfy the boundary conditions along $\eta = 0$ and $\eta = \phi$, and we can apply the boundary conditions to solve for the arbitrary constants c_j in terms of the applied load amplitudes E_n and O_n for the second building block.

With Levy solutions for the second building block established, we now turn our attention to the third building block. The boundary conditions along the edges $\eta = 0$ and $\eta = \phi$ are slip shear boundary conditions, which are identical to the conditions for the second building block. .Therefore we can use the same Levy solutions as the second building block and we will obtain $\mathbf{Z}' = \left[\mathbf{C}\right]\mathbf{Z}$ where $\mathbf{C}$ for the third building block is the same as $\mathbf{C}$ for the second the building block. The only difference in the formulation is that the iterator the trigonometric series are summed over is changed (we will use p for the third building block), therefore p replaces n in (6.2.25) to obtain the Levy solutions for the third building block, and we will let $\gamma = \frac{p\pi}{\phi}$ which replaces β in (6.2.26). The solution to $\mathbf{Z}' = \left[\mathbf{C}\right]\mathbf{Z}$ for the third building block is given by (6.2.33) where $\chi = \xi$ and we will establish the boundary conditions along the edges $\xi = 0$ and $\xi = 1$.

Along the edge $\xi = 0$ we apply distributed loads that are set equal to the distributed edge reactions of the rotations normal to the edge (i.e. P_ξ and M_ξ) while setting the transverse deflection W_3 and the rotation $\psi_{1\eta}$ to zero. The conditions on this edge are different than the edges with applied loads for the first and second building blocks, the reason for this difference is because this corresponds to the clamped edge of the superimposed solution.

The applied load that corresponds to the rotation $W_{3,\xi}$ and the associated edge reaction $M_{3\xi}$ along $\xi = 0$ is taken to be

$$M_{3\xi} = \sum_{p=0}^{\infty} E_p \cos\frac{p\pi\eta}{\phi} \tag{6.2.34}$$

equating the applied load to the edge reaction the following boundary condition is obtained

$$E_n = \frac{(D_1 + D_3)}{a}\left(Z_7 - \nu\gamma^2 Z_5\right)\Big|_{\xi=0} \tag{6.2.35}$$

similarly, the applied load equal to the edge reaction $P_{3\xi}$ associated with the rotation $\psi_{3\xi}$ along $\xi = 0$ is taken to be

$$P_{3\xi} = \sum_{p=0}^{\infty} O_p \cos\frac{p\pi\eta}{\phi} \tag{6.2.36}$$

which results in the boundary condition

$$O_p = \frac{h_c}{a}\left(Z_2 + \gamma\nu Z_3\right)\Big|_{\xi=0} \tag{6.2.37}$$

the remaining boundary conditions at $\xi = 0$ are obtained by setting the transverse deflection W_3 and the rotation $\psi_{3\eta}$ along the edge to zero, which in state space is represented as

$$Z_3 = Z_5 = 0\big|_{\xi=0} \tag{6.2.38}$$

We now turn are attention to the slip shear conditions along the edge $\xi = 1$, by substituting the Levy solutions into the slip shear conditions (6.2.3), the reader can verify that the following conditions must be satisfied

$$Z_1 = Z_4 = Z_6 = Z_8 = 0\big|_{\xi=1} \tag{6.2.39}$$

The boundary conditions are established at $\xi = 0$ and $\xi = 1$ in terms of the Levy solutions, which by definition satisfy the boundary conditions along $\eta = 0$ and $\eta = \phi$, and we can apply the boundary conditions to solve for the arbitrary constants c_j in terms of the applied load amplitudes E_p and O_p for the third building block.

The solution of the cantilever plate is obtained by superimposing the solutions of the three building block plates, therefore

$$\begin{aligned} W(\xi,\eta) &= W_1(\xi,\eta)+W_2(\xi,\eta)+W_3(\xi,\eta) \\ \psi_\xi(\xi,\eta) &= \psi_{1\xi}(\xi,\eta)+\psi_{2\xi}(\xi,\eta)+\psi_{3\xi}(\xi,\eta) \\ \psi_\eta(\xi,\eta) &= \psi_{1\eta}(\xi,\eta)+\psi_{2\eta}(\xi,\eta)+\psi_{3\eta}(\xi,\eta) \end{aligned} \tag{6.2.40}$$

The superimposed Levy Solutions of the three building blocks must satisfy the boundary conditions of the cantilever plate (6.2.1) and this is achieved by determining the effect of the applied loads on the boundary conditions and adjusting the amplitudes of the applied loads to satisfy the boundary conditions exactly for each term of each trigonometric series.

Along the edge $\eta=\phi$ all of the building blocks have boundary conditions that correspond to the edge reactions Q_η and $P_{\eta\xi}$ set equal to zero, which are two of the four necessary conditions for a free edge (6.2.3). The other two conditions are that the edge reactions M_η and P_η must be zero. These reactions were not set to zero for the three building blocks, therefore using (6.2.40) the edge reaction M_η at $\eta=\phi$ of the superimposed solution is

$$\begin{aligned} M_\eta = E_m \sin\frac{m\pi\xi}{2} &+ \frac{(D_1+D_3)}{a}\left[\beta^2 Z_n(\xi)-\nu Z_n''(\xi)\right]\cos n\pi \\ &+ \frac{(D_1+D_3)}{a}\left[\gamma^2 Z_p(\xi)-\nu Z_p''(\xi)\right]\cos p\pi = 0 \end{aligned} \tag{6.2.41}$$

All of the terms of (6.2.41) are defined in ξ on the interval $[0,1]$, the first term is a trigonometric series of m involving the applied load amplitude E_m, while the other terms involving the iterators n and p are functions of the form (6.2.14) where the arbitrary constants c_j are functions of the amplitudes of the applied loads (e.g. E_n).

If the terms involving n and p could be expanded in terms of a Fourier series of the type $\sin\frac{m\pi\xi}{2}$, we could impose the constraint that the sum of the coefficients of the Fourier series must be equal to zero, resulting in a algebraic relation of the applied load amplitudes that satisfies the boundary condition $M_\eta=0$ at $\eta=\phi$ for the cantilever plate.

Let $f(\xi)$ be a function that continuous on the interval $[0,1]$, we can represent the function in this interval by the Fourier Series

$$f(\xi)=\sum_{m=1,3,5}^{\infty} A_m \sin\frac{m\pi\xi}{2} \tag{6.2.42}$$

To determine the coefficients of the series A_m we multiply (6.2.42) by $\sin\frac{\grave{m}\pi\xi}{2}$ and integrate both sides over the interval $[0,1]$ and using the relation

$$\int_0^1 \sin\frac{\grave{m}\pi\xi}{2}\sin\frac{m\pi\xi}{2}d\xi=\frac{1}{2}\delta_{m\grave{m}} \tag{6.2.43}$$

where δ is the Kronecker delta function (2.2.1), we obtain the relation

$$A_m=2\int_0^1 f(\xi)\sin\frac{m\pi\xi}{2}d\xi \tag{6.2.44}$$

we now represent the terms involving n and p in (6.2.41) as Fourier Series of the type $\sin\frac{m\pi\xi}{2}$, as a result (6.2.41) becomes

$$\begin{aligned} &A_{mm}\sin\frac{m\pi\xi}{2}+A_{mn}\sin\frac{m\pi\xi}{2}+A_{mp}\sin\frac{m\pi\xi}{2}=0\\ &A_{mm}+A_{mn}+A_{mp}=0 \end{aligned} \tag{6.2.45}$$

where

$$\begin{aligned} A_{mm}&=E_m\\ A_{mn}&=\frac{2}{a}(D_1+D_3)\cos n\pi\int_0^1\left[-\beta^2 Z_n(\xi)+\nu Z_n''(\xi)\right]\sin\frac{m\pi\xi}{2}d\xi\\ A_{mp}&=\frac{2}{a}(D_1+D_3)\cos p\pi\int_0^1\left[-\gamma^2 Z_p(\xi)+\nu Z_p''(\xi)\right]\sin\frac{m\pi\xi}{2}d\xi \end{aligned} \tag{6.2.46}$$

and A_{mn} is an expression with terms involving E_n and O_n for appropriate values of m and n, and A_{mp} is an expression with terms involving E_p and O_p for appropriate values of m and p.

Using the same procedure the edge reaction P_η at $\eta=\phi$ of the superimposed solution given by

$$\begin{aligned} P_\eta=O_m\sin\frac{m\pi\xi}{2}&+\frac{h_c}{a}\left[\beta Y_n(\xi)+\nu X_n'(\xi)\right]\cos n\pi\\ &+\frac{h_c}{a}\left[\gamma Y_p(\xi)+\nu X_p'(\xi)\right]\cos n\pi=0 \end{aligned} \tag{6.2.47}$$

is expanded in terms of the Fourier series (6.2.42) resulting in

$$B_{mm} + B_{mn} + B_{mp} = 0 \tag{6.2.48}$$

where

$$\begin{aligned} B_{mm} &= O_m \\ B_{mn} &= \frac{2h_c}{a}\cos n\pi \int_0^1 \left[\beta Y_n(\xi) + \nu X_n'(\xi)\right] \sin\frac{m\pi\xi}{2} d\xi \\ B_{mp} &= \frac{2h_c}{a}\cos p\pi \int_0^1 \left[\gamma Y_p(\xi) + \nu X_p'(\xi)\right] \sin\frac{m\pi\xi}{2} d\xi \end{aligned} \tag{6.2.49}$$

and B_{mn} and B_{mp} are expressions of similar form to A_{mn} and A_{mp}, respectively.

Along the edge $\xi = 1$ all of the building blocks have boundary conditions that correspond to the edge reactions Q_ξ and $P_{\xi\eta}$ set equal to zero, which are two of the four necessary conditions for a free edge (6.2.3). The other two conditions are that the edge reactions M_ξ and P_ξ must be zero. These reactions were not set to zero for the three building blocks therefore using (6.2.40) the edge reaction M_ξ at $\xi = 1$ of the superimposed solution is

$$\begin{aligned} M_\xi = &\frac{(D_1 + D_3)}{a}\left[-\alpha^2 Z_m(\eta) + \nu Z_m''(\eta)\right]\sin\frac{m\pi}{2} + E_n\cos\frac{n\pi}{\phi} \\ &+ \frac{(D_1 + D_3)}{a}\left[Z_p''(\xi) - \nu\gamma^2 Z_p(\xi)\right]\Big|_{\xi=1}\cos\frac{p\pi\eta}{\phi} = 0 \end{aligned} \tag{6.2.50}$$

The terms of (6.2.50) are defined in η on the interval $[0,\phi]$, using the same approach taken for the edge reactions along $\eta = \phi$; the terms involving m and p are expanded in terms of a Fourier series of the type $\cos\frac{n\pi\eta}{\phi}$.

Let $f(\eta)$ be a continuous function on the interval $[0,\phi]$, we can represent this function in this interval by the Fourier series

$$f(\eta) = \sum_{n=0}^{\infty} A_n \cos\frac{n\pi\eta}{\phi} \tag{6.2.51}$$

where the coefficients A_n are given by

$$A_n = \begin{cases} \dfrac{1}{\phi}\int_0^{\phi} f(\eta)\cos\dfrac{n\pi\eta}{\phi}\,d\eta & n=0 \\ \dfrac{2}{\phi}\int_0^{\phi} f(\eta)\cos\dfrac{n\pi\eta}{\phi}\,d\eta & n\neq 0 \end{cases} \tag{6.2.52}$$

using (6.2.51) to represent the terms involving m and p in terms of a Fourier series of the type $\cos\dfrac{n\pi\eta}{\phi}$, (6.2.50) becomes

$$\begin{aligned} &A_{nm}\cos\frac{n\pi\eta}{\phi} + A_{nn}\cos\frac{n\pi\eta}{\phi} + A_{np}\cos\frac{n\pi\eta}{\phi} = 0 \\ &A_{nm} + A_{nn} + A_{np} = 0 \end{aligned} \tag{6.2.53}$$

where

$$\begin{aligned} A_{nm} &= \frac{If(n)}{a\phi}(D_1 + D_3)\sin\frac{m\pi}{2}\int_0^{\phi}\left[-\alpha^2 Z_m(\eta) + \nu Z_m''(\eta)\right]\cos\frac{n\pi\eta}{\phi}\,d\eta \\ A_{nn} &= E_n \\ A_{np} &= \frac{(D_1 + D_3)}{a}\left[Z_p''(\xi) - \nu\gamma^2 Z_p(\xi)\right]\Big|_{\xi=1}\delta_{np} \end{aligned} \tag{6.2.54}$$

with $If(n)$ defined as

$$If(n) = \begin{cases} 1 & n=0 \\ 2 & n\neq 0 \end{cases} \tag{6.2.55}$$

and A_{nm} is an expression with terms involving E_m and O_m for appropriate values of n and m, and A_{np} is an expression with terms involving E_p and O_p for appropriate values of n and p.

Using the same procedure the edge reaction P_ξ at $\xi = 1$ of the superimposed solution given by

$$\begin{aligned} P_\xi &= \frac{h_c}{a}\left[-\alpha X_m(\eta) + \nu Y_m'(\eta)\right]\sin\frac{m\pi}{2} + O_n\cos\frac{n\pi\eta}{\phi} \\ &+ \frac{h_c}{a}\left[X_p'(\xi) + \nu\gamma Y_p(\xi)\right]\Big|_{\xi=1}\cos\frac{p\pi\eta}{\phi} = 0 \end{aligned} \tag{6.2.56}$$

which is expanded in terms of the Fourier series (6.2.51) resulting in

$$B_{nm} + B_{nn} + B_{np} = 0 \tag{6.2.57}$$

where

$$B_{nm} = \frac{If(n)h_c}{\phi a}\sin\frac{m\pi}{2}\int_0^{\phi}\left[-\alpha X_m(\eta)+\nu Y_m'(\eta)\right]\cos\frac{n\pi\eta}{\phi}d\eta$$
$$B_{nn} = O_n \tag{6.2.58}$$
$$B_{np} = \frac{h_c}{a}\left[X_p'(\xi)+\nu\gamma Y_p(\xi)\right]\Big|_{\xi=1}\delta_{np}$$

and B_{nm} and B_{np} are expressions of similar form to A_{nm} and A_{np}, respectively.

Along the edge $\xi = 0$ all of the building blocks have boundary conditions where the transverse deflection W and the rotation ψ_η are set equal to zero, which are two of the four boundary conditions necessary for a clamped edge (6.2.3). The other two conditions involve setting the rotations $W_{,\xi}$ and ψ_ξ equal to zero at the edge $\xi = 0$. Using (6.2.40) the rotation $W_{,\xi}$ at $\xi = 0$ of the superimposed solution is

$$W_{,\xi} = \alpha Z_m(\eta)+\left[Z_n'(\xi)\right]\Big|_{\xi=0}\cos\frac{n\pi\eta}{\phi} + \left[Z_p'(\xi)\right]\Big|_{\xi=0}\cos\frac{p\pi\eta}{\phi} = 0 \tag{6.2.59}$$

The terms of (6.2.59) are defined in η on the interval $[0,\phi]$, using the same approach taken for the edge reactions along $\eta = \phi$ the terms involving m and n are expanded in terms of the Fourier series (6.2.51) with n replaced with p, which results in

$$A_{pm}\cos\frac{p\pi\eta}{\phi} + A_{pn}\cos\frac{p\pi\eta}{\phi} + A_{pp}\cos\frac{p\pi\eta}{\phi} = 0$$
$$A_{pm} + A_{pn} + A_{pp} = 0 \tag{6.2.60}$$

where

$$A_{pm} = \frac{\alpha If(p)}{\phi}\int_0^{\phi} Z_m(\eta)\cos\frac{p\pi\eta}{\phi}d\eta$$
$$A_{pn} = \left[Z_n'(\xi)\right]\Big|_{\xi=0}\delta_{pn} \tag{6.2.61}$$
$$A_{pp} = \left[Z_p'(\xi)\right]\Big|_{\xi=0}$$

and A_{pm} is an expression with terms involving E_m and O_m for appropriate values of n and p, A_{pn} is an expression with terms involving E_n and O_n for appropriate values of p and n and A_{pp} is an expression with terms involving E_p and O_p for appropriate values of p.

Using the same procedure the rotation ψ_ξ at $\xi = 0$ of the superimposed solution given by

$$\psi_\xi = X_m(\eta) + X_n(\xi)\Big|_{\xi=0} \cos\frac{n\pi\eta}{\phi} + X_p(\xi)\Big|_{\xi=0} \cos\frac{p\pi\eta}{\phi} = 0 \tag{6.2.62}$$

which is expanded in terms of the Fourier series (6.2.51) with n replacing p resulting in

$$B_{pm} + B_{pn} + B_{pp} = 0 \tag{6.2.63}$$

where

$$\begin{aligned} B_{pm} &= \frac{If(p)}{\phi} \int_0^\phi \left[X_m(\eta)\right] \cos\frac{p\pi\eta}{\phi} d\eta \\ B_{pn} &= \left[X_n(\xi)\right]\Big|_{\xi=0} \delta_{np} \\ B_{pp} &= \left[X_p(\xi)\right]\Big|_{\xi=0} \end{aligned} \tag{6.2.64}$$

and B_{pm} and B_{pn} are expressions of similar form to A_{pm} and A_{pn}, respectively.

Finally, along the edge $\eta = 0$ we have imposed slip shear conditions for the symmetric modes of the cantilever plate. All of the building blocks satisfy this condition as a result the superimposed solution also satisfies these conditions, so we need not formulate conditions for the edge $\eta = 0$ for the superimposed solution.

We have developed a system of equations in terms of the amplitudes of the loads applied to the boundaries of the building block plates to satisfy the boundary conditions of the cantilever plate. We can arrange the system of equations in the form given by the following schematic

$$\begin{bmatrix}
\begin{bmatrix} - & 0 & 0 \\ 0 & A_{mm} & 0 \\ 0 & 0 & - \end{bmatrix} & \begin{bmatrix} - & - & - \\ - & A_{mn} & - \\ - & - & - \end{bmatrix} & \begin{bmatrix} - & - & - \\ - & A_{mp} & - \\ - & - & - \end{bmatrix} \\
\begin{bmatrix} - & 0 & 0 \\ 0 & B_{mm} & 0 \\ 0 & 0 & - \end{bmatrix} & \begin{bmatrix} - & - & - \\ - & B_{mn} & - \\ - & - & - \end{bmatrix} & \begin{bmatrix} - & - & - \\ - & B_{mn} & - \\ - & - & - \end{bmatrix} \\
\begin{bmatrix} - & - & - \\ - & A_{nm} & - \\ - & - & - \end{bmatrix} & \begin{bmatrix} - & 0 & 0 \\ 0 & A_{nn} & 0 \\ 0 & 0 & - \end{bmatrix} & \begin{bmatrix} - & 0 & 0 \\ 0 & A_{np} & 0 \\ 0 & 0 & - \end{bmatrix} \\
\begin{bmatrix} - & - & - \\ - & B_{nm} & - \\ - & - & - \end{bmatrix} & \begin{bmatrix} - & 0 & 0 \\ 0 & B_{nn} & 0 \\ 0 & 0 & - \end{bmatrix} & \begin{bmatrix} - & 0 & 0 \\ 0 & B_{np} & 0 \\ 0 & 0 & - \end{bmatrix} \\
\begin{bmatrix} - & - & - \\ - & A_{pm} & - \\ - & - & - \end{bmatrix} & \begin{bmatrix} - & 0 & 0 \\ 0 & A_{pn} & 0 \\ 0 & 0 & - \end{bmatrix} & \begin{bmatrix} - & 0 & 0 \\ 0 & A_{pp} & 0 \\ 0 & 0 & - \end{bmatrix} \\
\begin{bmatrix} - & - & - \\ - & B_{pm} & - \\ - & - & - \end{bmatrix} & \begin{bmatrix} - & 0 & 0 \\ 0 & B_{pn} & 0 \\ 0 & 0 & - \end{bmatrix} & \begin{bmatrix} - & 0 & 0 \\ 0 & B_{pp} & 0 \\ 0 & 0 & - \end{bmatrix}
\end{bmatrix} = \underline{0}$$

(6.2.65)

however we wish to solve for the applied load amplitudes $\left(E_m, O_m, E_n, O_n, E_p, O_p\right)$ which then gives the following system of equations in the form given by the following schematic

$$\begin{array}{c}
m= \\ 1 \\ 3 \\ 5
\end{array}
\begin{array}{c}
\begin{array}{ccc} 1 & 3 & 5 \end{array} \\
\begin{bmatrix} 1 & & \\ & 1 & \\ & & 1 \end{bmatrix}
\end{array}
\begin{array}{c}
m= \\ 1 \\ 3 \\ 5
\end{array}
\begin{array}{c}
\begin{array}{ccc} 1 & 3 & 5 \end{array} \\
\begin{bmatrix} & & \\ & 0 & \\ & & \end{bmatrix}
\end{array}
\begin{array}{c}
n= \\ 0 \\ 1 \\ 2
\end{array}
\begin{array}{c}
\begin{array}{ccc} 0 & 1 & 2 \end{array} \\
\begin{bmatrix} - & - & - \\ - & - & - \\ - & - & - \end{bmatrix}
\end{array}
\begin{array}{c}
n= \\ 0 \\ 1 \\ 2
\end{array}
\begin{array}{c}
\begin{array}{ccc} 0 & 1 & 2 \end{array} \\
\begin{bmatrix} - & - & - \\ - & - & - \\ - & - & - \end{bmatrix}
\end{array}
\begin{array}{c}
p= \\ 0 \\ 1 \\ 2
\end{array}
\begin{array}{c}
\begin{array}{ccc} 0 & 1 & 2 \end{array} \\
\begin{bmatrix} - & - & - \\ - & - & - \\ - & - & - \end{bmatrix}
\end{array}
\begin{array}{c}
p= \\ 0 \\ 1 \\ 2
\end{array}
\begin{array}{c}
\begin{array}{ccc} 0 & 1 & 2 \end{array} \\
\begin{bmatrix} - & - & - \\ - & - & - \\ - & - & - \end{bmatrix}
\end{array}
\left\{ \begin{array}{c}
\begin{bmatrix} E_m \end{bmatrix} \\ \begin{bmatrix} O_m \end{bmatrix} \\ \begin{bmatrix} E_n \end{bmatrix} \\ \begin{bmatrix} O_n \end{bmatrix} \\ \begin{bmatrix} E_p \end{bmatrix} \\ \begin{bmatrix} O_p \end{bmatrix}
\end{array} \right\} = \underline{0}$$

(6.2.66)

where the following schematic shows a three term expansion of the each of the building block plate solutions, but the in analysis the number of the terms should be determined by convergence tests with the understanding that increasing the number of terms increases the accuracy of the solution.

The coefficient matrix in (6.2.66) is represented by Δ and the applied load amplitude vector is represented by $\underline{\mathbf{E}}$, therefore (6.2.66) can be represented as $\Delta\underline{\mathbf{E}} = 0$. The integrals used to compute Δ are Fourier series expansions of the state space solutions for the three building blocks. We know that depending if the complex part of an eigenvalue used in the state space solution is zero, positive, or negative the part of the solution will take on the three possible forms

$$\begin{array}{lll} \lambda_j & r_i^{(j)} & z_i = c_j r_i^{(j)} e^{\lambda_j \chi} \\ \lambda_j = \sigma + i\tau & r_i^{(j)} = s_i^{(j)} + i t_i^{(j)} & z_i = c_j e^{\sigma_j \chi}\left(s_i^{(j)} \cos\tau_j\chi - t_i^{(j)} \sin\tau_j\chi\right) \\ \lambda_j = \sigma - i\tau & r_i^{(j)} = s_i^{(j)} - i t_i^{(j)} & z_i = c_j e^{\sigma_j \chi}\left(s_i^{(j)} \sin\tau_j\chi + t_i^{(j)} \cos\tau_j\chi\right) \end{array} \tag{6.2.67}$$

given this and that the integrals are with respect to the spatial variable χ on the intervals $[0,1]$ and $[0,\phi]$, there are six possible integrals that are encountered in computing Δ, of the form

$$\begin{aligned} IntES &= \int_0^1 e^{\lambda\chi} \sin\alpha\chi d\chi \\ IntECS &= \int_0^1 e^{\sigma\chi} \cos\tau\chi \sin\alpha\chi d\chi \\ IntESS &= \int_0^1 e^{\sigma\chi} \sin\tau\chi \sin\alpha\chi d\chi \\ IntEC &= \int_0^\phi e^{\lambda\chi} \cos\beta\chi d\chi \\ IntECC &= \int_0^\phi e^{\sigma\chi} \cos\tau\chi \cos\beta\chi d\chi \\ IntESC &= \int_0^\phi e^{\sigma\chi} \sin\tau\chi \cos\beta\chi d\chi \end{aligned} \tag{6.2.68}$$

where the solutions to these integrals are given in **APPENDIX 2** and β can be replaced by γ where necessary for integrals involving the third building block solution and its iterator p.

However examination of (6.2.66) shows that p can be replaced by n because no terms of Δ exist for values where $n \neq p$ and this is done with the understanding that the state space solutions involving the iterators n and p (i.e. building block plate 2 and 3) are not equal.

There are 36 components of Δ with 16 components computed using integrals of the form (6.2.68) we will take two components and show how the integrals in (6.2.68) are used to obtain the terms of the components for values of the iterators. Taking the components A_{mn} given by (6.2.46) and knowing that it can be decomposed into two components of Δ by virtue of the fact that the arbitrary constants of the state space solutions of the second building block will be composed of a part involving E_n and a part involving O_n so we can represent c_j as $c_j = c_j^E E_\Sigma + c_j^O O_\Sigma$. Therefore we have $A_{mn} = \Delta^E{}_{mn} E_n + \Delta^O_{mn} O_n$ and in general

$$A_{\Sigma\Sigma'} = \Delta^E{}_{\Sigma\Sigma'} E_{\Sigma'} + \Delta^O_{\Sigma\Sigma'} O_{\Sigma'} \qquad \Sigma, \Sigma' = m, n, p \tag{6.2.69}$$

this decomposition takes use from the schematic (6.2.65) to the schematic (6.2.66). Therefore Δ^E_{mn} is given in terms of the integrals (6.2.68) by

$$\Delta^E_{mn} = \sum_j^8 \begin{cases} \frac{2}{a}(D_1 + D_3)\cos n\pi \times \left(c_j^E\right)_n \left[-\beta^2 r_1^{(j)} + \nu r_3^{(j)}\right]_n \left(IntES|_{\lambda=\lambda_j}\right)_n & \lambda_j = \lambda_j \\ \frac{2}{a}(D_1 + D_3)\cos n\pi \times \left(c_j^E\right)_n \left\{\left[-\beta^2 s_1^{(j)} + \nu s_3^{(j)}\right]_n \left(IntECS|_{\sigma=\sigma_j, \tau=\tau_j}\right)_n - \left[-\beta^2 \mathrm{t}_1^{(j)} + \nu \mathrm{t}_3^{(j)}\right]_n \left(IntESS|_{\sigma=\sigma_j, \tau=\tau_j}\right)_n\right\} & \lambda_j = \sigma_j + i\tau_j \\ \frac{2}{a}(D_1 + D_3)\cos n\pi \times \left(c_j^E\right)_n \left\{\left[-\beta^2 s_1^{(j)} + \nu s_3^{(j)}\right]_n \left(IntESS|_{\sigma=\sigma_j, \tau=\tau_j}\right)_n + \left[-\beta^2 \mathrm{t}_1^{(j)} + \nu \mathrm{t}_3^{(j)}\right]_n \left(IntECS|_{\sigma=\sigma_j, \tau=\tau_j}\right)_n\right\} & \lambda_j = \sigma_j - i\tau_j \end{cases}$$

(6.2.70)

where the subscript n denotes that the constants, eigenvectors and eigenvalues are from the second building block Levy solutions involving the iterator n, and only the first three integrals of (6.2.68) are used because Δ^E_{mn} is an expansion in terms of the series $\sin \alpha\chi$, where $\chi = \xi$.

Taking the components of A_{nm} given by (6.2.54) and examining the corresponding component of Δ, Δ^E_{nm} is given in terms of the integrals (6.2.68) by

$$\Delta^E_{nm} = \sum_j^8 \begin{cases} \frac{If(n)}{a\phi}(D_1 + D_3)\sin \alpha \times \left(c_j^E\right)_m \left[-\alpha^2 r_1^{(j)} + \nu r_3^{(j)}\right]_m \left(IntEC|_{\lambda=\lambda_j}\right)_m & \lambda_j = \lambda_j \\ \frac{If(n)}{a\phi}(D_1 + D_3)\sin \alpha \times \left(c_j^E\right)_m \left\{\left[-\alpha^2 s_1^{(j)} + \nu s_3^{(j)}\right]_m \left(IntECC|_{\sigma=\sigma_j, \tau=\tau_j}\right)_m - \left[-\alpha^2 \mathrm{t}_1^{(j)} + \nu \mathrm{t}_3^{(j)}\right]_m \left(IntESC|_{\sigma=\sigma_j, \tau=\tau_j}\right)_m\right\} & \lambda_j = \sigma_j + i\tau_j \\ \frac{If(n)}{a\phi}(D_1 + D_3)\sin \alpha \times \left(c_j^E\right)_m \left\{\left[-\alpha^2 s_1^{(j)} + \nu s_3^{(j)}\right]_m \left(IntESC|_{\sigma=\sigma_j, \tau=\tau_j}\right)_m + \left[-\alpha^2 \mathrm{t}_1^{(j)} + \nu \mathrm{t}_3^{(j)}\right]_m \left(IntECC|_{\sigma=\sigma_j, \tau=\tau_j}\right)_m\right\} & \lambda_j = \sigma_j - i\tau_j \end{cases}$$

(6.2.71)

where the subscript m denotes that the constants, eigenvectors and eigenvalues are from the first building block Levy solutions involving the iterator m, and only the last three integrals of (6.2.68) are used because Δ^E_{nm} is an expansion in terms of the series $\cos \beta\chi$, where $\chi = \eta$ ..

To obtain Δ^{O}_{nm} the constant $\left(c^{E}_{j}\right)_{m}$ is replaced with $\left(c^{O}_{j}\right)_{m}$ in (6.2.71) and this is the general case all $\Delta^{O}_{\Sigma\Sigma'}$ can be obtained from $\Delta^{E}_{\Sigma\Sigma'}$ by replacing $\left(c^{E}_{j}\right)_{m}$ with $\left(c^{O}_{j}\right)_{m}$.

Of the 20 remaining components of Δ, 4 are identity matrices and 4 are null matrices the remaining 12 do not involve integration and are computed from the straight forward evaluation of state space solutions at a specified edge using the decomposition $z_i = z^{E}_{i} E_{\Sigma} + z^{O}_{i} O_{\Sigma}$.

Finally, in order for the relation $\Delta\underline{\mathbf{E}} = 0$ to be true the determinant of Δ must be zero for a given frequency, thus making that frequency for which the determinant of Δ vanishes a frequency of free vibration.

We now have an equation for the determination of the frequencies of vibration of the cantilever plate which is given by

$$\mathbf{Det}\left[\Delta\right]\Big|_{\omega=\omega_n} = 0 \tag{6.2.72}$$

and given that this condition is satisfied then we can solve for the applied load amplitudes in the same manor eigenvectors are calculated (i.e. arbitrarily setting one of the amplitudes to unity). The amplitudes can then be substituted into the expressions for arbitrary constants of the state space solutions and the state space solutions are in tern used to complete the Levy solutions of the building block plates which are superimposed resulting in mode shapes of the of the sandwich cantilever plate, given that the frequency of vibration satisfies the condition (6.2.72).

6.2.2 Symmetric Modes Computer Implementation

This section outlines the steps a computer program must perform and lists all of the equations developed in the previous section that are necessary for creating a program that determines the frequencies of vibration and corresponding mode shapes of the a cantilever plate modeled using the USPT.

STEP 1: Input the Material and Geometric properties and calculate the associated constants for the non-dimensional transverse simplified USPT given by (3.7.4).

STEP 2: Determine a starting frequency for which the building block plate solutions are calculated and Δ is found and store it. It is *important* to remember that all of the building block plate solutions are functions of the vibration frequency which we must provide prior to calculation and then by the condition (6.2.72) we can determine if the frequency is a natural frequency of vibration.

STEP 3: Determine the number of terms of the iterators (m, n, p) used in each of the Levy solutions, then for each of the building block plates compute and store the eigenvalues

λ_j and corresponding eigenvectors $r_i^{(j)}$ from $\mathbf{C}$ for each term of the solution. Then apply the necessary boundary conditions to the state space solutions given by (6.2.14) for each term to solve for the arbitrary constants c_j, which will be in terms of the applied load amplitudes $\left(E_\Sigma, O_\Sigma\right)$ of the building block, and store them for each term. It is *important* that considerations are made for complex eigenvalues to ensure that the Levy solutions are real, an IF statement can be used based on the condition of the eigenvalue to use the appropriate form of the three possible forms of the components of the state space solution.

STEP 4: Compute Δ by using the appropriate stored eigenvalues, eigenvectors and constants c_j to form the coefficients of the integral expansions of the conditions required to ensure that the applied load amplitudes satisfy the cantilever boundary conditions. Once again an IF statement can be used based on the condition of the eigenvalue in conjunction with the appropriate form of the exact integrals given in (6.2.68), as done in (6.2.70) to compute Δ.

STEP 5: Compute and store the determinant, rank and minimum eigenvalue of Δ. In order for the determinant of Δ to vanish it must be rank deficient or similarly it must have a zero eigenvalue, therefore numerically we have three measures to use in determining if a frequency is a natural frequency of vibration.

STEP 6: Repeat *STEP 3 – STEP 5* for an incremental increase in frequency over a desired frequency range.

STEP 7: Analyze the data stored and if necessary increase terms of the Levy solutions or refine the range of frequencies examined and the increment of the frequency, until a natural frequency of vibration is determined.

STEP 8: Given that a frequency is determined to be a natural frequency of vibration obtain the solution for the applied load amplitudes from Δ and use them to determine the mode shapes corresponding to the natural frequency of vibration.

Having listed the general steps to the numeric superposition method (NSM) and given a detailed example of a program to implement the solution, the equations necessary to create the solution will now be listed for convenience, all of which appear in the previous section which details the theoretical development.

6.2.2.1 First Building Block Equations

First Building Block Levy Solutions

$$W_1(\xi,\eta) = \sum_{m=1,3,5}^{\infty} Z_m(\eta)\sin\alpha\xi$$

$$\psi_{1\xi}(\xi,\eta) = \sum_{m=1,3,5}^{\infty} X_m(\eta)\cos\alpha\xi \qquad \alpha = m\pi/2$$

$$\psi_{1\eta}(\xi,\eta) = \sum_{m=1,3,5}^{\infty} Y_m(\eta)\sin\alpha\xi$$

State Space Matrix

$$\mathbf{C} = \begin{bmatrix} 0 & 1 & 0 & 0 & 0 & 0 & 0 & 0 \\ C_6 & 0 & 0 & C_4 & C_5 & 0 & 0 & 0 \\ 0 & 0 & 0 & 1 & 0 & 0 & 0 & 0 \\ 0 & C_1 & C_3 & 0 & 0 & C_2 & 0 & 0 \\ 0 & 0 & 0 & 0 & 0 & 1 & 0 & 0 \\ 0 & 0 & 0 & 0 & 0 & 0 & 1 & 0 \\ 0 & 0 & 0 & 0 & 0 & 0 & 0 & 1 \\ C_9 & 0 & 0 & C_8 & C_{10} & 0 & C_7 & 0 \end{bmatrix}$$

$$C_1 = \alpha\bar{v} \qquad C_2 = g_1 \qquad C_3 = g_1 + \alpha^2\bar{v}^* \qquad C_4 = -\alpha\frac{\bar{v}}{\bar{v}^*} \qquad C_5 = \alpha\frac{g_1}{\bar{v}^*}$$

$$C_6 = \frac{\alpha^2 + g_1}{\bar{v}^*} \qquad C_7 = 2\alpha^2 + g_2 \qquad C_8 = g_2 \qquad C_9 = -\alpha g_2 \qquad C_{10} = \omega^2 g_0 - \alpha^4 - \alpha^2 g_2$$

Boundary Conditions on State Space Solutions

$$E_m = \frac{(D_1 + D_3)}{a}\left(Z_7 - \nu\alpha^2 Z_5\right)\Big|_{\eta=\phi}$$

$$O_m = \frac{h_c}{a}\left(Z_4 - \alpha\nu Z_1\right)\Big|_{\eta=\phi}$$

$$\bar{v}^*\frac{h_c}{a}\left(\alpha Z_3 + Z_2\right) = 0\Big|_{\eta=\phi}$$

$$g_2\left(Z_3 + Z_6\right) - \left(Z_8 - \alpha^2\left(2-\nu\right)Z_6\right) = 0\Big|_{\eta=\phi}$$

$$Z_2 = Z_3 = Z_6 = Z_8 = 0\Big|_{\eta=0}$$

6.2.2.2 Second Building Block Equations

Second Building Block Levy Solutions

$$W_2(\xi,\eta)=\sum_{n=0}^{\infty} Z_n(\xi)\cos\beta\eta$$

$$\psi_{2\xi}(\xi,\eta)=\sum_{n=0}^{\infty} X_n(\xi)\cos\beta\eta \qquad \beta=n\pi/\phi$$

$$\psi_{2\eta}(\xi,\eta)=\sum_{n=0}^{\infty} Y_n(\xi)\sin\beta\eta$$

State Space Matrix

$$[\mathbf{C}]=\begin{bmatrix} 0 & 1 & 0 & 0 & 0 & 0 & 0 & 0 \\ C_6 & 0 & 0 & C_4 & 0 & C_5 & 0 & 0 \\ 0 & 0 & 0 & 1 & 0 & 0 & 0 & 0 \\ 0 & C_1 & C_3 & 0 & C_2 & 0 & 0 & 0 \\ 0 & 0 & 0 & 0 & 0 & 1 & 0 & 0 \\ 0 & 0 & 0 & 0 & 0 & 0 & 1 & 0 \\ 0 & 0 & 0 & 0 & 0 & 0 & 0 & 1 \\ 0 & C_9 & C_8 & 0 & C_{10} & 0 & C_7 & 0 \end{bmatrix}$$

$$C_1=\beta\frac{\overline{\nu}}{\overline{\nu}^*} \qquad C_2=-\beta\frac{g_1}{\overline{\nu}^*} \qquad C_3=\frac{g_1+\beta^2}{\overline{\nu}^*} \qquad C_4=-\beta\overline{\nu} \qquad C_5=g_1$$

$$C_6=\beta^2\overline{\nu}^*+g_1 \qquad C_7=2\beta^2+g_2 \qquad C_8=\beta g_2 \qquad C_9=g_2 \qquad C_{10}=\omega^2 g_0-\beta^4-\beta^2 g_2$$

Boundary Conditions on State Space Solutions

$$E_n=\frac{(D_1+D_3)}{a}\left(Z_7-\nu\beta^2 Z_5\right)\Big|_{\xi=1}$$

$$O_n=\frac{h_c}{a}\left(Z_2+\beta\nu Z_3\right)\Big|_{\xi=1}$$

$$\overline{\nu}^*\frac{h_c}{a}\left(Z_4-\beta Z_1\right)=0\Big|_{\xi=1}$$

$$g_2\left(Z_1-Z_6\right)-\left(Z_8-\beta^2\left(2-\nu\right)Z_6\right)=0\Big|_{\xi=1}$$

$$Z_2=Z_3=Z_5=Z_7=0\Big|_{\xi=0}$$

6.2.2.3 Third Building Block Equations

The Levy Solutions and State Space Matrix for the third building block can be obtained from the second building block by replacing n with p and β with γ, where $\gamma=p\pi/\phi$.

$$E_n = \frac{(D_1 + D_3)}{a}\left(Z_7 - \nu\gamma^2 Z_5\right)\Big|_{\xi=0}$$

$$O_p = \frac{h_c}{a}\left(Z_2 + \gamma\nu Z_3\right)\Big|_{\xi=0}$$

$$Z_3 = Z_5 = 0\big|_{\xi=0}$$

$$Z_1 = Z_4 = Z_6 = Z_8 = 0\big|_{\xi=1}$$

6.2.2.4 Coefficients of the Determinant Matrix

$$A_{mm} = E_m$$

$$A_{mn} = \frac{2}{a}(D_1 + D_3)\cos n\pi \int_0^1 \left[-\beta^2 Z_n(\xi) + \nu Z_n''(\xi)\right]\sin\frac{m\pi\xi}{2}\,d\xi$$

$$A_{mp} = \frac{2}{a}(D_1 + D_3)\cos p\pi \int_0^1 \left[-\gamma^2 Z_p(\xi) + \nu Z_p''(\xi)\right]\sin\frac{m\pi\xi}{2}\,d\xi$$

$$B_{mm} = O_m$$

$$B_{mn} = \frac{2h_c}{a}\cos n\pi \int_0^1 \left[\beta Y_n(\xi) + \nu X_n'(\xi)\right]\sin\frac{m\pi\xi}{2}\,d\xi$$

$$B_{mp} = \frac{2h_c}{a}\cos p\pi \int_0^1 \left[\gamma Y_p(\xi) + \nu X_p'(\xi)\right]\sin\frac{m\pi\xi}{2}\,d\xi$$

$$A_{nm} = \frac{If(n)}{a\phi}(D_1 + D_3)\sin\frac{m\pi}{2}\int_0^\phi \left[-\alpha^2 Z_m(\eta) + \nu Z_m''(\eta)\right]\cos\frac{n\pi\eta}{\phi}\,d\eta$$

$$A_{nn} = E_n$$

$$A_{np} = \frac{(D_1 + D_3)}{a}\left[Z_p''(\xi) - \nu\gamma^2 Z_p(\xi)\right]\Big|_{\xi=1}\delta_{np}$$

$$B_{nm} = \frac{If(n)h_c}{\phi a}\sin\frac{m\pi}{2}\int_0^\phi \left[-\alpha X_m(\eta) + \nu Y_m'(\eta)\right]\cos\frac{n\pi\eta}{\phi}\,d\eta$$

$$B_{nn} = O_n$$

$$B_{np} = \frac{h_c}{a}\left[X_p'(\xi) + \nu\gamma Y_p(\xi)\right]\Big|_{\xi=1}\delta_{np}$$

$$A_{pm} = \frac{If(p)}{\phi}\int_0^\phi \left[\alpha Z_m(\eta)\right]\cos\frac{p\pi\eta}{\phi}\,d\eta$$

$$A_{pn} = \left[Z_n'(\xi)\right]\Big|_{\xi=0}\delta_{pn}$$

$$A_{pp} = \left[Z_p'(\xi)\right]\Big|_{\xi=0}$$

$$B_{pm} = \frac{If(p)}{\phi}\int_0^{\phi}\left[X_m(\eta)\right]\cos\frac{p\pi\eta}{\phi}d\eta$$

$$B_{pn} = \left[X_n(\xi)\right]\Big|_{\xi=0}\delta_{np}$$

$$B_{pp} = \left[X_p(\xi)\right]\Big|_{\xi=0}$$

6.2.2.5 *Forms of the Components of the State Space Solutions and resulting Integrals*

Possible Forms of the Components of the State Space Solutions

$$\begin{array}{lll} \lambda_j & r_i^{(j)} & z_i = c_j r_i^{(j)} e^{\lambda_j \chi} \\ \lambda_j = \sigma + i\tau & r_i^{(j)} = s_i^{(j)} + i t_i^{(j)} & z_i = c_j e^{\sigma_j \chi}\left(s_i^{(j)}\cos\tau_j\chi - t_i^{(j)}\sin\tau_j\chi\right) \\ \lambda_j = \sigma - i\tau & r_i^{(j)} = s_i^{(j)} - i t_i^{(j)} & z_i = c_j e^{\sigma_j \chi}\left(s_i^{(j)}\sin\tau_j\chi + t_i^{(j)}\cos\tau_j\chi\right) \end{array}$$

Forms of Integrals that Result from Formulating the Coefficients of the Determinant Matrix using the Possible Forms of the Components of the State Space Solutions

$$IntES = \int_0^{\phi} e^{\lambda\chi}\sin\alpha\chi d\chi$$

$$IntECS = \int_0^{\phi} e^{\sigma\chi}\cos\tau\chi\sin\alpha\chi d\chi$$

$$IntESS = \int_0^{\phi} e^{\sigma\chi}\sin\tau\chi\sin\alpha\chi d\chi$$

$$IntEC = \int_0^{\phi} e^{\lambda\chi}\cos\beta\chi d\chi$$

$$IntECC = \int_0^{\phi} e^{\sigma\chi}\cos\tau\chi\cos\beta\chi d\chi$$

$$IntESC = \int_0^{\phi} e^{\sigma\chi}\sin\tau\chi\cos\beta\chi d\chi$$

6.3 *TSDT*

For the analysis of the cantilever plate with the TSDT we will restrict ourselves to the equations of motion (4.7.5) and the corresponding boundary conditions (4.7.6) and. (4.7.7) The reader should refer to sections **4.6** and **4.7** for the derivation of these equations, they are uncoupled from the inplane motions of the plate and simplified by only considering the transverse inertia of the plate.

The boundary conditions for the cantilever plate are along the edge

$\xi = 0$	$\xi = 1$
$\psi_{\xi} = 0$	$\Xi_1\psi_{\xi,\xi} + \Xi_2\psi_{\eta,\eta} + \Xi_3 W_{,\xi\xi} + \Xi_4 W_{,\eta\eta} = 0$
$\psi_{\eta} = 0$	$\Xi_9\psi_{\xi,\eta} + \Xi_{10}\psi_{\eta,\xi} + \Xi_{11} W_{,\xi\eta} = 0$
$W_{,\xi} = 0$	$\Xi_{26}\psi_{\xi,\xi} + \Xi_{27}\psi_{\eta,\eta} + \Xi_{28} W_{,\xi\xi} + \Xi_{29} W_{,\eta\eta} = 0$
$W = 0$	$\Xi_{12}\psi_{\xi} + \Xi_{13}\psi_{\xi,\xi\xi} + \Xi_{14}\psi_{\xi,\eta\eta} + \Xi_{15}\psi_{\eta,\xi\eta} + \Xi_{16} W_{,\xi} + \Xi_{17} W_{,\xi\xi\xi} + \Xi_{18} W_{,\xi\eta\eta} = 0$

and

$$\eta = 0 \text{ and } \eta = \phi$$

$$\Xi_9\psi_{\xi,\eta} + \Xi_{10}\psi_{\eta,\xi} + \Xi_{11} W_{,\xi\eta} = 0$$
$$\Xi_5\psi_{\eta,\eta} + \Xi_6\psi_{\xi,\xi} + \Xi_7 W_{,\eta\eta} + \Xi_8 W_{,\xi\xi} = 0$$
$$\Xi_{30}\psi_{\eta,\eta} + \Xi_{31}\psi_{\xi,\xi} + \Xi_{32} W_{,\eta\eta} + \Xi_{33} W_{,\xi\xi} = 0$$
$$\Xi_{19}\psi_{\eta} + \Xi_{20}\psi_{\eta,\eta\eta} + \Xi_{21}\psi_{\eta,\xi\xi} + \Xi_{22}\psi_{\xi,\xi\eta} + \Xi_{23} W_{,\eta} + \Xi_{24} W_{,\eta\eta\eta} + \Xi_{25} W_{,\eta\xi\xi} = 0 \quad (6.3.1)$$

where the plate is clamped along the edge $\xi = 0$ as shown in Figure 6.1.

Variable	Distributed Edge Reactions at 1 and 2 in Figure 6.2 for the TSDT
$\psi_{\hat{n}}$	$P_{\hat{n}}$
$\psi_{\hat{s}}$	$P_{\hat{n}\hat{s}}$
$W_{,\hat{n}}$	$M_{\hat{n}}$
W	$Q_{\hat{n}}$

(6.3.2)

The general formulation of the distributed edge reactions in terms of the normal and tangential coordinates is not possible because depending on whether $\hat{n} = \xi$ or $\hat{n} = \eta$, that is depending if the ξ-axis is normal to the edge of the plate or η-axis is, the formulation of the edge reactions contains coefficients which differ depending on the edge unlike the UPST. In other words the P_{ξ} can not be obtained from P_{η} by interchanging η and ξ for the TSDT because the coefficients are not identical.

However since the boundary conditions used for the solution are only dependent on the spatial variables and their derivates they can be expressed generally in terms of the normal and tangential coordinates and are given by (6.3.3).

Edge Type	Conditions at 1 and 2 in Figure 6.2
Simply Supported (SS)	$W=0,\ W_{,\hat{n}\hat{n}}=0,\ \psi_{\hat{n}},_{\hat{n}}=0,\ \psi_{\hat{s}}=0$
Free (F)	$Q_{\hat{n}}=0,\ M_{\hat{n}}=0,\ P_{\hat{n}}=0,\ P_{\hat{n}\hat{s}}=0$
Clamped (C)	$W=0,\ W_{,\hat{n}}=0,\ \psi_{\hat{n}}=0,\ \psi_{\hat{s}}=0$
Slip Shear (∘∘)	$W_{,\hat{n}\hat{n}\hat{n}}=0,\ W_{,\hat{n}}=0,\ \psi_{\hat{n}},_{\hat{n}\hat{n}},\ \psi_{\hat{n}}=0,\ \psi_{\hat{s}},_{\hat{n}}=0$

(6.3.3)

The general boundary conditions in (6.3.3) are almost identical to those of the USPT (6.2.3), the only difference is an addition requirement for the slip shear but from inspection it is clear that a Levy solution will satisfy it. On the basis of the similarity of the boundary conditions of the TSDT it should be evident that identical building block Levy solutions can be used and the only difference between the USPT and TSDT solutions will be state space solutions due to the different edge reactions and state space matrices as a result of the different equations of motion

6.3.1 Symmetric Modes

The solution for the modes of vibration symmetric about the centerline of the plate perpendicular to the clamped edge of the plate (see Figure 6.3) for the symmetric cross-ply laminate using the non-dimensional transverse simplified TSDT is presented. As noted in the previous section the procedure for developing the necessary equations to implement the numerical superposition method is identical to that which was detailed in depth for the USPT. With this in mind only the necessary equations needed to perform the numerical superposition method will be listed for the symmetric modes of the TSDT and left for the reader to verify.

6.3.1.1 First Building Block Equations

First Building Block Levy Solutions

$$W_1(\xi,\eta)=\sum_{m=1,3,5}^{\infty} Z_m(\eta)\sin\alpha\xi$$

$$\psi_{1\xi}(\xi,\eta)=\sum_{m=1,3,5}^{\infty} X_m(\eta)\cos\alpha\xi \qquad \alpha=m\pi/2$$

$$\psi_{1\eta}(\xi,\eta)=\sum_{m=1,3,5}^{\infty} Y_m(\eta)\sin\alpha\xi$$

State Space Matrix

$$\mathbf{C}=\begin{bmatrix} 0 & 1 & 0 & 0 & 0 & 0 & 0 & 0 \\ C_5 & 0 & 0 & C_6 & C_7 & 0 & C_8 & 0 \\ 0 & 0 & 0 & 1 & 0 & 0 & 0 & 0 \\ 0 & C_1 & C_2 & 0 & 0 & C_3 & 0 & C_4 \\ 0 & 0 & 0 & 0 & 0 & 1 & 0 & 0 \\ 0 & 0 & 0 & 0 & 0 & 0 & 1 & 0 \\ 0 & 0 & 0 & 0 & 0 & 0 & 0 & 1 \\ C_9 & 0 & 0 & C_{10} & C_{11} & 0 & C_{12} & 0 \end{bmatrix}$$

$$C_1=\alpha\frac{\Theta_4}{\Theta_2} \qquad C_2=\frac{\alpha^2\Theta_3-\Theta_1}{\Theta_2}$$

$$C_3=\frac{\alpha^2\Theta_7-\Theta_5}{\Theta_2} \qquad C_4=-\frac{\Theta_6}{\Theta_2}$$

$$C_5=\frac{\alpha^2\Theta_9-\Theta_8}{\Theta_{10}} \qquad C_6=-\alpha\frac{\Theta_{11}}{\Theta_{10}}$$

$$C_7=\frac{\alpha^3\Theta_6-\alpha\Theta_{12}}{\Theta_{10}} \qquad C_8=-\alpha\frac{\Theta_7}{\Theta_{10}}$$

$$C_9=\frac{\alpha C_5\Theta_{19}-\alpha^3\Theta_{18}-C_1C_5\Theta_{20}+\alpha\Theta_{22}}{\Theta_{17}+C_4\Theta_{20}} \qquad C_{10}=\frac{\alpha C_6\Theta_{19}+\alpha^2\Theta_{21}-\left(C_2+C_1C_6\right)\Theta_{20}-\Theta_{23}}{\Theta_{17}+C_4\Theta_{20}}$$

$$C_{11}=\frac{\alpha C_7\Theta_{19}-\alpha^4\Theta_{15}-C_1C_7\Theta_{20}-\omega^2 g_0+\alpha^2\Theta_{24}}{\Theta_{17}+C_4\Theta_{20}} \qquad C_{12}=\frac{\alpha C_8\Theta_{19}+\alpha^2\Theta_{16}-\left(C_3+C_1C_8\right)\Theta_{20}-\Theta_{25}}{\Theta_{17}+C_4\Theta_{20}}$$

Boundary Conditions on State Space Solutions

$$E_m=\Xi_{30}Z_4-\alpha\Xi_{31}Z_1+\Xi_{32}Z_7-\alpha^2\Xi_{33}Z_5\Big|_{\eta=\phi}$$

$$O_m=\Xi_5Z_4-\alpha\Xi_6Z_1+\Xi_7Z_7-\alpha^2\Xi_8Z_5\Big|_{\eta=\phi}$$

$$\Xi_9Z_2+\alpha\Xi_{10}Z_3+\alpha\Xi_{11}Z_6=0\Big|_{\eta=\phi}$$

$$\Xi_{19}Z_3+\Xi_{20}\left(C_1Z_2+C_2Z_3+C_3Z_6+C_4Z_8\right)-\alpha^2\Xi_{21}Z_3-\alpha\Xi_{22}Z_2+\Xi_{23}Z_6+\Xi_{24}Z_8-\alpha^2\Xi_{25}Z_6=0\Big|_{\eta=\phi}$$

$$Z_2=Z_3=Z_6=Z_8=0\Big|_{\eta=0}$$

6.3.1.2 Second Building Block Equations

Second Building Block Levy Solutions

$$W_2(\xi,\eta)=\sum_{n=0}^{\infty}Z_n(\xi)\cos\beta\eta$$

$$\psi_{2\xi}(\xi,\eta)=\sum_{n=0}^{\infty}X_n(\xi)\cos\beta\eta \qquad \beta=n\pi/\phi$$

$$\psi_{2\eta}(\xi,\eta)=\sum_{n=0}^{\infty}Y_n(\xi)\sin\beta\eta$$

State Space Matrix

$$\mathbf{C}=\begin{bmatrix}0&1&0&0&0&0&0&0\\C_5&0&0&C_6&0&C_7&0&C_8\\0&0&0&1&0&0&0&0\\0&C_1&C_2&0&C_3&0&C_4&0\\0&0&0&0&0&1&0&0\\0&0&0&0&0&0&1&0\\0&0&0&0&0&0&0&1\\0&C_9&C_{10}&0&C_{11}&0&C_{12}&0\end{bmatrix}$$

$$C_1=\beta\frac{\Theta_4}{\Theta_3} \qquad C_2=\frac{\beta^2\Theta_2-\Theta_1}{\Theta_3}$$

$$C_3=\frac{\beta\Theta_5-\beta^3\Theta_6}{\Theta_3} \qquad C_4=\beta\frac{\Theta_7}{\Theta_3}$$

$$C_5=\frac{\beta^2\Theta_{10}-\Theta_8}{\Theta_9} \qquad C_6=-\beta\frac{\Theta_{11}}{\Theta_9}$$

$$C_7=\frac{\beta^2\Theta_{14}-\Theta_{12}}{\Theta_9} \qquad C_8=-\frac{\Theta_{13}}{\Theta_9}$$

$$C_9=\frac{-\beta C_1\Theta_{21}+\beta^2\Theta_{19}-(C_2+C_1C_6)\Theta_{18}-\Theta_{22}}{\Theta_{15}+C_8\Theta_{18}} \qquad C_{10}=\frac{-\beta C_2\Theta_{21}+\beta^3\Theta_{20}-C_2C_6\Theta_{18}-\beta\Theta_{23}}{\Theta_{15}+C_8\Theta_{18}}$$

$$C_{11}=\frac{-\beta C_3\Theta_{21}-\beta^4\Theta_{17}-C_3C_6\Theta_{18}-\omega^2g_0+\beta^2\Theta_{25}}{\Theta_{15}+C_8\Theta_{18}} \qquad C_{12}=\frac{-\beta C_4\Theta_{21}+\beta^2\Theta_{16}-(C_7+C_4C_6)\Theta_{18}-\Theta_{24}}{\Theta_{15}+C_8\Theta_{18}}$$

Boundary Conditions on State Space Solutions

$$E_n=\Xi_{26}Z_2+\beta\Xi_{27}Z_3+\Xi_{28}Z_7-\beta^2\Xi_{29}Z_5\Big|_{\xi=1}$$

$$O_n=\Xi_1Z_2+\beta\Xi_2Z_3+\Xi_3Z_7-\beta^2\Xi_4Z_5\Big|_{\xi=1}$$

$$-\beta\Xi_9 Z_1 + \Xi_{10} Z_4 - \beta\Xi_{11} Z_6 = 0\Big|_{\xi=1}$$

$$\Xi_{12} Z_1 + \Xi_{13}\left(C_5 Z_1 + C_6 Z_4 + C_7 Z_6 + C_8 Z_8\right) - \beta^2\Xi_{14} Z_1 + \beta\Xi_{15} Z_4 + \Xi_{16} Z_6 + \Xi_{17} Z_8 - \beta^2\Xi_{18} Z_6 = 0\Big|_{\xi=1}$$

$$Z_2 = Z_3 = Z_5 = Z_7 = 0\Big|_{\xi=0}$$

6.3.1.3 Third Building Block Equations

The Levy Solutions and State Space Matrix for the third building block can be obtained from the second building block by replacing n with p and β with γ, where $\gamma = p\pi/\phi$.

Boundary Conditions on State Space Solutions

$$E_p = \Xi_{26} Z_2 + \gamma\Xi_{27} Z_3 + \Xi_{28} Z_7 - \gamma^2\Xi_{29} Z_5\Big|_{\xi=0}$$

$$O_p = \Xi_1 Z_2 + \gamma\Xi_2 Z_3 + \Xi_3 Z_7 - \gamma^2\Xi_4 Z_5\Big|_{\xi=0}$$

$$Z_3 = Z_5 = 0\Big|_{\xi=0}$$

$$Z_1 = Z_4 = Z_6 = Z_8 = 0\Big|_{\xi=1}$$

6.3.1.4 Coefficients of the Determinant Matrix

$$A_{mm} = E_m$$

$$A_{mn} = 2\cos n\pi \int_0^1 \left[\beta\Xi_{30} Y_n(\xi) + \Xi_{31} X_n'(\xi) - \beta^2\Xi_{32} Z_n(\xi) + \Xi_{33} Z_n''(\xi)\right] \sin\frac{m\pi\xi}{2}\, d\xi$$

$$A_{mp} = 2\cos p\pi \int_0^1 \left[\gamma\Xi_{30} Y_p(\xi) + \Xi_{31} X_p'(\xi) - \gamma^2\Xi_{32} Z_p(\xi) + \Xi_{33} Z_p''(\xi)\right] \sin\frac{m\pi\xi}{2}\, d\xi$$

$$B_{mm} = O_m$$

$$B_{mn} = 2\cos n\pi \int_0^1 \left[\beta\Xi_5 Y_n(\xi) + \Xi_6 X_n'(\xi) - \beta^2\Xi_7 Z_n(\xi) + \Xi_8 Z_n''(\xi)\right] \sin\frac{m\pi\xi}{2}\, d\xi$$

$$B_{mp} = 2\cos p\pi \int_0^1 \left[\gamma\Xi_5 Y_p(\xi) + \Xi_6 X_p'(\xi) - \gamma^2\Xi_7 Z_p(\xi) + \Xi_8 Z_p''(\xi)\right] \sin\frac{m\pi\xi}{2}\, d\xi$$

$$A_{nm} = \frac{If(n)}{\phi} \sin\frac{m\pi}{2} \int_0^{\phi} \left[-\alpha\Xi_{26} X_m(\eta) + \Xi_{27} Y_m'(\eta) - \alpha^2\Xi_{28} Z_m(\eta) + \Xi_{29} Z_m''(\eta)\right] \cos\frac{n\pi\eta}{\phi}\, d\eta$$

$$A_{nn} = E_n$$

$$A_{np} = \left[\Xi_{26} X_p'(\eta) + \gamma\Xi_{27} Y_p(\eta) + \Xi_{28} Z_p''(\eta) - \gamma^2\Xi_{29} Z_p(\eta)\right]\Big|_{\xi=1} \delta_{np}$$

$$B_{nm} = \frac{If(n)}{\phi} \sin\frac{m\pi}{2} \int_0^{\phi} \left[-\alpha \Xi_1 X_m(\eta) + \Xi_2 Y_m'(\eta) - \alpha^2 \Xi_5 Z_m(\eta) + \Xi_6 Z_m''(\eta) \right] \cos\frac{n\pi\eta}{\phi} d\eta$$

$$B_{nn} = O_n$$

$$B_{np} = \left[\Xi_1 X_p'(\eta) + \gamma \Xi_2 Y_p(\eta) + \Xi_3 Z_p''(\eta) - \gamma^2 \Xi_4 Z_p(\eta) \right]\Big|_{\xi=1} \delta_{np}$$

$$A_{pm} = \frac{If(p)}{\phi} \int_0^{\phi} \left[\alpha Z_m(\eta) \right] \cos\frac{p\pi\eta}{\phi} d\eta$$

$$A_{pn} = \left[Z_n'(\xi) \right]\Big|_{\xi=0} \delta_{pn}$$

$$A_{pp} = \left[Z_p'(\xi) \right]\Big|_{\xi=0}$$

$$B_{pm} = \frac{If(p)}{\phi} \int_0^{\phi} \left[X_m(\eta) \right] \cos\frac{p\pi\eta}{\phi} d\eta$$

$$B_{pn} = \left[X_n(\xi) \right]\Big|_{\xi=0} \delta_{np}$$

$$B_{pp} = \left[X_p(\xi) \right]\Big|_{\xi=0}$$

6.3.1.5 Forms of the Components of the State Space Solutions and resulting Integrals

The forms of the components of the state space solutions and resulting integrals are identical to those obtained for the USPT and listed in **6.2.2.5**.

7 Numerical Results 2

7.1 Introduction

This chapter contains the numerical results obtained using the numerical superposition method (NSM) for both the USPT and TSDT for undamped cantilever plate with results obtained using the finite element software ANSYS. The first ten frequencies of vibration and corresponding mode shapes are presented for the symmetric modes of vibration of the cantilever rectangular sandwich plate.

7.2 USPT Symmetric Modes

This section presents the results found for the solution of the cantilever sandwich plate with modes of vibration that are symmetric with respect to the centerline of the plate perpendicular to the clamped edge presented in **6.2.1**. All of the results are for the sandwich plate with the initial material and geometric properties given in Table 5.5, where all of the values are real and damping is *not* introduced at any time in the analysis.

The results are found using the a computer program created in Mathematica which is computes Δ for a given frequency of vibration ω and computes the corresponding transverse displacement $W(\xi,\eta)$ using the method outlined in **6.2.2**.

For a frequency range of $10-1000\ rad/s$ $\mathrm{Det}[\Delta]$ and the degree of rank deficiency is plotted for various numbers of term expansions of the solution, with equal number of terms taken for each iterator m, n, and p in Figure 7.1.

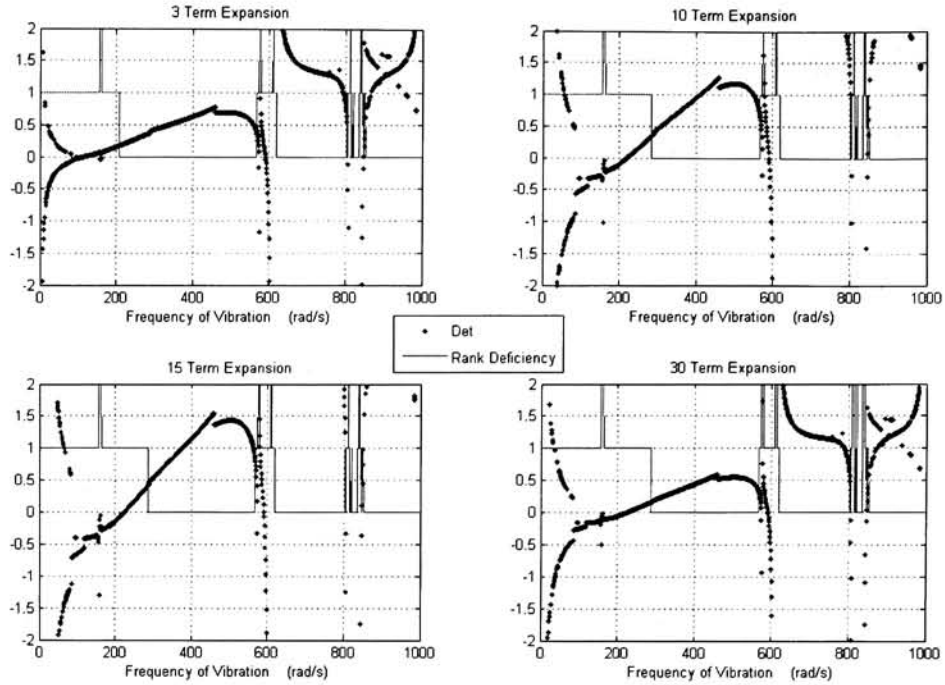

Figure 7.1 Characteristic Equation for Symmetric Modes of the USPT Cantilever Sandwich Plate

The plots obtained in Figure 7.1 are representative of what can be considered the characteristic equation of the symmetric modes. The reader is reminded that the condition for a frequency to be a natural frequency of vibration and the resulting solution a mode shape can be expressed by three equivalent conditions: $\mathrm{Det}[\Delta]=0$, an eigenvalue of Δ is zero and the Δ is rank deficient.

Numerically these conditions cannot be achieved exactly, but examining Figure 7.1 we can approximate where $\mathrm{Det}[\Delta]=0$ and then search for local minimums of the absolute values of the determinant (i.e. areas where $\mathrm{Det}[\Delta]=0$ will be a minimum when considering the absolute value of $\mathrm{Det}[\Delta]=0$, we cannot exactly find where $\mathrm{Det}[\Delta]=0$) and minimum eigenvalue of Δ under the additional requirement of Δ being rank deficient. Using these three numerical tests natural frequencies of vibration are readily determined, and the corresponding mode shape is obtained.

The technique of finding natural frequencies of vibration is a largely graphical process starting with an initial search over a wide frequency range (e.g. Figure 7.1) and then zooming in on areas where the determinant of Δ appears to be zero. It is necessary to have a graphical representation of the data along with the three numerical conditions to determine if a frequency is a natural frequency of vibration due to the sensitivity of the numerical calculations.

In addition to the numerical conditions and graphical representation of the data the transverse displacement (as well as the rotations) can be calculated for each frequency and the convergence to a mode shape can be visually observed (see Figure 7.2) as an additional method of ensuring that a frequency is a natural frequency of vibration.

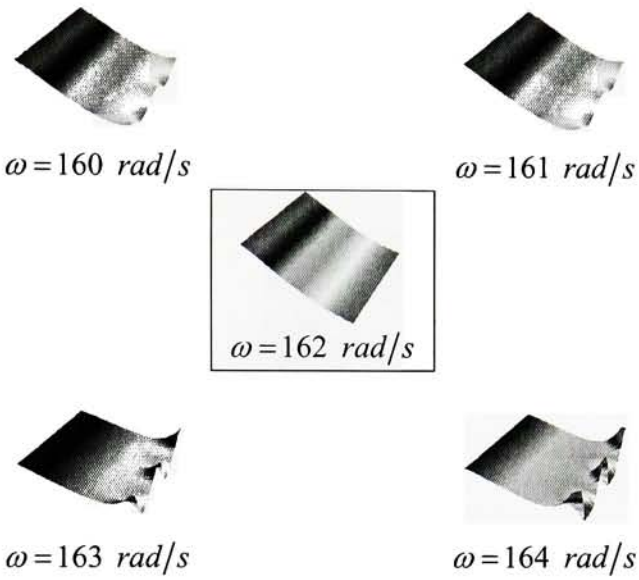

Figure 7.2 Convergence to a Mode Shape at $\omega = 162\ rad/s$

The convergence of the transverse displacement in Figure 7.2 directly corresponds to a local minimum with respect to the absolute value of the determinant and minimum eigenvalue of Δ in a region where Δ is rank deficient. It is a very attractive feature of this method solution that the mode shapes appear distinctly in a relatively small frequency range which is in an indication of a rapid convergence of the amplitudes of the applied loads to satisfy the boundary conditions of the cantilever plate.

The last point of importance found when obtaining numerical results was that Δ was found to be extremely rank deficient for certain frequencies (see Figure 7.1) which corresponded for regions where the determinant of Δ went to infinity (positive and negative). These locations are important because in general this corresponds to a region where the determinant is zero and a frequency of vibration exists. It also is very similar to the appearance of the characteristic equations found analytically for the free vibration of beams.

Having exhausted the particular methodology and characteristics of obtaining the natural frequencies of vibration and corresponding symmetric mode shapes for the cantilever sandwich plate modeled using the uncoupled transversely simplified USPT subject to the initial material and geometric properties given in Table 5.5 the results for the first ten natural frequencies are presented.

NSM for USPT	SHELL91	SOLID95 stacked through thickness
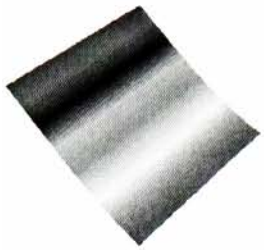	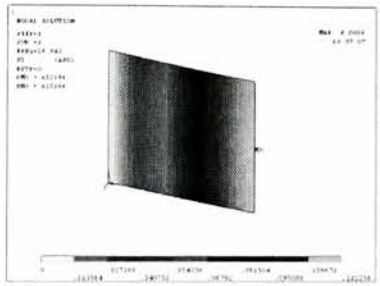	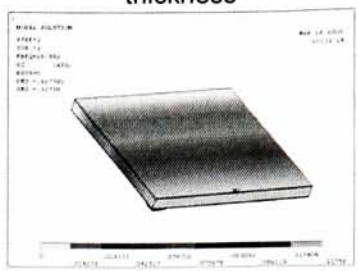
162 *rad/s*	160.485 *rad/s*	182.162 *rad/s*
	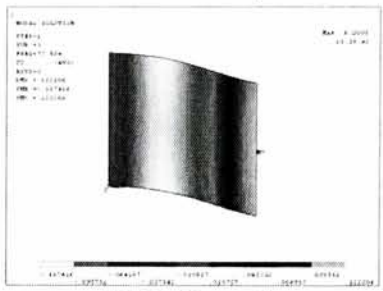	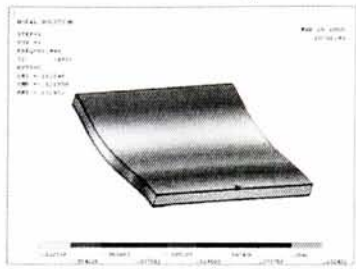
589.995 *rad/s*	486.972 *rad/s*	574.560 *rad/s*
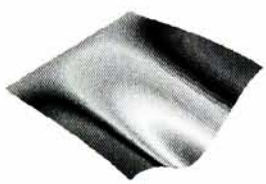	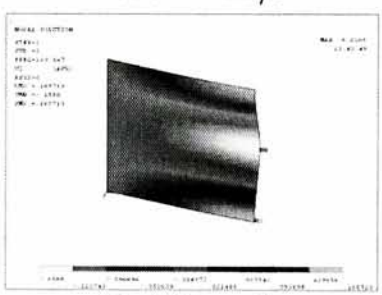	
805.914 *rad/s*	694.587 *rad/s*	797.462 *rad/s*
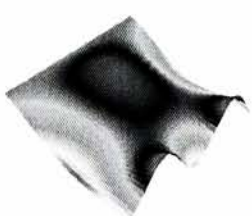	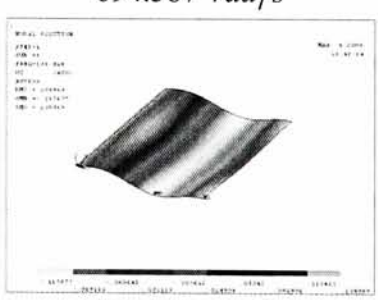	
847.766 *rad/s*	853.985 *rad/s*	1021.275 *rad/s*
	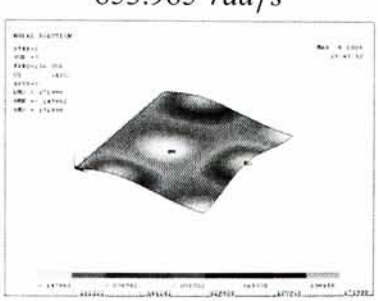	
1074.890 *rad/s*	856.436 *rad/s*	1054.614 *rad/s*

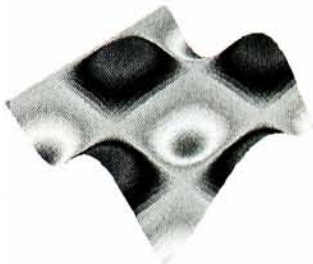

1341.715 *rad/s*

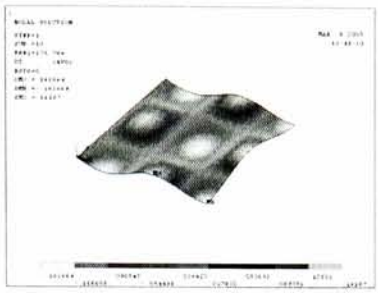

1104.358 *rad/s*

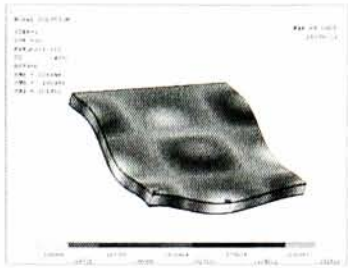

1389.922 *rad/s*

1529.293 *rad/s*

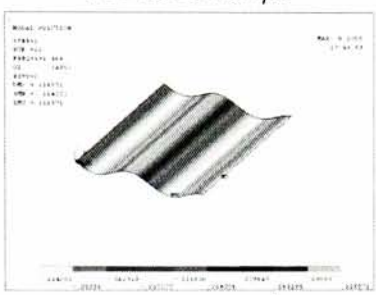

1203.016 *rad/s*

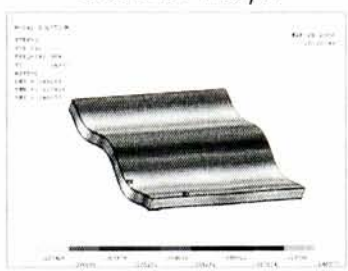

1570.671 *rad/s*

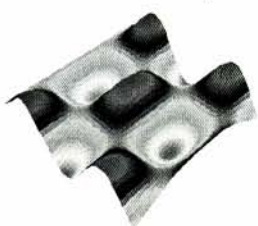

1734.5 *rad/s*

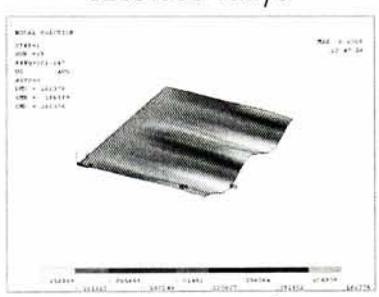

1389.507 *rad/s*

1754.014 *rad/s*

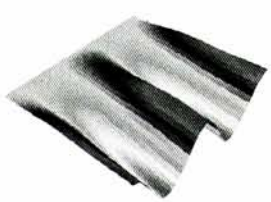

1818.672 *rad/s*

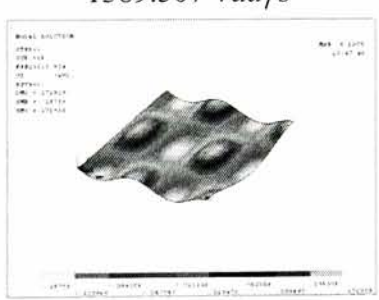

1394.327 *rad/s*

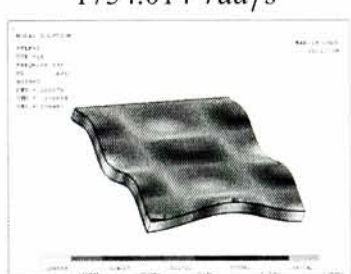

1863.593 *rad/s*

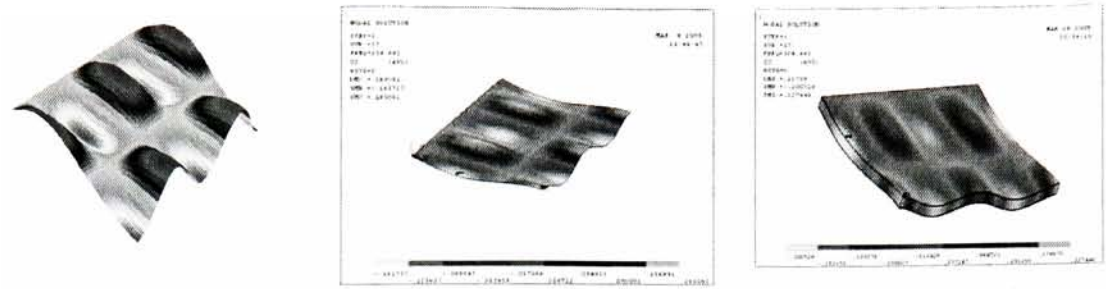

1982 *rad/s* 1475.870 *rad/s* 1913.865 *rad/s*

Figure 7.3 First Ten Mode Shapes Symmetric about the Centerline of the Sandwich Plate Perpendicular to the Clamped Edge of the Plate found using the NSM for the USPT, SHELL91 w/ sandwich option and SOLID46

The natural frequencies of the cantilever sandwich plate are also determined by finite element analysis using the standard FEA package ANSYS for the first ten symmetric modes. The results are calculated using the SHELL91 element with the sandwich option and the SOLID95 element stacked through the thickness with 3 elements through the core and one element through each of the face layers and presented in Figure 7.3 along with the USPT.

The first mode for SHELL91 agrees with the NSM, beyond that the frequencies and modes differ with the fourth and fifth and eighth and ninth modes interchanged. All of the mode shapes are identical with the NSM for the stacked SOLID95 element and frequencies are in close agreement with exception fourth frequency.

Comparison of Natural Frequencies of Vibration for Similar Modes				
NSM USPT	SHELL91		SOLID95 stacked	
ω_n (rad/s)	ω_n (rad/s)	% Diff	ω_n (rad/s)	% Diff
162.000	160.485	0.94%	182.2	12.5%
589.995	486.972	17.46%	574.6	2.6%
805.914	694.587	13.81%	797.5	1.0%
847.766	853.985	-	1021.3	20.5%
1074.890	856.436	-	1054.6	1.9%
1341.715	1104.358	17.69%	1389.9	3.6%
1529.293	1203.016	21.34%	1570.7	2.7%
1734.500	1389.507	-	1754	1.1%
1818.672	1394.327	-	1863.6	2.5%
1982.000	1475.870	25.54%	1913.9	3.4%

Table 7.1 Comparison of first ten natural frequencies of vibration between FEA and NSM for the USPT

The results for the symmetric modes of cantilever sandwich plate modeled with the USPT are theoretically exact and satisfy the boundary conditions of the cantilever plate exactly for each term of the solution. The only approximation made in the analysis is by truncating the series

solutions, however 15 term of each series were used to obtain these results and the order of the truncation is on the order of the errors introduced by numerically obtaining the necessary eigenvalues and eigenvectors. Compared to the formulation of the elements used in FEA which generally relax the derivative conditions on the displacements in the equations of motion and assume an approximated solution for the displacements the NSM is theoretically more accurate.

7.3 TSDT Symmetric Modes

This section presents the results found for the solution of the cantilever sandwich plate with modes of vibration that are symmetric with respect to the centerline of the plate perpendicular to the clamped edge presented in **6.2.1**. All of the results are for the sandwich plate with the initial material and geometric properties given in Table 5.5, where all of the values are real and damping is *not* introduced at any time in the analysis.

The results for the TSDT are obtained using same method as the USPT for the equations presented in **6.3.1**. Once again the results for the TSDT will be presented without the detail that the USPT results were presented because the solution method is identical and the only difference is in the equations used.

NSM TSDT	SOLID46	SOLID191
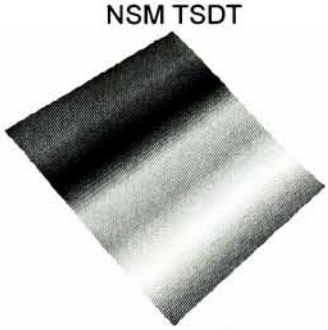		
213 rad/s	163 rad/s	270 rad/s
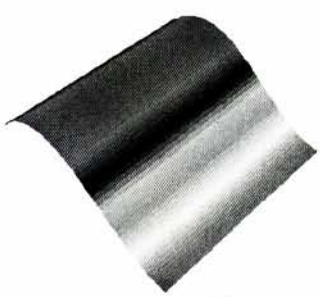	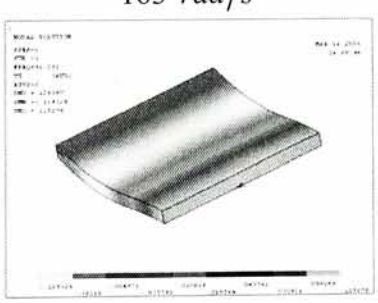	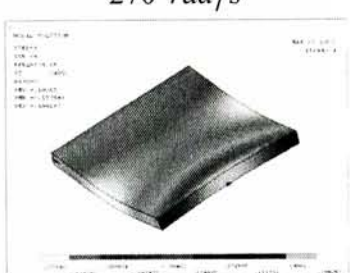
1221 rad/s	525 rad/s	1606 rad/s

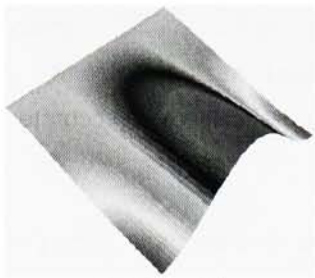

2725 *rad/s*

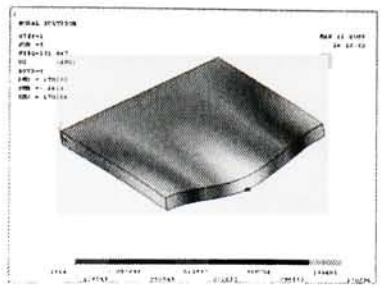

772 *rad/s*

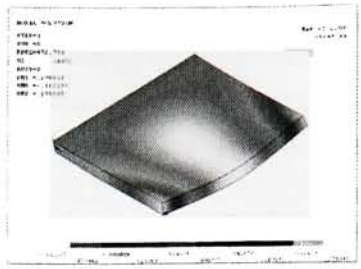

2034 *rad/s*

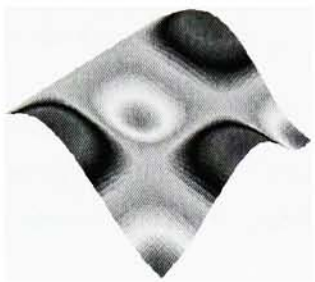

3697 *rad/s*

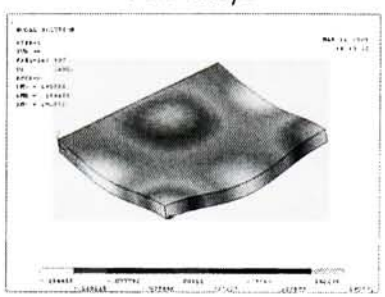

990 *rad/s*

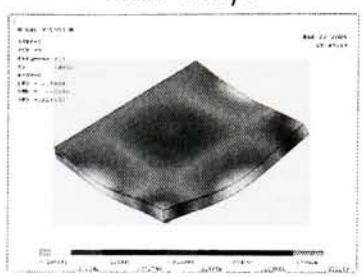

3859 *rad/s*

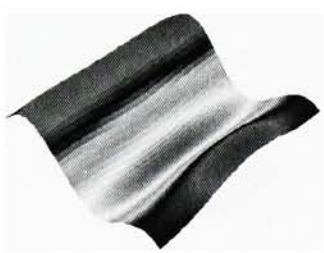

3869 *rad/s*

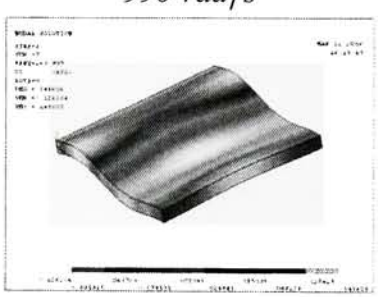

995 *rad/s*

4418 *rad/s*

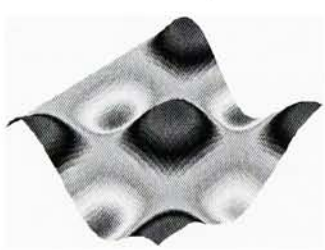

5253 *rad/s*

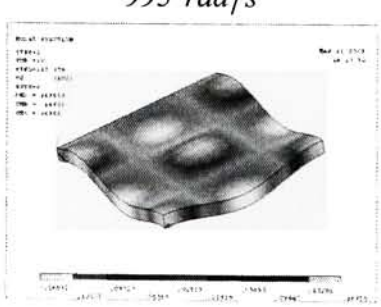

1307 *rad/s*

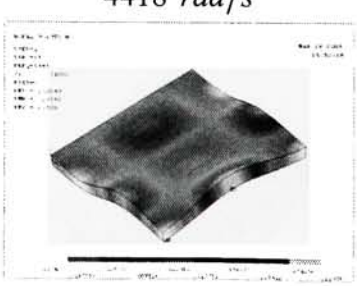

6635 *rad/s*

Figure 7.4 First Ten Mode Shapes Symmetric about the Centerline of the Sandwich Plate Perpendicular to the Clamped Edge of the Plate found using the NSM for the TSDT, SOLID191 and SOLID95 stacked through the thickness

The first ten mode shapes and corresponding frequencies are presented for the TSDT along with finite element models obtained using the in Figure 7.4. The mode shapes obtained using the SOLID191 element are identical to those obtained for the TSDT, while the mode shapes for the SOLID46 differ for the last three modes.

Comparison of Natural Frequencies of Vibration for Similar Modes				
NSM TSDT	SOLID46		SOLID191	
ω_n (rad/s)	ω_n (rad/s)	% Diff	ω_n (rad/s)	% Diff
213.0	163	23.53%	270	26.93%
1221.0	525	56.98%	1606	31.57%
2725.0	772	71.68%	2034	25.36%
3697.0	990	73.23%	3859	4.39%
3869.0	995	74.29%	4418	14.20%
5253.0	1307	75.13%	6635	26.31%
5643.0	1441	74.47%	8112	43.75%
6103.0	1615	73.53%	8533	39.81%
6468.5	1673	74.14%	9934	53.57%
6704.0	1679	74.95%	10279	53.33%

Table 7.2 Comparison of first ten natural frequencies of vibration between FEA and NSM for the TSDT

The frequencies of vibration for the modes in Figure 7.4 are compared in Table 7.2 for the NSM TSDT, SOLID191 and stacked SOLID46. It is clear that the TSDT does not agree with either of the finite element models; the SOLID191 predicts frequencies that are relatively close for the first six frequencies while the SOLID46 appears to predict frequencies similar to the USPT.

The results for the cantilever plate are the same as those found in the simply supported analysis; although both the SOLID46 and SOLID191 are single equivalent layer models the SOLID46 agrees with the USPT and the SOLID191 predicts frequencies that are larger that the TSDT.

7.4 Symmetric Modes Comparison

This section compares the symmetric modes of the cantilever sandwich plate for TSDT, USPT and FEA generated in ANSYS using the SOLID95 20 node element stacked through the thickness, which is believed to be the most accurate model available. Table 7.3 shows that the USPT is in agreement with the stacked SOLID95 validating the NSM, while the results for the TSDT are not correct in terms of their accuracy in modeling the symmetric modes of the cantilever sandwich plate, but are correct in terms of the implementation of the NSM because the method is identical to that of the USPT.

Comparison of Natural Frequencies of Vibration for Similar Modes				
NSM USPT	NSM TSDT		SOLID95 stacked	
ω_n (rad/s)	ω_n (rad/s)	% Diff w/ USPT	ω_n (rad/s)	% Diff w/ USPT
162	213	23.9%	182.2	12.5%
589.995	1221	51.7%	574.6	2.6%
805.914	2725	70.4%	797.5	1.0%
847.766	3697	77.1%	1021.3	20.5%
1074.89	3869	72.2%	1054.6	1.9%
1341.715	5253	74.5%	1389.9	3.6%
1529.293	5643	72.9%	1570.7	2.7%
1734.5	6103	71.6%	1754	1.1%
1818.672	6468.5	71.9%	1863.6	2.5%
1982	6704	70.4%	1913.9	3.4%

Table 7.3 Comparison of first ten natural frequencies of vibration between FEA and NSM

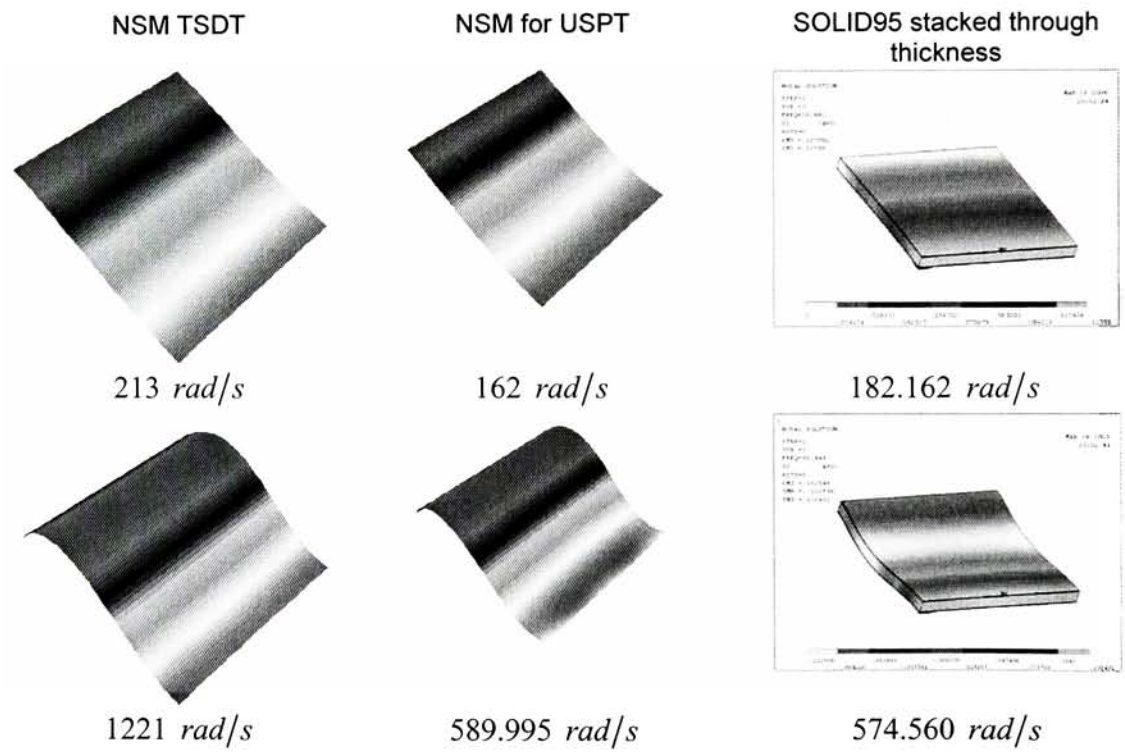

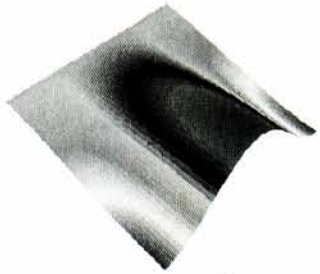

2725 *rad/s*

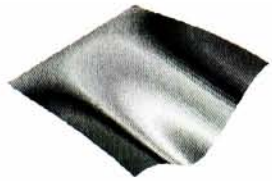

805.914 *rad/s*

797.462 *rad/s*

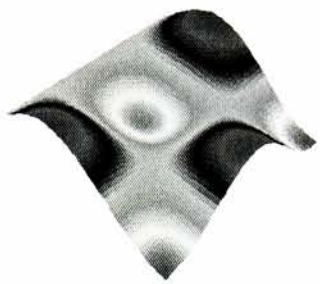

3697 *rad/s*

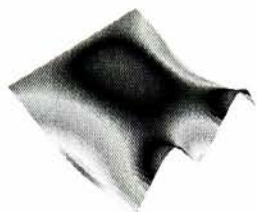

847.766 *rad/s*

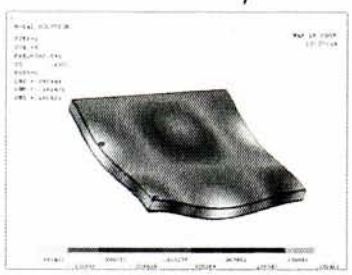

1021.275 *rad/s*

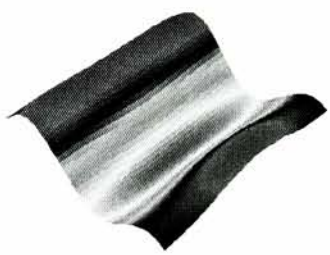

3869 *rad/s*

1074.890 *rad/s*

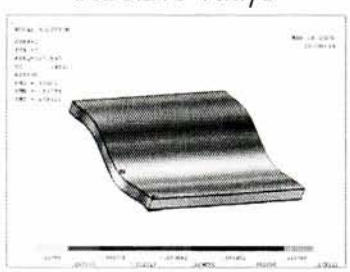

1054.614 *rad/s*

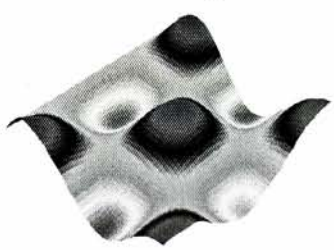

5253 *rad/s*

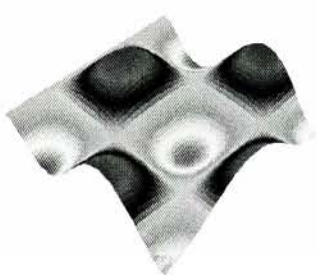

1341.715 *rad/s*

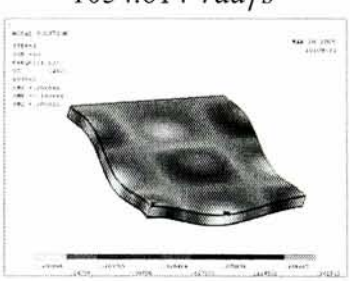

1389.922 *rad/s*

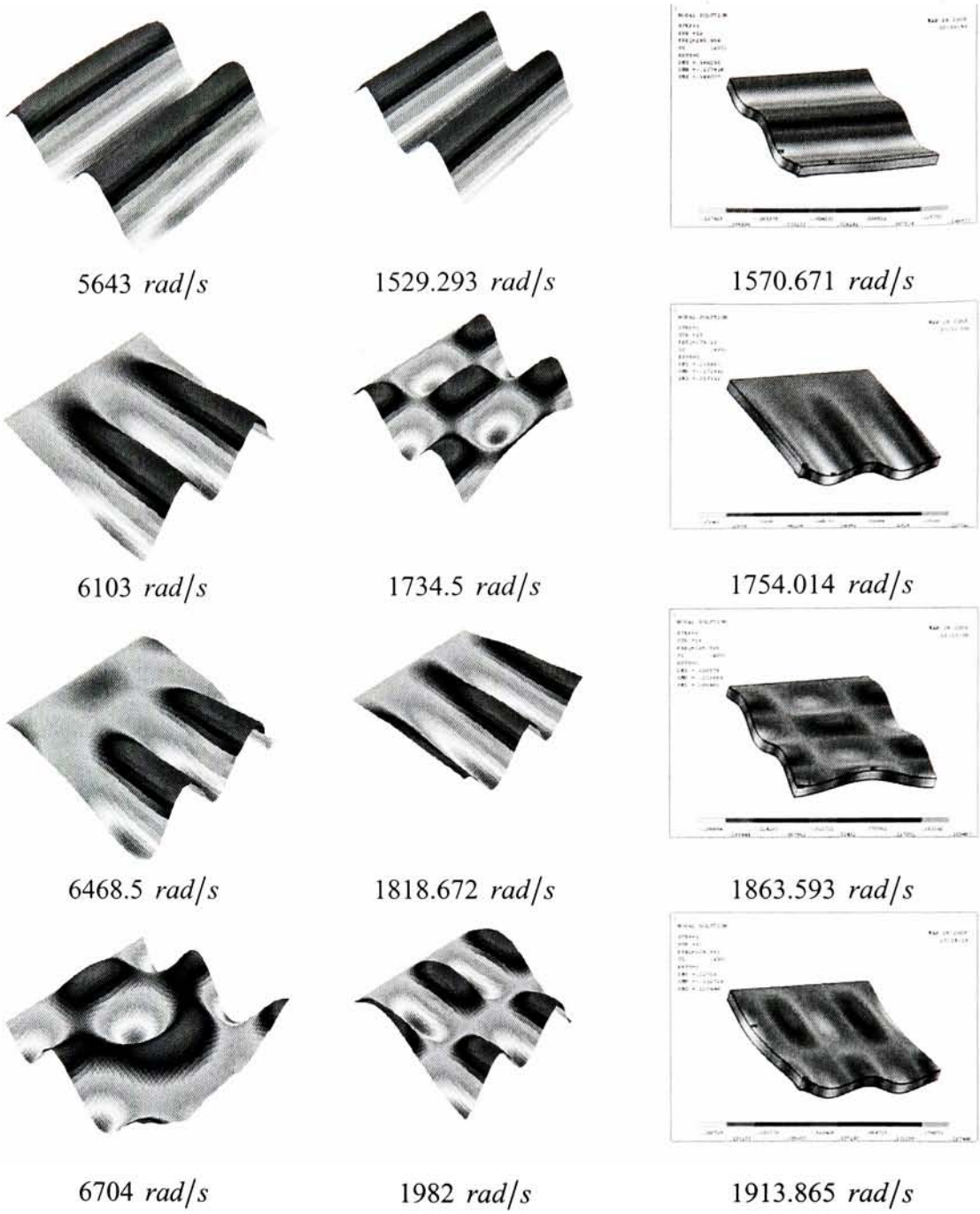

Figure 7.5 First Ten Mode Shapes Symmetric about the Centerline of the Sandwich Plate Perpendicular to the Clamped Edge of the Plate found using the NSM for the TSDT, SOLID191 and SOLID95 stacked through the thickness

8 Conclusions and Recommendations

8.1 Conclusions

The ANSYS results are not conclusive, depending on the element used results for natural frequencies of both the simply supported and cantilever boundary conditions can be obtained that are larger than the TSDT (SOLID191, SHELL91) or erratically stays within range of the USPT (SHELL91 w/ sandwich option). The two of the single equivalent layer elements, SOLID191 and SHELL91, are in the range of the TSDT but do not consistently agree while the other equivalent layer element, SOLID46, predicted results consistently similar to the USPT. However when higher order elements (SOLID95) are stacked through the thickness of each layer of the sandwich plates the results obtained agreed exactly with the USPT.

The two methods adopted of analysis of the free vibration of rectangular sandwich cantilever plates are comparable. Though the displacement field of the TSDT is capable of the true shear strain distribution across the thickness of the plate, it also averages the material properties across the thickness of the plate and applies the displacement field to an equivalent single layer. The results of the simply supported analysis showed that the TSDT does not accurately predict the transverse shear strain of the plate resulting over prediction of the natural frequencies of vibration and under predicting the corresponding loss factors for the damped case. The USPT is more accurate based on the results of the simply supported solution in contrast to the TSDT and the very close agreement to the results obtained from the SOLID95 element stacked through the thickness. The interlaminate (e.g. face and core layer interface) effects of the sandwich plate must be taken into consideration (USPT) and a bulk approximation of the sandwich plate (TSDT) does not consider these effects.

In general the proposed numerical superposition method (NSM) for the analysis of the rectangular sandwich cantilever plates produces accurate results. The results obtained for the USPT are in close agreement with the results obtained from the SOLID95 element stacked through the thickness for the cantilever plate. The NSM produces series solutions that satisfy the boundary conditions of the cantilever plate exactly term by term and the only error introduced in the solution are those related to the numerical computation of eigenvalues.

8.2 Recommendations

The analysis of the sandwich plate by the TSDT is not adequate, however the USPT does not accommodate for face layers composed of fiber reinforced laminates or in general stacked orthotropic layers. It is recommended that further development of sandwich plate theory

consist of a layerwise theory with the TSDT applied to each layer which obviously lends itself to the creation of a finite element model.

The numerical superposition method is a strong compliment to the finite element method, although FEA is widely used and developed the NSM provides a much needed means of verification of FEA models. It is recommended that the NSM is modified to solve for loss factors of the damped plate or solutions obtained are used in eigenfunction expansions to solve for forced vibration problems.

Appendix 1 References

Chapter 1

[1] Reissner, E. 1945 *Journal of Applied Mechanics* **12**, A69-A77. The effect of transverse shear deformation on the bending of elastic plates.

[2] Mindlin, R.D. 1951 *Journal of Applied Mechanics* **18**, A31-A38. Influence of rotatory inertia and shear on flexural motions of isotropic, elastic plates.

[3] Reddy, J.N. 1984 *Journal of Applied Mechanics* **45**, 745-752. A simple higher-order theory for laminated composite plates.

[4] Reddy, J.N. 1997 *Mechanics of Laminated Composite Plates.* New York: CRC Press

[5] Reissner, E. 1948 *Journal of the Aeronautical Sciences* **15**, 435-440. Finite deflections of sandwich plates.

[6] Rao, Y.V.K.S. and Nakra, B.C. 1973 *Archive of Mechanics* **25**, 213-225. Theory of vibratory bending of unsymmetrical sandwich plates.

[7] Rao, Y.V.K.S. and Nakra, B.C. 1974 *Journal of Sound and Vibration* **34**, 309-326. Vibrations of unsymmetrical sandwich beams and plates with viscoelastic cores.

[8] Cupial, P. and Niziol, J. 1995 *Journal of Sound and Vibration* **183**, 99-114. Vibration and damping analysis of a three-layered composite plate with a viscoelastic mid-layer.

[9] Meunier, M. and Shenoi, R.A. 1999 *Journal of Mechanical Engineering Science* **Part C 213**, 715-727. Free vibration analysis of composite sandwich plates.

[10] Meunier, M. and Shenoi, R.A. 2001 *Composite Structures* **54**, 243-254. Dynamic analysis of composite sandwich plates with damping modelled using high-order shear deformation theory.

[11] Meunier, M. and Shenoi, R.A. 2002 *Composite Structures* **Part B 33**, 505-519. Free Vibration analysis of composite sandwich plates based on Reddy's higher-order theory.

[12] Meunier, M. and Shenoi, R.A. 2003 *Journal of Sound and Vibration* **263**, 131-151. Forced response of FRP sandwich panels with viscoelastic materials.

[13] Gorman, D. J. 1982 *Free Vibration Analysis of Rectangular Plates* New York: Elsevier

Chapter 2

[1] Ref. Chapter 1, [4]
p.139

[2] Christensen, R.M. 1982 *Theory of Viscoelasticity An Introduction Second Edition.* New York: Academic Press

General References

Reddy, J.N. 1997 *Mechanics of Laminated Composite Plates.* New York: CRC Press

Reddy J.N. 1984 *Energy and Variational Methods in Applied Mechanics* New York: John Wiley & Sons

Fung, Y.C. 1965 *Foundations of Solid Mechanics* Englewood Cliffs, New Jersey: Prentice-Hall, Inc.

Chapter 3

[1] Ref. Chapter 1, [6]

[2] Ref. Chapter 1, [7]

[3] Ref. Chapter 1, [7]
p.317

[4] He, J.-F. and Ma, B.-A. 1988 *Journal of Sound and Vibration* **126**, 37-47. Analysis of flexural vibration of viscoelastically damped sandwich plates

Chapter 4

[1] Ref. Chapter 1, [3]

[2] Ref. Chapter 1, [4]
Chapter 5 section 4-2, p 161-2

[3] Ref Chapter 1, [4]
Chapter 11 section 4-1

Chapter 5

[1] Ref. Chapter 1, [6]
Table 1. Frequencies of Sandwich Plates, p.223

[2] Reddy, J.N. 1985 *Journal of Sound and Vibration* **98**, 157-170. Stability and vibration of isotropic, orthotropic and laminated plates according to a higher-order shear deformation theory
Table 1. Comparison of natural frequencies, $\bar{\omega} = \omega h \Big/ \left(\sqrt{\rho/G}\right)$, of isotropic $(\nu = .3)$ plates $\left((a/h) = 10\right)$, p161

[3] Ref. Chapter 1, [4]
Chapter 11 section 4-4, Table 11.4-5. Nondimensionalized frequencies $\bar{\omega}$ of $(0/90/90/0)$ cross-ply laminates as functions of modulus ratio, p.621

[4] Ref. Chapter 1, [12]
Table 2. Measured Dynamic material properties of HEREX C70.130 PVC foam at 30°C, p.140

Chapter 6

[1] Ref. Chapter 1, [13]

[2] Ref. Chapter 1, [13]
p.71

Appendix 2 Integrals

$$IntES = \int_0^t e^{\lambda\chi} \sin\alpha\chi d\chi = \frac{\alpha - \alpha e^{\lambda}\cos\alpha + \lambda e^{\lambda}\sin\alpha}{\alpha^2+\lambda^2}$$

$$IntECS = \int_0^t e^{\sigma\chi}\cos\tau\chi\sin\alpha\chi d\chi = \frac{\alpha\left(\alpha^2+\sigma^2-\tau^2\right)}{\alpha^4+2\alpha^2\left(\sigma^2-\tau^2\right)+\left(\sigma^2+\tau^2\right)^2}$$

$$+\frac{1}{2}e^{\sigma}\left(\frac{(-\alpha+\tau)\cos(\alpha-\tau)+\sigma\sin(\alpha-\tau)}{\alpha^2+\sigma^2-2\alpha\tau+\tau^2}+\frac{-(\alpha+\tau)\cos(\alpha+\tau)+\sigma\sin(\alpha+\tau)}{\alpha^2+\sigma^2+2\alpha\tau+\tau^2}\right)$$

$$IntESS = \int_0^t e^{\sigma\chi}\sin\tau\chi\sin\alpha\chi d\chi = \frac{2\alpha\sigma\tau}{\alpha^4+2\alpha^2\left(\sigma^2-\tau^2\right)+\left(\sigma^2+\tau^2\right)^2}$$

$$+\frac{1}{2}e^{\sigma}\left(\frac{\sigma\cos(\alpha-\tau)+(\alpha-\tau)\sin(\alpha-\tau)}{\alpha^2+\sigma^2-2\alpha\tau+\tau^2}-\frac{\sigma\cos(\alpha+\tau)+(\alpha+\tau)\sin(\alpha+\tau)}{\alpha^2+\sigma^2+2\alpha\tau+\tau^2}\right)$$

$$IntEC = \int_0^{\phi} e^{\lambda\chi}\cos\beta\chi d\chi = \frac{-\lambda+e^{\lambda\phi}\left(\lambda\cos(\beta\phi)+\beta\sin(\beta\phi)\right)}{\beta^2+\lambda^2}$$

$$IntECC = \int_0^{\phi} e^{\sigma\chi}\cos\tau\chi\cos\beta\chi d\chi = \frac{-\sigma}{2}\left(\frac{1}{\beta^2+\sigma^2-2\beta\tau+\tau^2}+\frac{1}{\beta^2+\sigma^2+2\beta\tau+\tau^2}\right)$$

$$+\frac{e^{\sigma\phi}}{2}\left(\frac{\sigma\cos\left[(\beta-\tau)\phi\right]+(\beta-\tau)\sin\left[(\beta-\tau)\phi\right]}{\beta^2+\sigma^2-2\beta\tau+\tau^2}+\frac{\sigma\cos\left[(\beta+\tau)\phi\right]+(\beta+\tau)\sin\left[(\beta+\tau)\phi\right]}{\beta^2+\sigma^2+2\beta\tau+\tau^2}\right)$$

$$IntESC = \int_0^{\phi} e^{\sigma\chi}\sin\tau\chi\cos\beta\chi d\chi = \frac{1}{2}\left(\frac{2\tau\left(-\beta^2+\sigma^2+\tau^2\right)}{\beta^4+2\beta^2\left(\sigma^2-\tau^2\right)+\left(\sigma^2+\tau^2\right)^2}\right)$$

$$+\frac{e^{\sigma\phi}}{2}\left(\frac{(\beta-\tau)\cos\left[(\beta-\tau)\phi\right]-\sigma\sin\left[(\beta-\tau)\phi\right]}{\beta^2+\sigma^2-2\beta\tau+\tau^2}+\frac{-(\beta+\tau)\cos\left[(\beta+\tau)\phi\right]+\sigma\sin\left[(\beta+\tau)\phi\right]}{\beta^2+\sigma^2+2\beta\tau+\tau^2}\right)$$